Role of ERK3 in the regulation of IL-8 and epithelial secretome-mediated chemotaxis

Dissertation

Zur Erlangung des Grades Doktor der Naturwissenschaften

Am Fachbereich Biologie

Der Johannes Gutenberg-Universität Mainz

Katarzyna Bogucka

Geb. am 14.02.1989 in *Płock*, Poland

Mainz, 2019

Table of Contents

Abbreviations

3'UTR	3' Untranslated region
AP-1	Activator protein 1
AP-2α	Activating enhancer binding protein 2 alpha
CBP	CREB binding protein
C/EBP	CAAT/enhancer-binding protein
CDK1	Cyclin-dependent kinase 1
CHX	Cycloheximide
CREB	cAMP-responsive element-binding protein
CRM1	Chromosome region maintenance 1
CSCs	Cancer stem cells
DCs	Dendritic cells
DE	Differentially expressed
DUB	Deubiqutinating enzyme
DUSP	Dual-specificity phosphatase
EGF	Epidermal growth factor
Elk-1	ETS domain-containing protein
EMT	Epithelial-mesenchymal transition
ERK1/2	Extracellular-regulated kinase 1/2
ERK3	Extracellular-regulated kinase 3
ERK4	Extracellular-regulated kinase 4
FBS	Fetal bovine serum
GCP-2	Granulocyte chemotactic protein-2
H	Hour
HCPECs	Human colonic primary epithelial cells
HDAC-1	Histone deacetylase 1
HGF	Hepatocyte growth factor
HRP	Horseradish peroxidase
Hsp27	Heat shock protein 27
HUVEC	Human umbilical vein endothelial cells
IAPs	Inhibitors of apoptosis proteins (BIRCs)

ICAM-1	Intercellular adhesion molecule-1
IECs	Intestinal epithelial cells
IL	Interleukin
IL-8R	Interleukin 8 receptor
IKK	IκB kinase
IRAK	Interleukin-1 receptor-associated kinase
JNK	Jun-N-terminal kinases
KD	Kinase dead
LB	Luria Bertani
LPS	Lipopolysaccharide
MAPK	Mitogen activated protein kinase
MAPKAPK	MAPK-activated protein kinase
MCP-1	Monocyte chemoattractant protein- 1
MEK1/2	MAPK/ERK kinase 1/2
MET	Mesenchymal-epithelial transition
MMP	Matrix metalloproteinase
NAP-2	Neutrophil-activating peptide-2
NES	Nuclear export signal
NGF	Nerve growth factor
NK	Natural killer
NLS	Nuclear localization sequence
NREs	Negative regulatory elements
NRF	NF-κB repressing factor
NTS	Nuclear translocation sequence
Oct-1	Octamer-1
PAMPs	Pathogen-associated molecular patterns
PGE2	Prostaglandin E2
PI3K	Phospatydyloinositol-3 kinase
PRRs	Pattern recognition receptors
RAF	Rapidly accelerated fibrosarcoma
RNF157	Really interesting new gene (RING) finger protein 157
ROK-α	Rho-associated kinase alpha

RSK	Ribosomal S6 kinase
RTKs	Receptor Tyrosine Kinases
SAPK	Stress-activated protein kinases
SCF	Skp1-Cullin1-F-box ligase
SDS	Sodium dodecyl sulphate
shRNA	Short hairpin RNA
siRNA	Small interfering RNA
SP1	Specificity protein 1
SRC-3	Steroid receptor coactivator-3
TAK1	TGF beta-activated kinase 1
TDP2	Tyrosyl DNA phosphodiesterase 2
TFAP2A	Branchio-oculo-facial syndrome-related transcription factor
TF	Transcription factor
TGFβ	Transforming growth factor beta
TLR	Toll-like receptor
TNFα	Tumor necrosis factor alpha
Tpl2	Tumor progression locus 2 kinase MAP3
TRAF6	TNF receptor-associated factor 6
Tris	Tris-hydroxymethyl-aminomethane
USP	Ubiquitin-specific protease
VCAM1	Vascular cell adhesion molecule 1
VEGFR2	Vascular endothelial growth factor receptor 2
WT	Wild type

Summary

Extracellular signal-regulated kinase 3 (ERK3) is a member of mitogen-activated protein kinases (MAPKs) and along with ERK4 and MK5 constitutes one of the less understood atypical MAPK modules. Recently, ERK3 gained due attention for its role in mediating tumor cell migration and metastasis. As the molecular mechanisms regulating ERK3 expression and function are unclear, the aim of this study is to decipher the activation dynamics and functional significance of this atypical MAPK. In this study, we primarily aimed to evaluate the role of ERK3 in regulating innate immune responses. Loss of function studies revealed a critical role of ERK3 in the control of LPS-regulated gene expression in epithelial cells. During the course of this study, we detected that CXCL8/IL-8 expression is strictly reliant on the expression of ERK3 in human colonic primary epithelial cells as well as in cancer cell lines. ERK3 controls IL-8 production and secretion in a kinase independent manner. It was further characterized that IL-8 promoter activity is dependent on ERK3 and several known transcription factors that control IL-8 expression are regulated by ERK3. Moreover, ERK3 plays a critical role in AP-1 signaling by interacting with and regulating nuclear localization of c-Jun protein in response to LPS. Furthermore, ERK3 also regulates MCP-1 (Monocyte chemoattractant protein-1), GCP-2 (Granulocyte chemotactic protein-2) or CXCL10, which are critically required for maintaining proper epithelial secretome and leukocytes chemotaxis *in vitro* and *in vivo*. We also detect that LPS elicits differential effects on ERK3 protein stability in a cell type dependent manner. Whilst in primary cells, LPS stimulation induced rapid ubiquitination and proteasomal degradation of ERK3, LPS seems to stabilize levels of ERK3 by blocking its proteasomal degradation in HT-29 cells. However, the IL-8 levels correlate to the expression of ERK3 irrespective of the cell types.

Blocking of the proteasomal degradation led to an accumulation of ERK3 protein and consequently rescued IL-8 levels regardless of the inhibition of MEK1/2-ERK1/2 pathway. Most importantly, loss of ERK3 levels led to a strong reduction in IL-8 levels despite the inhibition of the classical MAPK cascades or activation of NF-κB. In addition, MK5 and ERK4 exhibit opposing effects on ERK3 levels.

While the well-studied ERK1/2, p38, JNK and NF-κB pathways are reported as the main regulating pathways controlling IL-8 expression, this study unveiled a obligatory and yet

synergistic role for ERK3 in the regulation of epithelial secretome, including IL-8. The study further demonstrated that the secretome of ERK3 depleted cells failed to promote leukocyte chemotaxis both *in vitro* and *in vivo*, suggesting a critical role for this atypical MAPK in the maintenance of epithelial secretome. ERK3 has been shown to be required for the maintenance of epithelial architecture and some of the observations made here may possibly contribute to this phenotype. Further, as IL-8 has been shown to play a pivotal role in tumourigenesis and metastasis, attempts could be made to target ERK3 in these settings. Taken together, the body of the work presented here unveils a critical role for this atypical MAPK in the regulation of epithelial secretome and leukocyte chemotaxis.

Zusammenfassung

Extracellular-signal regulated kinase 3 (ERK3) gehört zu der Familie der Mitogen-aktivierten Proteinkinasen (MAPK) und zusammen mit ERK4 und MK5 bildet ERK3 die Gruppe der noch wenig untersuchten atypischen MAPK. Kürzlich wurde die Rolle von ERK3 in Tumorzellmigration und Metastasierung beschrieben. Über die zugrunde liegenden molekularen Mechanismen der Regulation sowie die Funktion von ERK3 ist bislang nur wenig bekannt. Daher war ein Ziel dieser Arbeit die Aktivierung sowie die funktionelle Bedeutung der atypischen MAPK näher zu untersuchen. Hierbei lag der Fokus auf der Rolle von ERK3 in der Regulation des angeborenen Immunsystems. Der Verlust von ERK3 in Epithelzellen führte zu Veränderungen in der LPS-vermittelten Genexpression und legt somit eine entscheidende Rolle dieses Faktors nahe.

Im Verlauf unserer Untersuchungen konnten wir zeigen, dass die CXCL8/IL-8 Expression strikt über die Expression von ERK3 in primären Kolonepithelzellen und weiteren Tumorzelllinien reguliert wird. Interessanterweise kontrolliert ERK3 die IL-8 Produktion und Sekretion unabhängig von seiner Kinaseaktivität. Darüberhinaus kontrolliert ERK3 direkt die IL-8 Promotoraktivität sowie die Aktivität zahlreicher weiterer Transkriptionsfaktoren, die in der IL-8 Expression und Sekretion von Bedeutung sind. Darüberhinaus spielt ERK3 eine wesentliche Rolle in der AP-1 vermittelten Signalweiterleitung: Nach LPS Stimulation interagiert ERK3 mit c-Jun und reguliert dessen Translokation in den Nukleus. Neben IL-8, reguliert ERK3 ebenfalls die Expression von weiteren Chemokinen wie MCP-1 (*Monocyte chemoattractant protein-1*), GCP-2 (*Granulocyte chemotactic protein-2*) und CXCL10. Diese Chemokine sind zum einen für die Zusammensetzung des epithelialen Sekretoms mit verantwortlich und zum anderen spielen sie in der Chemotaxis von Leukozyten *in vitro* und *in vivo* eine wichtige Rolle.

Es konnte gezeigt werden, dass LPS Zelltyp-abhängige Effekte auf die ERK3 Proteinstabilität hat: Während in primären Zellen eine LPS Stimulation eine schnelle Ubiquitinierung und den Abbau von ERK3 durch das Proteasom induzierte, löste die LPS Stimulation in HT-29 Zellen eine Blockade des Proteasoms aus, was letzlich zu einer Stabilisierung des ERK3 Proteins führte. Hierbei korrelierte die Expression von IL-8 mit der von ERK3. Eine Inhibierung des Proteasoms führte dies zu einer Akkumulierung von

ERK3 Protein, wodurch die IL-8 Level ebenfalls aufrecht erhalten wurden. Diese Ergebnisse wurden ebenfalls erzielt, wenn der MEK-ERK1/2 Signalweg blockiert wurde. Von großer Bedeutung ist in diesem Zusammenhang die Beobachtung, dass der Verlust von ERK3 die IL-8 Level drastisch senkte. Die Blockade der klassischen MAPK Signalkaskaden oder die Aktivierung von NFkappaB führte zu keinen anderen Ergebnissen. Zusätzlich zeigte sich, dass MK5 und ERK4 gegensätzliche Effekte auf das ERK3 Expressionslevel ausüben.

Während der regulatorische Effekt von ERK1/2, p38, JNK und NF-κB induzierten SIgnalwegen auf die IL-8 Expression bereits bekannt war, konnte in dieser Arbeit gezeigt werden, dass ERK3 eine wesentliche Rolle im Sekretom von Epithelzellen spielt und hierbei zwingend erforderlich ist jedoch synergistisch wirkt.

Die Ergebnisse dieser Arbeit legen nahe, dass das Sekretom ERK3 depletierter Zellen nicht in der Lage ist die Chemotaxis von Leukozyten *in vitro* und *in vivo* zu unterstützen, wodurch dieser atypischen MAPK eine essentielle Rolle in der Zusammensetzung des Sekretoms von Epithelzellen zugesprochen werden kann. In der Literatur wurde bereits beschrieben, dass ERK3 wesentlich zum Erhalt epithelialer Strukturen beiträgt. Einige Ergebnisse dieser Arbeit unterstreichen dies.

Darüberhinaus ist bekannt, dass IL-8 eine Schlüsselrolle in der Tumorigenese und Metastasierung spielt. Daher könnte ERK3 eine valide Zielstruktur sein, um neue therapeutische Ansätze zu entwickeln.

Zusammengenommen zeigen die Ergebnisse dieser Arbeit, dass atypische Kinasen wie ERK3 eine entscheidende Rolle in der Regulation des epithelialen Sekretoms und der Chemotaxis von Leukozyten haben.

1. Introduction

1.1 Mitogen Activated Protein Kinases (MAPKs)

Mitogen-activated protein kinases (MAPKs) are a group of serine/threonine-specific protein kinases. Ubiquitously expressed, they regulate crucial biological processes by transducing the extracellular signals into the cells via a three-tiered catalytic cascade of sequential phosphorylation events. In mammals, 14 MAPKs are organized into seven cascades and some of them are well characterized. Based on the shared and distinct features of individual MAP kinases they were classified into two subfamilies: conventional and atypical MAPKs [1, 2].

1.1.1 Conventional MAPKs

Each activation module of conventional MAPKs consists of three evolutionarily conserved kinases, organized in three-tired cascade (Fig.1) [1].

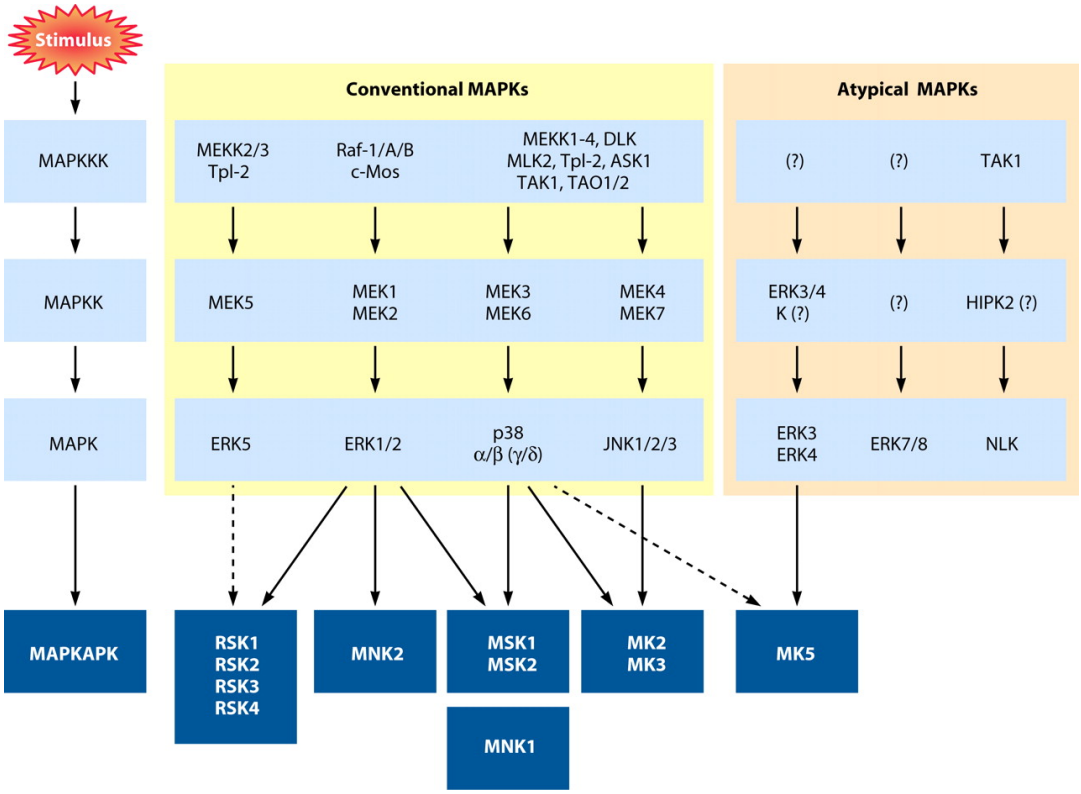

Fig. 1. MAPKs signaling cascades. Extracted from [1].

In response to external stimuli a chain of cellular events is initiated by activation of MAPKKK phosphorylation, leading to the downstream substrate (MAPKK) activation and further phosphorylation of threonine and tyrosine residues within the conserved Thr-X-Tyr motif of MAPK [1, 3]. Dual-phosphorylation in the activation loop is a hallmark of classical MAP kinases, which is essential for their enzymatic activity [1].

Four conventional MAPKs signaling cascades have been identified and four major members were characterized over the years: extracellular-regulated kinase 1/2 (ERK1/2), p38 kinase, Jun-N-terminal kinases (JNK) and ERK5. They exhibit specific and synergistic roles by regulating gene expression and controlling a variety of cellular processes like migration, proliferation, cell death, differentiation and immune responses [2].

1.1.2 Activation and regulation of conventional MAPKs

The Ras-Raf-MEK1/2-ERK1/2 canonical pathway was the first fully characterized cascade that is activated in response to growth factors and cytokines. Typically, this module is triggered by ligand-induced dimerization of receptor tyrosine kinases (RTKs) and autophosphorylation of its intracellular tyrosine residue. This pathway is regulated by Ras GTPase, which recruits MAPKKK kinases (RAF) to the plasma membrane for its activation. Activated RAFs phosphorylate and activate MAPK/ERK kinase 1/2 (MEK1/2), which in turn leads to the activation of ERK1/2 MAPKs [1, 4]. Activated ERK phosphorylates multitude of cytoplasmic and cytoskeletal proteins including MAPK-activated protein kinases (MAPKAPKs) and ribosomal S6 kinases (RSK) [5]. Additionally, nuclear translocation sequence (NTS) of ERK1/2 is phosphorylated in response to stimuli, MAPK is translocated to the nucleus and activates a variety of transcription factors [1, 5]. ERK1/2 phosphorylates Elk-1 and by regulating its transcriptional activity controls c-Fos gene expression and protein activity, allowing its dimerization with c-Jun and activation of activator protein 1 (AP-1), leading to complex formation [6]. Apart from phosphorylation and activation of the downstream substrates, ERK1/2 was proved to be a direct repressor of transcription for IFNγ-induced genes by competing with the C/EBP activator-binding protein [7].

Despite the high impact of ERK1 on a variety of biological processes, its knockout was demonstrated to have no effect on mouse development or fertility [8]. It was also shown

by the same authors, that ERK2 is indispensable for fetal development and transgenic expression of ERK1 on the ERK2-null background is able to compensate the loss of ERK2 in those animals [8].

Over the past years, it has become clear that the kinetics of RAS-RAF-ERK1/2 pathway determine cell fate. Studies of ERK1/2 signaling cascade in the embryonic PC12 phaeochromocytoma cells determining cellular outcomes in response to the epidermal growth factor (EGF) and nerve growth factor (NGF) revealed that EGF induces proliferation of the cells due to the transient activation of ERK1/2, whereas NGF simulation triggered differentiation, which is suggested to be mediated by the persistent elevation of active Ras [9, 10]. These data were supported by the observed translocation of ERK1/2 from the cytosol to the nucleus after NGF stimulation, which was not observed in case of the EGF-mediated transient activation of MAPK [11, 12]. It was also discussed that in different cell types, converse mechanism of action might be implemented, as for example in fibroblasts where sustained ERK1/2 activation is associated with proliferation. Taken together, these findings demonstrate that cells can employ transient and sustained activation of ERK1/2 to exert different responses. Duration of the signal is regulated by several mechanisms including MAP kinase phosphatases [13].

As phosphorylation of both threonine and tyrosine in the activation loop is required for ERK1/2 activity, dephosphorylation of one of them is sufficient for its inactivation. This deactivation process is exerted by dual-specificity MAP kinase phosphatases (DUSPs/MKPs) [14]. DUSPs differ in their cellular distribution and affinity for individual MAPKs. ERK1/2 can be dephosphorylated by cytosolic DUSP6, DUSP7 or DUSP9 as well as by DUSP1, DUSP4 and DUSP5, which are inducible nuclear phosphatases [14, 15]. It was reported that DUSPs play a crucial role in regulating ERK1/2 activity and therefore the cell fate. Activation and nuclear translocation of ERK1/2 triggers transcription of DUSP1 and DUSP6, which creates a negative feedback loop [16]. The physiological outcome of the RTKs signaling depends on the duration of the ERK1/2 activation and DUSP-mediated dephosphorylation events [14]. Sustained activation of RAS-RAF-ERK1/2 cascade via the RAS and RAF mutations is reported in many cancers and DUSPs as major regulators of MAPK activity are key players to consider in this process [14, 17].

JNKs (c-Jun N terminal kinases) are also known as stress-activated protein kinases (SAPK). Three isoforms were identified in humans (1,2,3), which are 85% identical, but

differ in tissue distribution. While JNK1 and JNK2 are expressed in a broad range of tissues, JNK3 seems to be a neuronal-specific isoform [18-20]. As the name indicates, they are activated by cellular stress like heat shock, UV exposure or cytokines. Like in case of other MAPKs, activation of JNKs occurs via a cascade of kinases being phosphorylated at Thr/Tyr residues. MKK4 and MKK7 are two upstream MAPKKs, which are responsible for docking of JNKs and its activation. When it comes to the substrate specificity, as their name implies, JNKs primarily regulate c-Jun transcription factors, thus marking their biological function in promoting AP-1 protein complex formation with Fos proteins family. They also seem to play an important role in apoptotic response of the cells to cellular stress inducers like UV damage [21, 22]. Embryonic fibroblasts isolated form JNK1/2-deficient mice proved to be resistant to UV irradiation and treatment with DNA–damaging agents [21].

The p38 MAPK family is represented by four isoforms - α, β, γ and δ. P38α, which is 50% identical to ERK2 and p38β are ubiquitously expressed in both cytosolic and nuclear cellular compartments [1, 23]. Majority of the published data refers to the regulation of p38α. Chemical inhibition of p38 does not affect activity of any other canonical MAPKs [23, 24]. Like in the case of JNK, p38 pathway is activated in response to cellular stress, released cytokines like IL-8, UV irradiation and lipopolysaccharide (LPS), tumor necrosis factor alpha (TNFα) or Interleukin 1 (IL-1). In response to the aforementioned stimuli, upstream kinases like MKK3 and MKK6 are activated, enabling phosphorylation of the targeted p38 isoform. As for all canonical MAPKs, substrate specificity is not strict and many of them are shared between p38, JNK and ERK1/2. The most potent MAPKAPKs interacting with p38 in generating cellular responses are MK2 and MK3 [1].

1.2 Atypical MAPKs

Based on the structural similarities to the classical MAPKs, new kinases were discovered and due to their distinct characteristics a new group emerged, atypical MAPKs (Fig.2). Unconventional and/or atypical MAP kinases comprise of ERK3, ERK4, ERK7/8 and Nemo-like kinase (NLK) [25]. The distinguishing feature of this novel subfamily of MAPKs is the lack of the classical three-tiered cascade organization and limited substrate specificity [1, 25]. Out of the mentioned atypical MAPKs, ERK3 and to some extent ERK4 will be the focus of this work.

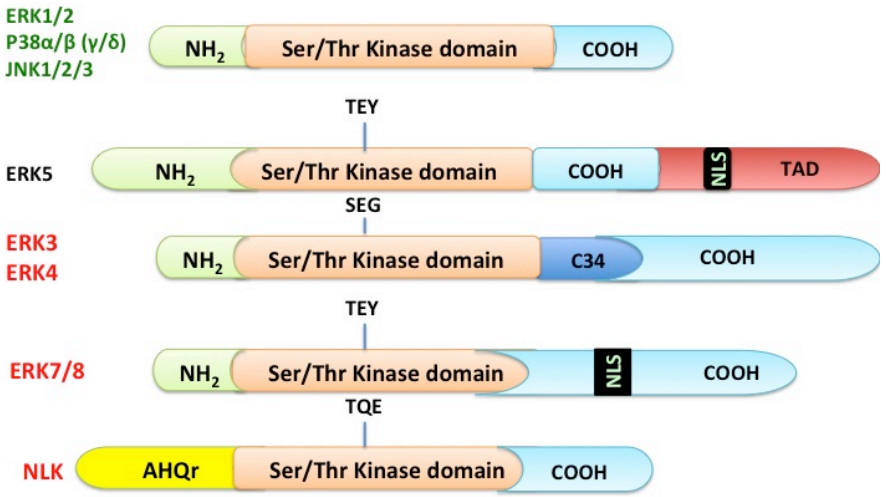

Fig. 2. Schematic representation of differences in the domain organization and phospho-acceptor sites in the activation loop of conventional and atypical MAPKs. NLS-nuclear localization sequence, C34-conserved region, TAD- Transactivation domain. Adapted from [1].

1.2.1 Structure of ERK3 and ERK4

Among the few members of atypical MAPKs, ERK3 and ERK4 are very distinctive kinases expressed only in vertebrates that share few peculiarities. Dual phospho-acceptor site within the classical Thr-X-Tyr motif present in all other MAPKs is replaced by a single phosphorylation site at Serine 189 and 186 in ERK3 and ERK4 respectively and placed within the signature SEG motif in their activation loop (Fig. 3) [25].

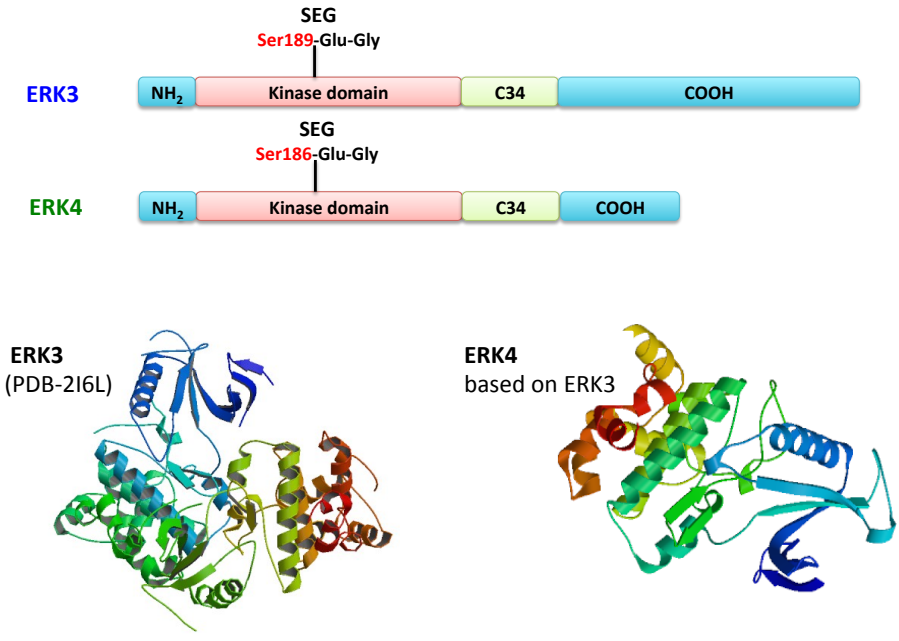

Fig.3 Schematic representation of the structure of ERK3 and ERK4. C-34 conserved region. Adapted from [1]**.** Shown below are the crystal structures of ERK3 (Protein data bank-2I6L (PDB-2I6L)) and a model of ERK4 based on the ERK3 structure.

Both, ERK3 and ERK4 were cloned over 20 years ago based on ERK1-derived probe and are considered orthologs as they share the distinct Ser-Pro-Arg sequence in their kinase domain, which replaced the conserved Ala-Pro-Glu found in all the other kinases in human genome [25]. They both contain a non-catalytic C-terminal domain, which accounts for the significant difference in size between ERK3/ERK4 (721/587 amino acids) and ERK1/2 (~360 amino acids) (Fig. 3) [25-27].

1.2.2 ERK3 module

ERK3 (MAPK6) mRNA is ubiquitously expressed in all tissues with highest expression levels in brain, muscles and gastrointestinal tract [25]. ERK3 is distributed in all subcellular compartments [25]. Expression of ERK3 was reported in both cytoplasm and nucleus and neither phosphorylation nor kinase activity of ERK3 seems to play a role in its subcellular distribution [25, 28]. Julien et al showed that chromosome region maintenance 1 (CRM1) exportin binds directly to ERK3 and contributes to its relocalization to the cytoplasm [29].

Loss of ERK3 leads to respiratory failure, disturbed growth and neonatal lethality in mice within the first days of life [30]. ERK3 contains a single phospho-acceptor site at serine 189 within its N-terminal domain, which is constitutively phosphorylated in resting cells. Very unique feature of ERK3 is the 400 amino acids C-terminal domain (Fig. 3) [31]. ERK3 is a highly unstable protein with a half-life of only 30-45 min. It is a remarkable example within MAPKs family, as the biological function of ERK3 seems to be regulated by protein stability [25]. Rapid turnover of the protein is not regulated by phosphorylation of the activation loop, also kinase activity of ERK3 and C-terminal extension seem to be irrelevant in this process. Two degradation domains were identified in the N-terminus (NDR1 and NDR2), that are ubiquitinated and required for proteasomal degradation of the protein [32].

Recent studies indicate, that ERK3 ubiquitination is lysine-independent, as the lysinless mutant of ERK3 is still degraded by the proteasome [33]. The free N-terminal domain of ERK3 serves as a conjugation site for polyubiquitin chains. Accumulation of ERK3 was

reported during muscle differentiation and in mitosis, due to the phosphorylation by cyclin-dependent kinase 1 (CDK1) [32, 34, 35]. Furthermore, Mikalsen et al reported that C-terminal tagging of ERK3 can protect the protein from ubiquitination [36]. While the E3 ligase/s that can ubiquitinate ERK3 remain/s unknown, the first deubiqutinating enzyme (DUB) for ERK3 was recently discovered [35, 37]. As reported by Mathienet et al, ubiquitin specific peptidase 20 (USP20) can directly bind and deubiquitinate ERK3 protein, leading to its stabilization [37]. Recent studies demonstrated, that ERK3 binds to DUSP2 *in vitro*. Furthermore, it has been demonstrated that ERK3, unlike ERK2, does not increase the activity of DUSP2 upon binding [38].

As for the biological function of ERK3, recent reports strongly suggest that expression of this atypical kinase is regulated by cytokines such as TNFα and IL-1β in both primary and cancer cells [39]. It was shown that ERK3 gene promoter contains c-Jun binding sites and chromatin-IP revealed direct interaction of the transcription factor to the discovered region of ERK3 [39]. Moreover, ERK3 emerged as a new factor regulating endothelial cell proliferation and migration. Depletions of either c-Jun or ERK3 were shown to impair the ability of human umbilical vein endothelial cells (HUVEC) to form endothelial tubes *in vitro*. Furthermore, experiments in ERK3 knockdown cells revealed that ERK3 is required for TNFα-stimulated capillary tube formation by HUVEC cells [39]. As an attribute to these findings, authors demonstrated that ERK3 controls VEGFR2 mRNA expression and signaling [39]. Another study revealed that ERK3 regulates the steroid receptor coactivator-3 (SRC-3) [40], a known co-activator of specificity protein-2 (SP1), which mediates VEGFR2 expression. Taken together, these studies showed a synergistic role for ERK3 and SRC-3 in regulating SP1-mediated VEGFR2 gene expression [39].

The role of ERK3 in immune response was also reported by two publications, indicating that like ERK2, ERK3 may play a role in T cell biology. According to the study by Marquis et al, ERK3 is highly expressed in activated $CD4^+$ and $CD8^+$ T cells and the depletion of ERK3 leads to an impaired proliferation rate and cytokine production in both T cell subtypes [41]. The same authors were also able to determine a role of ERK3 in the control of thymocytes selection. These findings suggest that atypical MAPK is a downstream effector of ERK1/2 signaling pathway [42].

Recently, ERK3 emerged as a potential therapeutic target in treating human cancers. It was shown that ERK3 regulates phosphorylation of tyrosyl DNA

phosphodiesterase 2 (TDP2), which repairs topoisomerase 2 (Top2)-linked DNA damage, thereby actively protecting lung cancer cells against DNA damage and growth inhibition [43]. Furthermore, ERK3 overexpression in MDA-MB231 breast cancer cells enhanced cell migration [44]. Interestingly, cells expressing exogenous kinase dead mutant of ERK3 exhibit the same migratory phenotype, indicating first kinase-independent function of ERK3 [44].

1.2.3 ERK4 module

ERK4 (MAPK4) gene displays similar organization of exons and introns as ERK3, which suggest the same ancestor for these two kinases [25]. Despite 62% overall similarity to ERK3 and 73% matching amino acids within its kinase domain, ERK4 lacks the distinct C-terminal extension present in ERK3 (Fig. 3). Only the first 150 residues are almost 50% identical. ERK4-depleted mice do not display any abnormalities in growth or reproduction [26]. Furthermore, additional loss of ERK4 in ERK3-null mice does not enhance the ERK3-loss-mediated phenotypes [26]. Highest expression levels of ERK4 were detected in murine brain tissue, which together with the fact that ERK4-null mice display depression-like behavior might suggest the importance of ERK4 in the proper function of the cerebrum [26]. It was shown that ERK4 in contrast to labile ERK3 is a stable protein [45]. ERK4 has one phosphorylation site at S186 in its activation loop. The biological function of ERK4 as well as its interactions with ERK3 remains unknown.

1.2.4 MK5 module

ERK3 and ERK4 exhibit very distinct substrate specificities. They do not phosphorylate or interact with any of the known substrates of classical MAPKs. One potent substrate of ERK3 and ERK4 described so far is MK5 (MAPKAPK5).

MAPK-activated protein kinase MK5 was first described as p38-regulated and activated protein kinase (PRAK). It was proved to share around 45% sequence similarity to the other known p38 substrates, MK2 and MK3 [46, 47]. MK5 as the other members of the subfamily MAPKAPKs carries a nuclear localization sequence (NLS), which is causing nuclear accumulation of the protein in untreated cells. Similar to other MKs, it can activate small heat shock protein 27 (Hsp27) [25, 48]. However, there are two substantial differences in MK5 C-terminus domain, which may attribute to the unique

regulation of MK5 when compared to MK2 and MK3. First, MAPKAPK5 lacks the extra phosphorylation site, which in other MAPKAPKs triggers nuclear export signal (NES) and due to that translocation of the mentioned kinases to the cytoplasm [49]. Second, it consists of a distinct extension of 100 amino acids at the C-terminus, which is essential for its interaction with ERK3 and ERK4 [25]. Although it was first described as a p38-related kinase, studies indicate that it can be phosphorylated *in vitro* by recombinant ERK2 as well [46]. Two MK5 encoding transcripts of 471 and 473 amino acids respectively were identified. MK5 is ubiquitously expressed in all tissues. Surprisingly, its deficiency does not have any impact on mice viability or fertility. Upon LPS-induced endotoxic shock, MK5-knocout animals responded like the wild type mice, showing no malfunction in cytokine production. These observations are in contrast to the phenotype exhibited by the MK2-deficient mice, which showed defects in LPS-induced biosynthesis of cytokines such as TNFα or IL-6 due to the mRNA destabilization. There was no compensatory mechanism involving MK5, which would 'switch on' in MK2-null mice. Moreover, compared to the other substrates of p38, like MK2, MK5 is not the most potent interaction partner of the kinase [48]. These results enlighten unexpected differences between MK5 and MK2 enzymes regulation and its interaction with p38, strongly suggesting that activation of endogenous MK5 by p38 kinase is largely unlikely [48].

As the mechanism behind MK5 activation remained unclear, the search continued to determine more potent interacting partners. Schumacher et al reported specific molecular interaction between ERK3 and MK5, using β-galactosidase luminometric assay. Furthermore, they showed five times higher affinity of MK5 to ERK3, than to p38 kinase. In the same study, it was also indicated that the C-terminal domain of ERK3 is required for the interaction but not its kinase activity. The nucleus to cytoplasm relocalization of MK5 was proposed to be a result of direct interaction with ERK3 (Fig. 4) and data showed that phosphorylation of MK5 at T182 is required for the activation of the kinase, but neither this phosphorylation nor its catalytic activity is relevant for ERK3-mediated translocation to the cytoplasm [31].

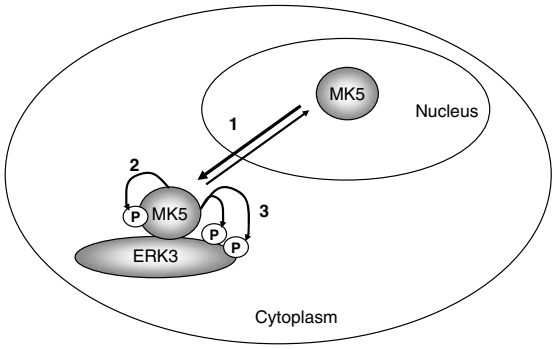

Fig. 4 Schematic representation of nuclear and cytoplasmic distribution of ERK3 and MK5 proteins and their interaction. (1) Increased cytoplasmic levels of ERK3 triggers docking of MK5 in the cytoplasm (2) Cytoplasmic scaffolding of MK5 by ERK3 triggers ERK3-mediated autophosphorylation at T182 and activation of MK5 (3) Activated MK5 can in turn phosphorylate ERK3. Adapted from [31].

Depletion of MK2, but not of MK5 from cells leads to a decrease in p38 expression [50]. Furthermore, it was reported that knockdown of MK5 leads to a dramatic decrease in ERK3 protein expression. Based on these findings, MAPKAPK5 was introduced as a stabilizing partner for ERK3 protein [31, 50].

In 2006, it was shown that ERK4 can also bind and regulate MK5 activity in a kinase-dependent manner. Authors demonstrated that ERK3 and ERK4 can form a multimeric protein complex at the same time suggesting completely different regions of ERK4 required for binding of ERK3 and MK5. Kinase dead mutants of ERK3 and ERK4 and their ability to activate MK5 were studied. Data revealed that catalytically inactive mutant of ERK3 is still able to induce phosphorylation of MK5 [45].

1.2.4.1 FRIEDE interaction motif

Localization of the residues 326-340 in C-terminus of ERK3 and ERK4 as an MK5-interacting region triggered new lines of studies, revealing new interesting facts about possible interactions between ERK3/4 and MK5 [27, 45, 51]. An MK5 mutant consisting of amino acids 1-432, despite present docking domain was unable to interact with ERK4. Small, around 20 residues long motifs of MAPKAPK5 fail to interact with ERK3 and ERK4 [27]. Furthermore, it was proved that activation loop phosphorylation, but not the catalytic activity of both atypical interacting partners of MK5 is required for binding to occur [27, 52]. These findings further prove unconventionality of the atypical ERK3 and ERK4 as compared to the canonical MAPKs, in which the catalytic domain interacts with

D motifs present in MAPKAPKs as short as 16 residues D motifs [27]. Further investigation of the mentioned findings led to a discovery that a single point mutation within distinct FRIEDE motifs of ERK3 and ERK4 (I334K and I330K, respectively) is sufficient to disrupt MK5 binding. Structural studies are required to determine the role of the activation loop phosphorylation of ERK3 and ERK4 for the MK5 binding [27].

1.2.5 Activation of ERK3 and ERK4

Up to date, upstream effectors of ERK3 and ERK4 remain elusive and therefore identification of factors responsible for phosphorylation and activation of those two atypical MAPKs is crucial to understand their physiological function. Two studies characterized Ser/Thr protein kinases PAK1 and PAK2 and their role in phosphorylation of ERK3 and ERK4 at S189 and S186 respectively. A link between Rac1/Cdc42-PAK and ERK3-MK5 was also described in the context of actin cytoskeleton and polymerization [53, 54].

Another study revealed that BRAF kinase controls expression levels of ERK3. BRAF V600E mutation occurs in approximately 90% of all BRAF mutations in melanoma and results in persistent catalytic activation of the BRAF kinase and the downstream MEK1/2-ERK1/2 signaling pathway [55]. Searched for novel targets of BRAF-MEK/1/2-ERK1/2 pathway revealed a role of BRAFV600E in regulating expression levels of ERK3 [56]. Results showed that both knockdown of ERK1/2 as well as inhibition of the kinase by U0126 inhibitor result in reduction of ERK3 levels in A375 melanoma cell line [56].

1.3 MAPKs and regulation of innate immune response

The innate immune response is the first defense line against infections. Rapid recognition of pathogen-associated molecular patterns (PAMPs) by the pattern recognition receptors (PRRs) like Toll-like receptors (TLRs) triggers translation of antimicrobial peptides that can directly target the pathogen as well as the multiple signaling cascades, leading to the production of proinflammatory cytokines and chemokines [57]. The group of immune cells present in the tissue consists of macrophages, fibroblast, mast cells, dendritic cells as well as leukocytes like granulocytes and monocytes. All of the immune cells present in peripheral tissues express multiple PPRs on their surface and in the cytoplasm, which can trigger either direct or indirect innate immune response [57].

MAP kinases like ERK1/2, p38 and JNK play distinct roles in translating the signal coming from the PRRs like TLRs into an effective immune response. Mechanisms controlled by MAPKs include transcriptional control as well as regulation of the mRNA stability of immunomodulatory cytokines [58].

1.3.1 Toll like receptors (TLRs)

TLRs are a group of transmembrane proteins that can recognize bacterial and viral PAMPs. Their extracellular leucine-rich domains can recognize PAMPs such as microbial lipoproteins or nucleic acids. Upon activation, TLRs assemble big complexes, which initiate signaling pathways, leading to a production of factors in consequence leading to the recruitment of granulocytes [58]. Signal transduction pathway is activated via a transmembrane residue followed by intracellular Toll/IL-1 receptor (TIR) domains that transfer the signal to the cytoplasmic adaptor proteins like MyD88 [58, 59]. The group of ten TLRs is expressed in humans and all of them with the exception of TLR3 signal via MyD88 adaptor protein [59]. The stimulation of TLR4 by LPS evokes an immediate immune response by inducing the release of critical proinflammatory cytokines and LPS/TLR4 pathway is one of the best-studied signal transduction pathways [60].

1.3.2 MyD88-dependent TLR4 pathway

MyD88 was the first identified member of TIR family. It triggers the activation of the transcription factor NF-κB and MAPKs signaling-induced cytokine production. TLR4 is the only family member that induces also TRIF-dependent NF-κB and MAP kinases late–phase pathways (Fig. 6). Interestingly, activation of both pathways is required for the production of inflammatory cytokines [59].

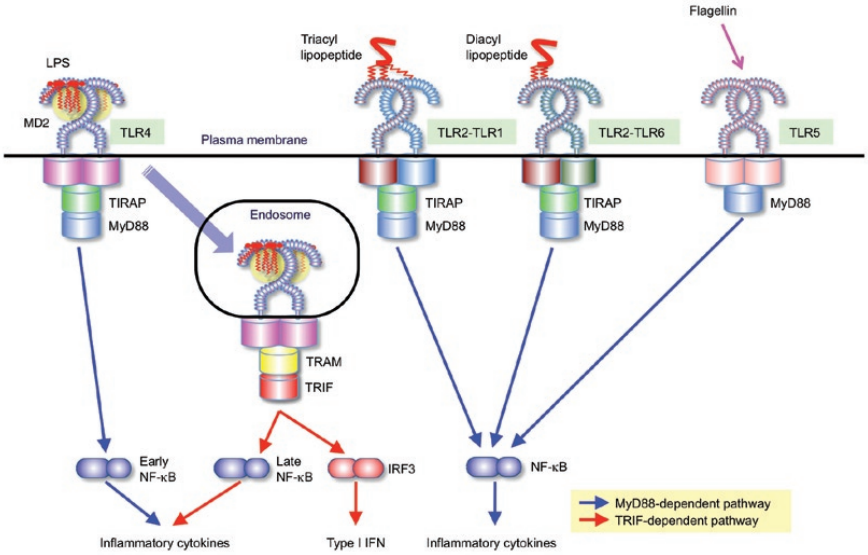

Fig. 5 Schematic representation of TLRs pathways, mediated via MyD88 adaptor protein. From [59].

In response to LPS, MAP kinases p38 and JNK are activated by transforming growth factor beta (TGFβ)-activated kinase 1 (TAK1) complex. TAK1 complex translocates to the cytoplasm and recruits MKK4/7 and MKK3/MKK6 that in turn will activate JNK and p38, respectively. The whole pathway consists of multiple steps, including phosphorylation of interleukin-1 receptor-associated kinase 1/2 (IRAK1/IRAK2) and their further interaction with TNF receptor-associated factor 6 (TRAF6), which can directly catalyze the synthesis of K63-pUb chains. Those complexes can then recruit and activate TAK1 and IκB kinase (IKK). Two distinct pathways can then be activated by TAK1: NF-κB pathway involving IKK and the MAPKs pathway (Fig.6) [57, 61].

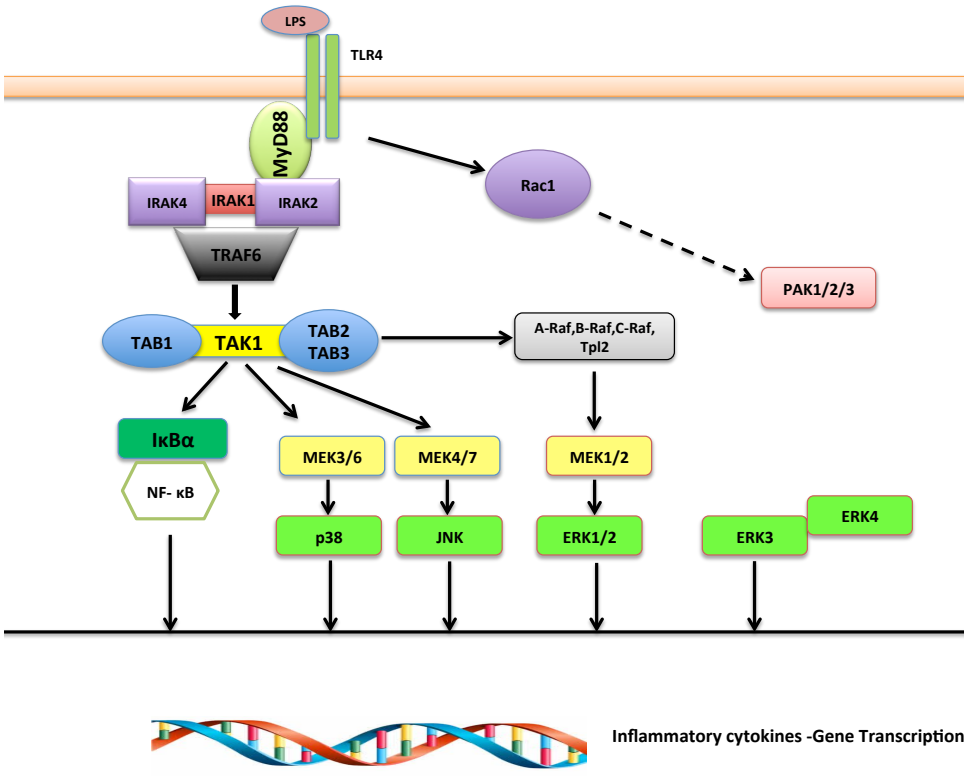

Fig. 6 Simplified scheme of activation of MAPKs and and NF-κB via TLR4 signaling pathway.

NF-κB is a transcription factor complex composed of five proteins: p65 (RelA), RelB, c-Rel, p105/p50 (NF-κB1) and p100/p52 (NF-κB1), which in unstimulated cells is retained in cytosol by IκB [62]. Therefore, activation of the canonical NF-κB pathway involves phosphorylation of the inhibitory IκB protein, which is ubiquitinated and degraded by the proteasome. This allows activation and nuclear translocation of NF-κB transcription factor, its binding to the DNA and in consequence regulation of multiple proinflammatory genes like IL-8 [61, 63].

The second pathway is linked to MAPKs: p38 and JNK and is activated via the sequential phosphorylation events in the three-tier cascade of regulated MAP kinases, which ultimately leads to translocation of AP-1 transcription factor.

Activation of ERK1 and ERK2 by TLRs was shown to be mediated by tumor progression locus 2 kinase MAP3 (Tpl2) (MAP3K), which functions as MEK1/2 in activating ERK1/2 [64]. In resting cells, Tpl2 occurs in complex with p105 precursor protein of NF-κB. Upon stimulation of TLRs, IκB complex is activated and K48-linked ubiquitination is triggered, leading to a phosphorylation of p105 and release of Tpl2, which can then further activate MKK1/MKK2 kinases and their downstream target ERK1/2 [57].

Alternative TLR pathways have also been described, including inhibitors of apoptosis protein 1 (IAP1, BIRC3) and 2 (IAP2, BIRC2) mediated signaling. The K48-linked ubiqutination of TRAF3 plays a crucial role in regulation of this pathways, consequently leading to the activation of MAPKs and cytokine production [65].

1.4 IL-8/CXCL8

Inflammation is the physiological response to tissue injury or infection. It is initiated by signaling cascades described earlier and activated by TLRs, which triggers secretion of proinflammatory factors that recruit first responders-leukocytes: neutrophils and monocytes to the region. At the same time, vascular alterations like vasodilation caused by histamine and prostaglandins will alter blood flow and increase the delivery of the circulating white blood cells to the site of the injury or infection. Released histamine and leukotrienes enhance permeability of the vessels to allow the exit of the cells and proteins into the circulation [58]. Cytokines such as CXCL8/IL-8 are potent factors regulating leukocytes chemotaxis and will be main subject of this study [66].

Chemokines are a group of small (8-15 kDa) proteins, which control the direct migration of leukocytes, resulting in the accumulation of these cells at the site of cytokine production [63, 67]. IL-8 mediated signaling is triggered by its binding to either chemokine receptor 1 (CXCR1, IL8-Rα), which has an affinity only to IL-8/CXCL8 and CXCL6 or CXCR2 (IL-8Rβ), which binds a wide range of cytokines including IL-8, CXCL1 and CXCL2 [68]. Ligand-receptor interaction leads to the activation of multiple pathways, including phospatidyloinositol-3 kinase PI3K/Akt, MAPKs signaling or Rho GTPases. The IL-8 and its roles in evoking proper immune responses, angiogenesis and tumor microenvironment modulation are very well characterized [67].

IL-8/CXCL8 belongs to the group of CXC chemokines, where two cysteine residues are separated by amino acid [69]. A number of studies demonstrated that nucleotides 1-133 in the 5’ region of the CXCL8 gene are sufficient to regulate its transcription, as this promoter sequence contains a binding site for NF-κB [70, 71]. IL-8 expression is controlled by multitude of coordinated signaling pathways and guarded on three levels: inhibition of the promoter, transcription and stabilization of the mRNA [63].

1.4.1 Regulation of IL-8/CXCL8 expression

In resting cells, IL-8 transcription is repressed either by octamer-1 (Oct-1) and NF-κB repressing factor (NRF) binding to negative regulatory elements (NREs) or by deacetylation of histones [72]. It has been shown that substitution of Oct-1 repressor protein by NF-κB and CAAT/enhancer-binding protein (C/EBP) boosted IL-1β-induced IL-8 transcription [73]. NRF binds to the NRE of the CXCL8 promoter, which partially overlaps with the NF-κB response element. Disruption of the NRF binding by implemented mutations in NRE led to an increase of basal IL-8 transcript levels. At the same time IL-1-induced IL-8 transcription was enhanced upon the introduced mutation of NRE. These findings suggest an interesting dual function of NRF, which works as a repressor only in unstimulated cells, while being a co-activator of the IL-8 transcription in IL-1 stimulated cells [74]. Histone acetylation increases the activity of transcriptional enhanceosomes, which allows efficient transcription factor binding. It was shown experimentally that inhibition of histone deacetylase 1 (HDAC-1) engages cAMP-responsive element-binding protein (CREB) binding protein (CBP)/p300, leading to the transcriptional stimulation by its histone acetyltransferase [75].

With the aim of characterizing the role of IL-8, its promoter was studied and transcription factors, which are able to bind to the promoter sites were characterized. Overexpression of IKKβ and IκB dominant-negative mutants or the use of antisense inhibition of NF-κB impaired IL-1- and TNFα-induced expression of IL-8 [63]. Binding of p65 subunit of the NF-κB complex to the IL-8 promoter was shown within half an hour upon IL-1 stimulation, providing yet another proof that NF-κB is indispensable for induction of the IL-8/CXCL8 gene expression. Besides NF-κB, the IL-8 promoter also contains binding sites for AP-1 and CAAT/enhancer-binding protein beta (C/EBPβ, NF-IL-6) [72].

1.4.2 MAPK-dependent regulation of IL-8 expression

MAPKs p38, ERK1/2 and JNK play an essential role in activating AP-1 by controlling homodimeric/heterodimeric protein complexes formed between Jun and Fos proteins [63]. Transcriptional potential of AP-1 is regulated by protein phosphorylation, its abundance and interaction with protein kinases like MAPKs. As MAP kinases are

"druggable targets" of our proteome, testing of various inhibitors targeting this specific family of protein kinases was implemented over the years to verify the role of each canonical pathway in IL-8 production [63].

As p38 kinase is always given a central role in regulating innate immune response in mammalian cells, most studies focused on determining its role in IL-8 production. Blocking p38 kinase activity by the SB203580 inhibitor proved to lead to a decrease in IL-1-induced IL-8 secretion [63, 76]. Inhibition of p38 kinase with even the highest concentrations did not affect mRNA levels of IL-8/CXCL8 in fibroblasts [77, 78]. These findings were then further explained by the hypothesis that p38 is involved in some post-transcriptional steps of IL-8 control. Expression of an active mutant of MKK6, the upstream kinase specific for p38, led to stabilization of IL-8 mRNA. In conclusion, it was shown that activation of the p38 signaling cascade is responsible for the IL-8 mRNA stabilization, via the MK2 [70].

JNK signaling has also been implied in regulating IL-8 production. As it has been already described for p38, JNK also possesses a stimulatory effect on NF-κB-mediated IL-8 production [76]. A model was proposed, in which NF-κB complex translocates to the nucleus and binds to the IL-8 promoter in close proximity to the bound AP-1. Subsequently, JNK activated by upstream MKK7 can then further phosphorylate NF-κB subunits, AP-1 and other regulatory components, enhancing IL-8 promoter activity. In contrast to p38, no stabilizing effect of MKK7 on IL-8 mRNA was found [70].

Different signal transduction pathways are highly involved in IL-8 regulation and each pathway plays a substantial role. Several proinflammatory agents like IL-1, LPS or TNFα were shown to activate previously described p38 and JNK, but they are not the most potent activators of ERK1/2 pathway. Growth factors in contrast are described as the strongest enhancers of the MEK/ERK signaling cascade. Hepatocyte growth factor (HGF)-and EGF-mediated activation of the pathway was shown to induce cell motility and production of metalloproteinases (MMPs), through the control of AP-1 protein complex. EGF was shown to slightly enhance IL-8 secretion with no effect on JNK or NF-κB pathway [70, 79]. The ERK1/2 pathway independently does not seem to have a dominant effect on IL-8 production. There are few reports testing MEK1/2 inhibitors and their role on the IL-8/CXCL8 secretion. Treatment of LPS-stimulated monocytes with MEK1 inhibitor (Trametinib) blocked cytokine production similarly to p38 inhibitor (SB203580) treatment [80].

In contrast to p38 studies, in case of MEK1/2 inhibitor treatment also exerted effects on the mRNA levels, which suggested that inhibition of MEK/ERK pathway prevents transcription of cytokines like IL-8, IL-6 and Prostaglandin E2 (PGE2) due to the block in ERK1/2 phosphorylation and direct inhibition of the activation of transcription factors like ETS domain-containing protein (Elk1), c-Myc and E-26-like protein 1 [6, 63, 72]. Studies from several groups demonstrated that Elk-1 phosphorylation by MAPKs in response to different stimuli is critical for the activation of c-Fos genes and mediates AP-1 complex formation. Stimulus dependency of these findings was discussed as MEK1/2 inhibitor treatment blocked IL-8 production only in LPS and IL-1 stimulated cells and did not have any effect on TNFα-mediated conditions [81]. It should be taken into account that the results for all the canonical MAP kinases presented so far are mostly based on the treatment with different inhibitors. Therefore, observed effects might also be explainable by off-target effects and existence of the secondary targets affecting IL-8 production [80].

IL-8/CXCL8 expression is controlled at three levels: transcription triggered by NF-κB, boosting the transcript levels by MAPKs signaling pathways and stabilization of the mRNA by p38 (Fig. 7) [63, 78].

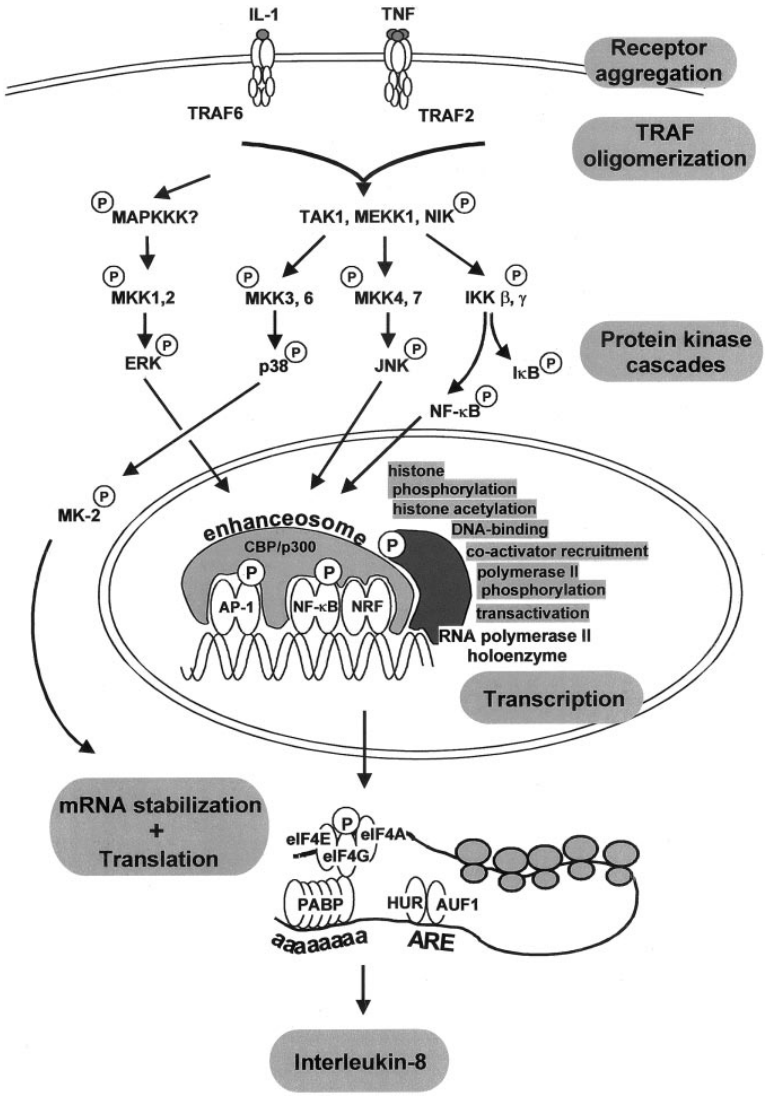

Fig. 7 Schematic representation of the signal transduction pathways involved in IL-8 transcriptional regulation. From [63].

1.4.3 Physiological roles of IL-8

The physiological role of IL-8 is to induce the immune response by promoting granulocyte chemotaxis to the site of the injury. Another very important function of this chemokine is its proangiogenic properties: It has direct, concentration dependent effect on endothelial cell proliferation and capillary network organization. It was also shown that expression levels of MMP-2 and -9 as well as their activity was enhanced in endothelial cells treated with recombinant IL-8. It is suggested that IL-8/CXCL8 is involved in extracellular matrix degradation and in consequence it might facilitates cell

migration and invasion [82, 83]. These findings support the notion that IL-8 is key player in neoangiogenesis and healing [67].

1.4.4 Leukocytes and chemotaxis

IL-8 emerged as the most potent activator of neutrophils and its migration. IL-8 stimulation of neutrophils induces actin polymerization and impressive lamellipodia formation (Fig. 8) [69]. IL-8/CXCL8 stimulation also induces the expression of integrins, thus enabling cell adhesion to endothelial cells, while migrating through the vessels [84].

Approximately 70% of white blood cells are neutrophils. Their life span is extremely short, around 6 h. Nevertheless, they play a fundamental role in innate immune responses: They regulate inflammation by production of chemokines such as IL-8, which enables recruitment of the other immune cells like monocytes and macrophages, altering the immune response and enabling elimination of pathogens [85].

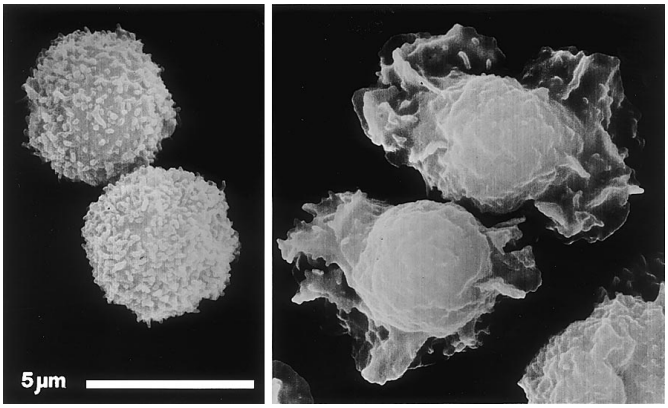

Fig. 8 Electron microscopy pictures of neutrophils captured in two conditions: without (left) and with (right) IL-8 chemokine treatment for 5 s. Extracted from [69].

IL-8 is not the only chemotactic factor important for proper migration of granulocytes and monocytes. It has been previously shown that granulocyte chemotactic protein-2 (GCP-2/CXCL6) can provoke chemotaxis and as in humans it seems to only complement the chemotactic properties of IL-8, in the mouse it was suggested to be a major chemotactic factor for neutrophils [86]. Neutrophil-activating peptide NAP-2 was reported to bind to the same site on neutrophils as IL-8 and was shown to regulate chemotaxis neutrophils and monocytes [87, 88]. Another example is CXCL10, which so far has been considered to be a chemotactic factor only for NK cells and T cells [89, 90]. However, recently it emerged as a main mediator of neutrophils infiltration in the lung

and seems to contribute to the pathogenesis of acute respiratory syndrome [91, 92]. Monocyte chemoattractant proteins (MCP) are as the name indicates predominantly associated with monocytes. It was demonstrated that MCP-1/CCL2 have a potent effect on THP-1 cells chemotaxis [93]. MCP-4 is highly upregulated in inflamed joint of rheumatoid arthritis patients and is used as a progression marker [94-96]. The IL-16 was first described as a lymphocyte chemoattractant factor, but since then it was also related to neutrophils and monocytes chemotaxis [97-99].

1.4.5 IL-8 and tumor biology

Tumor cells express different chemokines and their receptors, which potentially allows the exploitation of the involved pathways to abrogate cancer cells growth and survival. It was reported in many publications that tumor cells produce IL-8, which supports tumor growth, metastasis and angiogenesis [67, 78, 100-102]. Elevated levels of CXCL8/IL-8 correlate with cancer progression and are a poor prognostic factor in melanoma, breast, liver, lung or colon cancer [67]. Two signaling properties of IL-8 are very well established: paracrine by altering the tumor environment and autocrine by promoting metastasis [103].

Tumor microenvironment consists of host fibroblasts, endothelial cells and immune cells like macrophages, natural killer (NK) cells or leukocytes (Fig. 9) [103].

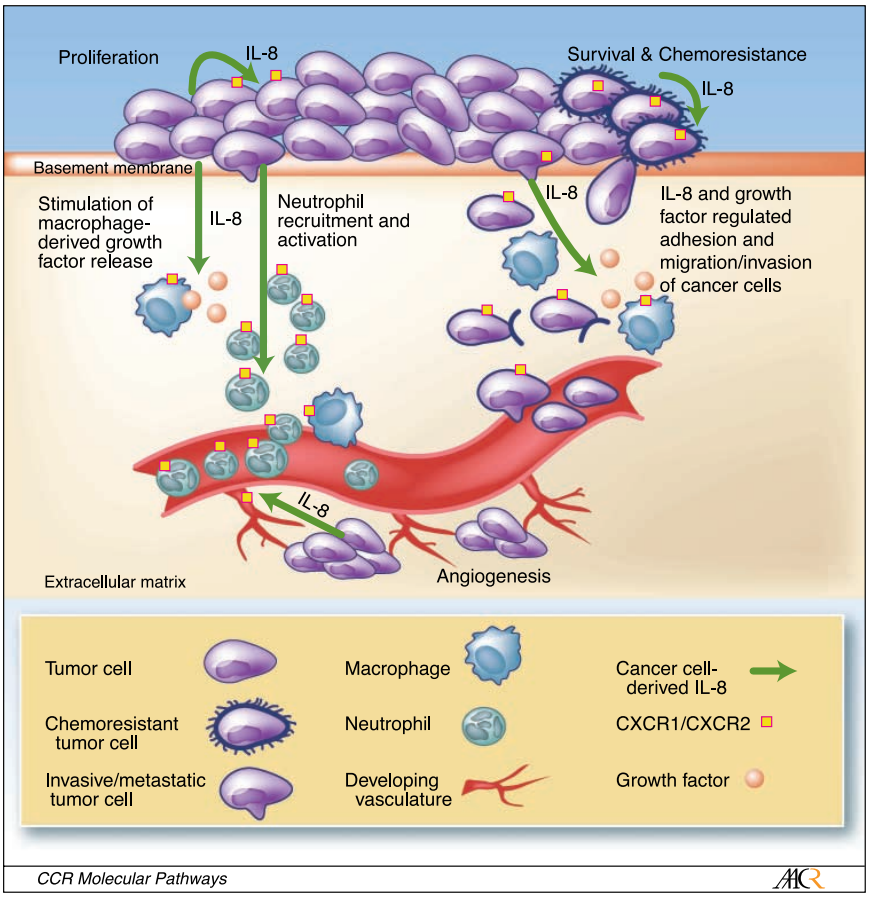

Fig. 9 Model representing tumor environment and IL-8 signaling. Tumor-derived IL-8 controls proliferation and survival of cancer cells via regulation of the autocrine signaling pathways. Moreover, secreted IL-8 enhances angiogenesis in the tumor endothelial cells and promotes chemotaxis of neutrophils into the tumor site. Additionally to its direct effect on tumor cell migration, IL-8 triggers tumor-associated macrophages to secrete growth factors, which further induces tumor cell proliferation and invasion. Extracted from [104].

Because of their short life span neutrophils were never considered as a potent member of this microenvironment, but tumor-associated neutrophils are reported to be a bad prognostic marker for colon [105], liver [106], esophageal [107], head and neck [108, 109], lung [109] cancer and melanoma [110]. Intratumoral IL-8 secretion is proposed to be a key regulator in neutrophil chemotaxis to the tumor microenvironment [104]. As consequence, IL-8 signaling promotes actin polymerization and reorganization, mediating motility and invasion of both, tumor and stroma cells like neutrophils (Fig. 9, 10) [82, 104]. Expression of CXCR1/CXCR2 chemokine receptors seems to correlate with metastasis and tumor progression.

Both receptors are highly expressed by cancer stem cells (CSCs), which are the population of tumor cells being responsible for tumor growth, maintenance and

metastasis. IL-8 has been reported to drive the CSCs phenotype. Recombinant IL-8 has been shown to enhance the CSC population and invasiveness in breast cancer model *in vitro*. Moreover, depletion of CXCR1 was shown to selectively deplete breast CSCs [111]. Furthermore, blockade of CXCR1 *in vivo* decreased metastasis and in combination with chemotherapy reduced primary tumor growth and brain metastasis [111, 112]. Inhibition of IL-8/IL-8R axis was also reported to reduce cell growth of colon cancer cells *in vitro* [113]. Inhibition of CXCR1/2 in lung cancer xenograft model decreased tumor growth, metastasis and angiogenesis [114]. Interestingly, in pancreatic cancer cells it was demonstrated that IL-8 mediated induction of CSC population and cell invasiveness could be reversed via CXCR1 blockade [115]. Targeting CXCR2 in acute myeloid leukemia model reduced the viability of leukemic stem cell both *in vitro* and *in vivo* [116]. These reports substantiate potential of IL-8/IL-8R axis in cancer prognosis and provide strong evidence that it is the promising target pathway to overcome tumor progression and immunoresistance [67].

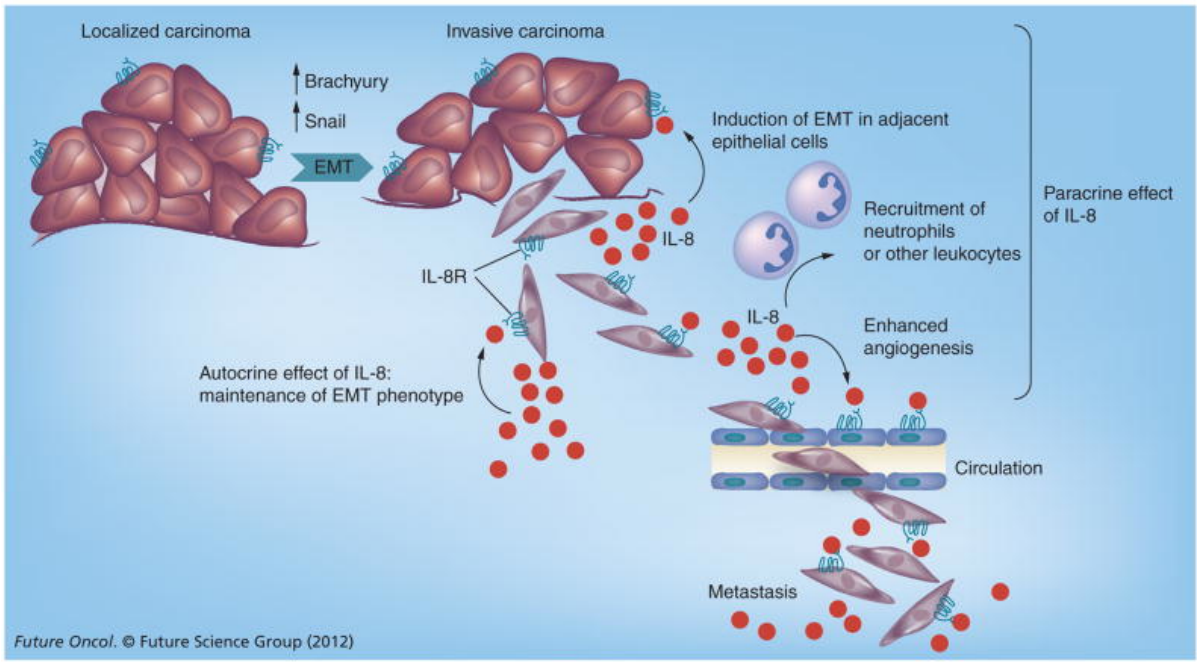

Fig. 10 Role of IL-8 in tumor progression. IL-8/IL-8R axis maintains mesenchymal status of cancer cells that undergone EMT. Moreover, high levels of IL-8 induce EMT of tumor adjacent epithelial cells and promote leukocyte chemotaxis. Extracted from [117].

1.4.6 IL-8 and intestinal epithelium

Epithelia establishment and maintenance of its architecture is essential in both early development and in adult physiology. Therefore, any deterioration in this carefully maintained structure might lead to a disease. Cytoskeletal network of actin-based microfilaments is crucial to maintain cellular polarity and contact of the neighbouring cells. Interactions between the intestinal epithelial cells (IECs) in the monolayer is mediated by specific junctions, which are regulated by epithelial genes like E-cadherin and keratin [118].

IL-8 is one of the first chemokines released by injured or inflamed epithelium and it is constitutively expressed by IECs [119]. Its inflammatory and chemotactic properties described previously participate in tumor microenvironment remodeling, by being one of the key regulators of the intestine architecture suggest for IL-8 to be markedly important.

Epithelial-mesenchymal transition (EMT) and reverse mesenchymal-epithelial transition (MET) are physiological processes, which are originally linked to embryogenesis and development (Type I EMT). In adult tissue, this differentiation program seems to be reinstated in wound healing and regeneration (Type II EMT) and in pathologies like cancer (Type III EMT). EMT causes a phenotypical switch of epithelial cells marked by a reduction of cell polarity, loss of contact growth inhibition or expression of epithelial markers such as E-cadherins, responsible for cell junction. In return, cells gain enhanced motility and invasiveness and greater resistance to cytotoxic agents [67, 117]. All these phenotypical changes are controlled by signaling pathways regulating transcription factors like zinc-finger proteins and secreted factors including IL-8 [67]. Interestingly, tumor cells that underwent EMT often produce the same cytokines and growth factors, which led to the process, maintaining protumorigenic microenviroment (Fig. 10) [117]. IL-8/CXCL8 was shown to promote EMT, activate stemness and anti-apoptotic processes, enabling cells to deceive cytotoxic immune cells [67, 103, 117].

1.5 The role of ERK3 in epithelial architecture

Transcription factor AP-2α (TFAP2A) is a key player in regulating gene expression in epithelial cells [120]. Among other factors, it regulates expression of E-cadherin and keratin 14, which are responsible for proper formation of cell junctions. Nothing is known so far about the mechanisms involved in TFAP2 regulation. Recent transcriptome analysis suggests that ERK3 regulates TFAP2A gene expression. It has been shown that ERK3 depletion leads to disturbance in epithelial architecture of human breast cancer cells: Knockdown cells were unable to maintain proper cell junction integrity and form flat epithelial monolayer. Interestingly, TFAP2A knockdown cells shared this phenotype with ERK3-depleted cells [121].

In *Xenopus laevis* embryos MET process was suggested to be regulated by ERK3 [121]. Knockdown of either ERK3 or TFAP2A in *X.laevis* embryos leads to kidney malformation. It was already reported that the same phenotype is exhibited by AP-2α knockout mice [122] and human patients with branchio-occulo-facial syndrome, caring mutations in TFAP2A gene [123]. Authors speculated that the ERK3-dependent and TFAP2A-mediated regulation of epithelial architecture might be involved in MTA during kidney development, but they do not narrow it down to just one organ, suggesting that abnormal epithelial architecture reported in this study might be associated with other developmental defects observed in ERK3 knockout mice [121].

Aim of the study

Mitogen-activated protein kinases (MAPKs) are a family of conserved enzymes with enormous potential in regulating all biological processes. Deregulation of MAPKs signaling is repeatedly reported to be associated with human diseases and over the years they have become a major drug targets. The main focus of the most influential studies are the canonical MAPKs, ERK1/2, p38 and JNK. Enormous effort was put into finding and defining new signaling modules within the MAPK family, which were further indicated as essential for regulation of physiological and pathological processes. Comparatively less is known about the members of the atypical subfamily of MAPKs such as an understudied ERK3. Most recent studies focused on dissecting a role of ERK3 in mediating tumorigenesis and this kinase has already been reported to contribute to tumor cells proliferation and migration, indicating prooncogenic potential of ERK3. The aim of this study was to assess biological role of ERK3 in the innate immune responses. Considering the role of innate immunity and its mediators in maintaining not only proper biological processes, but also its alteration in tumor progression, a full understanding of most potent regulatory mechanisms is of essence. To truly understand the biological role of ERK3, one of the major aims of this study is to crack the biochemistry of its regulation and its interaction with ERK4 and MK5. Main goal of the project was also to investigate a synergy between atypical ERK3 and other common regulators of the innate immune response like ERK1/2, p38 and NF-κB. Over the course of this study multiple loss-of-function experiments will be employed in order to assess role of ERK3 in regulation of human colonic epithelium. Different immune stimuli potency will be examined in modulating phosphorylation and expression of ERK3 and the role of LPS in its proteasomal degradation will be determined in both primary and malignant colonic epithelium. Role of kinase activity of ERK3 as well as significance of its protein abundance will be addressed in the regulation of CXCL8/IL-8. Impact of ERK3 depletion on TFs regulating IL-8 will be evaluated in LPS-dependent and independent manner. Physiological consequences of the implemented manipulations will be assessed by *in vitro* and *in vivo* epithelial-mediated leukocytes chemotaxis.

2. Materials and methods

2.1 Molecular Biology

2.1.1 Vectors and plasmid constructs

Vectors/plasmids:

pLenti4TO/V5-Dest (Invitrogen)
pcDNA3/V5-Dest40 (Addgene)
IL-8 promoter vector: PEZX-LvPG02 (Genecopoeia)
ERK3 wild type (ERK3 WT) in pDONR-223 (Human Kinase Library, Addgene)
ERK3 K49A K50A/pDONR-223
ERK3 WT/ pcDNA3-V5/Dest40
ERK3 K49A K50/pcDNA3/V5-Dest40

Lentiviral packaging plasmids:

HDM VSV-G → Addgene pHDMG
HDM Hgpm2 → Addgene pHDM-Hgpm2
HDM tat 1b → Addgene pHDM-tat1b
RC CMV-Rev → Addgene pRC/CMV-rev1b

Oligonucleotides/ mutagenesis primers:

ERK3 K49A K50A:	Frw_5' GCAATTGTCCTTACTGATCCCCAGAGTGTC,
	Rev_5' CGCGATGGCTACTCTTTTGTCACAGTC.
Sequencing primers:	ERK3 fix frw_5' CTGGATTTCCTGGAACAAATTTTGACAT
	ERK3 fix Rev_ 5' TGCTTCTCGACTAATTCCTG
	ERK3 frw_5' ATGGATGAGCCAATTTCAAG
	ERK3#3 frw_5' AAATGCTGACTGGTAAAACC

2.1.2 Site directed mutagenesis and preparation of expression constructs

To generate the ERK3 K49A K50A kinase dead mutant by site-directed mutagenesis, human full-length wild type ERK3 (ERK3 WT) in pDONR223 Gateway vector purified from Human Kinase Library (Addgene) was used as a template. Site directed mutagenesis was carried out using Q5 High-Fidelity DNA Polymerase (MO491, New England BioLabs) and the above mentioned mutagenesis primers. PCR setting and reaction mix are listed below:

Component	50µl reaction	PCR settings
5x Q5 Reaction Buffer	5 µl	Initial denaturation 98°C 1 min
10 mM dNTPs	1 µl	
100 mM Frw primer	0.5 µl	Denaturation 98°C 10 s
100 mM Rev primer	0.5 µl	Annealing 60°C 30 s
Template DNA	100 ng	Extension 72°C 9 min
Q5-High-FidelityDNA Polymerase	0.5µl	
RNase free water	to 50µl	Final extension 72°C 5 min

35 cycles

Component	10µl reaction
2x Ligation buffer	5µl
T4 Polynucleotide Kinase	1µl
T4 DNA Ligase	1µl
PCR product	1µl
RNase free water	to 10µl

The resulting PCR product was then ligated using T4 DNA Ligase (Cat# M0202, NEB) at 25°C for 4 h. To get rid of the non-mutated template the ligated product was digested with DpnI (Cat# R0176S, NEB) for 1 h at 37°C followed by 10 min at 70°C. The resulting plasmid was transformed into *Escherichia coli* as followed: 50 µl of competent DH5α cells were mixed with the DNA and incubated for 20 min on ice followed by the heat shock at 42°C for 90 s. 200 µl of SOC medium was added and samples were incubated for 1 h at 37°C with shaking at 700 rpm. Transformed bacteria were seeded on

Spectinomycin (Sigma) (for pDONR223 vector) containing Luria Bertani (LB) agar plates and incubated at 37°C overnight. Single colonies were then selected, inoculated in 2 ml of LB-medium and grown overnight at 37°C with shaking at 200 rpm. Plasmid DNA was purified using GeneJET-DNA purification kit (ThermoFisher) following manufacturer's instructions. Picked single clones were sequenced using the above-mentioned set of primers. The prepared ERK3 kinase dead construct as well as ERK3 WT was then cloned into the pLenti4TO-V5-Dest and pcDNA3-V5-Dest40 vectors using clonase (Gateway LR Clonase II Enzyme Mix Cat# 11791-020) according to the manufacturer's instructions.

2.1.3 Knock-down using shRNAs from the MISSION® shRNA Human Library

All shRNAs plasmids were purified from the MISSION® shRNA Human Library (Sigma).

shRNA sequences targeting ERK3
shERK3#1 TRCN0000001568, NM_002748.x-3734s1c1
CCGGGCTGTCCACGTACTTAATTTACTCGAGTAAATTAAGTACGTGGACAGCTTTTT
shERK3#2 TRCN0000001569, NM_002748.x-1564s1c1,
CCGGGACATGACTGAGCCACACAAACTCGAGTTTGTGTGGCTCAGTCATGTCTTTTT
shERK3#3 TRCN0000001570, NM_002748.x-798s1c1,
CCGGTGATCTGGGTTCTAGGTATATCTCGAGATATACCTAGAACCCAGATCATTTTT

shRNA sequences targeting MK5
shMK5#1 TRCN0000194823, NM_003668.2-475s1c1
CCGGCCCAAACATAGTTCAGATTATCTCGAGATAATCTGAACTATGTTTGGGTTTTTTG
shMK5#2 TRCN0000195129, NM_003668.2-319s1c1
CCGGCAGTATCAATTGGACTCAGAACTCGAGTTCTGAGTCCAATTGATACTGTTTTTTG
shMK5#5 TRCN0000000682, NM_003668.x-1622s1c1
CCGGGAAATTGTGAAGCAGGTGATACTCGAGTATCACCTGCTTCACAATTTCTTTTT

shRNA sequences targeting ERK4
shERK4#1 TRCN0000001374, NM_002747.x-3808s1c1
CCGGCTCACACCACACGCCTTAAATCTCGAGATTTAAGGCGTGTGGTGTGAGTTTTT
shERK4#2 TRCN0000001375, NM_002747.x-1105s1c1
CCGGACTACACCAAAGCCATCGACACTCGAGTGTCGATGGCTTTGGTGTAGTTTTTT

shERK4#4 TRCN0000001377, NM_002747.x-1331s1c1
CCGGAGTGAACAGTGAAGCCATCGACTCGAGTCGATGGCTTCACTGTTCACTTTTTT

The non-targeting control shRNA (shCo)
MISSION® pLKO.1 puro (Cat # SHC001)

2.1.4 Deletion of ERK3 by CRISPR/Cas

CRISPR/Cas constructs targeting ERK3 were designed by Manuel Kaulich (Goethe-University Frankfurt am Main, IBC2).

Three gRNA sequences targeting ERK3:
gRNA#1_ frw 5'CACCGAGCCAATTAACAGACGATGT
rv 5' AAACACATCGTCTGTTAATTGGCTC
gRNA#2_ frw 5'CACCGATACTTGTAACTACAAAACG
rv_5' AAACCGTTTTGTAGTTACAAGTATC
gRNA#3_ frw 5' CACCGCTGCTGTTAACCGATCCATG
rv 5' AAACCATGGATCGGTTAACAGCAGC
Vector control pLentiCRISPRv2.

2.1.5 siRNAs

The siRNAs directed against ERK3 and ERK4 were purchased from Qiagen.

siERK3#1 FlexiTube siRNA 5 nmol, siRNA Name: Hs_MAPK6_5, Cat# SI00606025
Sense strand: 5'- AGUUCAAUUUGAAAGGAAATT-3'
siERK3#2 FlexiTube siRNA 5 nmol, siRNA Name: Hs_MAPK6_6, Cat# SI00606032 (siRNA used only in Figure 4F)
siERK4#1 FlexiTube siRNA 5 nmol, siRNA Name: Hs_MAPK4_5, Cat# SI00606011
Sense strand: 5'-GGAUCGUUGAUCAGCAUUATT-3'
Negative control siRNA (siCo) Cat# 1027310

2.2 Cell biology

2.2.1 Cell lines

Cell line	Origin	Source
HT-29	Colon adenocarcinoma	ATCC HTB-38
HCPECs	Human Colonic Primary Epithelial cells	ATCC CRL-1790
MDA MB231	Breast carcinoma	DSMZ ACC 732
THP1	Acute monocytic leukemia cells	DSMZ ACC 16
Calu1	Lung cancer cells derived from metastatic site (pleura)	
293T	Embryonic kidney	Kind gift from Andreas Ernst lab (Goethe-University Frankfurt am Main, IBC2).
CaCo2	Colorectal adenocarcinoma	Kind gift from Monilola Olayioye lab (University of Stuttgart)
HeLa	Cervix adenocarcinoma	

2.2.2 Stimulations and treatments

LPS

Cells were seeded in 12-well plate at initial density of $2x10^5$ cells/well. Next day, when cells reached a confluence of 70-80%, medium was exchanged for serum free medium (HT-29) and MEM minus FBS, L-glutamine, sodium pyruvate (HCPECs). Cells were stimulated with 200 ng/ml lipopolysaccharide (LPS) (Cat# L6143, Sigma, 1 mg/ml) at indicated time points.

Human recombinant IL-1β was purchased from ImmunoTools (Cat# 11340013), cells were stimulated at 10 ng/µl working concentration for 0, 0.5 h, 1 h and 2 h.

Human recombinant TNFα was obtained from Corning (Cat# 354066) was used at a final concentration of 10 ng/ml to stimulate cells for 0, 0.5 h, 1 h and 2 h.

R848 TLR7/8 ligand (Cat# tlrl-r848) was purchased from InvivoGen and 2.5 µg/ml was used to stimulate HCPECs for 0, 0.5 h, 1 h and 2 h.

Cycloheximide (CHX) treatment

To investigate ERK3 protein half-life, cycloheximide (CHX) treatment was performed. Cells were seeded in 12-well plates at an initial density of $2x10^5$ cells/well. Next day medium was exchanged for serum free medium and protein biosynthesis was inhibited by treatment of cells with 100 µg/ml of CHX (Cat# C-7698, Sigma 100 mg/ml in DMSO) at indicated time points. If the LPS stimulation was included, cells were pre-treated for 1 h with 200 ng/ml of LPS prior CHX chase.

Inhibitors

To investigate the role of proteasome in the regulation of ERK3 protein degradation, MG-132 inhibitor (Callbiochem, Cat#474790, Merck Millipore) was used at 10 µM final concentration for 6 h.

The selective MEK1/2 inhibitor trametinib (GSK1120212, Cat#S2673, Selleckchem) was used at 1 μM working concentration for 1 h before LPS stimulation.

BRAF inhibitors PLX-4720 (Cat# S1152, Selleckchem) and GDC-0879 (Cat# S1104, Selleckchem) were used at a final concentration of 1 μM. Cells were pre-treated for 1 h prior LPS stimulation.

DMSO (Cat# A3672.0250, Applichem) was used as a solvent negative control for inhibitors treatments.

2.2.3 Transfections

2.2.3.1 siRNA

Cells were seeded one day before transfection at initial density of $2x10^5$ cells/well in 12-well plates or $3x10^5$ cells/well in 6-well plates. Cells were transfected using SAINT-sRNA transfection reagent (SR-2003, Synvolux) according to the manufacturer's instructions. Unless otherwise indicated, medium was exchanged 24 h post-transfection for medium without FBS and 48 h post–transfection supernatants were harvested. Collected supernatants were analysed by ELISA for IL-8 levels. Cells were analyzed by SDS-PAGE and real time-PCR for knockdown verification.

2.2.3.2 Generation of stable cells lines

Lentiviral supernatants were produced in 293T cells by co-transfection of the cells with lentiviral packaging plasmids (0.3 μg each), lentiviral expression constructs (1 μg) and 10,8 μl of 10 mM polyethylenimine (PEI). The virus particles were harvested after 48 h and sterile-filtered. HT-29, Calu1, CaCo2, MDA MB231, HeLa cells were infected with the respective lentiviral particles in the presence of 10 μg/ml of polybrene (10 mg/ml, sc-134220, Santa Cruz). Cells were then selected with puromycin (Cat# 0240.3, Carl Roth) at following concentrations: 3 μg/ml (MDA MB231, Calu1, CaCo2, HeLa), 8 μg/ml for HT-29, until a stable knockdown was achieved. For complementation assays, empty vector control (pLenti4TO/V5-Dest), WT or kinase dead (K49A K50A) mutant of ERK3 were reintroduced into shERK3 (3'UTR) background (shERK3#1) by lentiviral particle

transduction. Cells were double-selected with zeocin (100 µg/ml) (Cat # R25001, Invitrogen).

To generate CRISPR/Cas mediated ERK3 knockout in HT-29 cell line, cells were infected with lentiviral particles and selected with puromycin (30 µg/ml). Lentiviral particle containing supernatants for CRISPR ERK3 (CrispR ERK3) and CrispR control vector (pLentiCRISPRv2) (Crispr Co) were produced in 293T cells by co-transfection of lentiviral packaging plasmids (0.3 µg each) and 1.1µg of lentiviral vector containing the respective gRNAs in the presence of 21 µl of Lipofectamine2000 (Cat# 11668027, ThermoFisher).

2.2.3.3 Transient plasmid transfections

HeLa cells stably transfected with shRNA targeting ERK3 at the 3' untranslated region (3'UTR) (shERK3#1) or with control empty vector shRNA (shCo) were further transiently transfected with either an empty pcDNA3/V5-Dest40 vector (EV), ERK3 WT or ERK3 K49A K50A mutant construct (0.5 µg plasmid) in the presence of Lipofectamine2000 (ThermoFisher) (3 µl/well). Six hours post-transfection medium was exchanged for DMEM+FBS complete medium. Twenty-four hours post-transfection medium was exchanged again for DMEM–FBS medium. Forty-eight hours post-transfection supernatants were harvested for subsequent IL-8 ELISA. Cells were analysed by Western Blot

2.2.3.4 CXCL8/IL-8 Promoter Luciferase Reporter Assay

The CXCL8-Gaussia Luciferase GLuc-ON promoter reporter clone was purchased from Genecopoeia (HPRM15772) as a lentiviral expression construct along with the negative control plasmid (PEZX-LvPG02) with non-promoter sequence. MDA MB231 cells were infected with lentiviral supernatant produced in 293T cells as described before (section 2.2.3.2, polybrene) and selected with puromycin (3 µg/ml). Afterwards, stably transduced cells were transiently transfected with siCo or siRNA targeting ERK3. Twenty-four hours post-transfection medium was exchanged for serum free medium and cells were cultured for 24 h. Supernatants were harvested and IL-8 promoter activity was assessed by measurement of secreted Gaussia luciferase activity, using Secrete-Pair Gaussia Luciferase Assay Kit (Cat# SPGA-G) and GL-H buffer with GL

substrate according to the user manual. Relative Luminescence Units (RLU) were measured (integration 1 s). For quantification, RLU values of negative control were subtracted from IL-8 promoter expressing samples and presented as fold change of siERK3 RLU normalized to siCo samples.

2.3 Biochemical methods

2.3.1 Enzyme-linked Immunosorbent Assay (ELISA)

The concentration of secreted IL-8 was measured by ELISA. The assay was performed according to manufacturer's instructions (eBioscience, Human IL-8 ELISA Ready-SET-Go! Kit Cat# 88-8086).

2.3.2 Western Blotting

Cells were washed with ice-cold phosphate buffered saline (PBS) (10 mM sodium phosphate, 150 mM NaCl, pH 7.2) and lysed in cold RIPA lysis buffer: 250mM NaCl, 50mM Tris (pH 7.5), 10% Glycerin, 1% Triton X-100), supplemented with protease inhibitor cocktail set I-Calbiochem 1:100 (Cat# 539131, Merck Millipore) and phosphatase inhibtors: 1 mM sodium ortovanadate (Na_3VO_4) and 1 mM sodium fluoride (NaF). Cells were lysed for 30 min on ice, followed by 10 min centrifugation at 14000 rpm. Protein concentrations were determined using 660 nm Protein Assay (Cat# 22660, ThermoFisher). Samples were prepared by mixing with 4 x SDS-page sample buffer (277,8 mM Tris-HCl pH 6.8; 44.4% Glycerol, 4.4% SDS, 0.02% bromophenol blue) containing 50 mM DTT per 1 ml. Samples were boiled at 95°C for 5 min and subjected to 7.5-10% SDS-PAGE followed by transfer of the proteins onto nitrocellulose membranes (GE Healthcare, Chalfont St Giles, UK). Membranes were blocked in 3% BSA/PBST (1x PBS, pH 7.2 containing 0.05% Tween-20) for 1 h at room temperature. Membranes were then washed 3 x 5 min with PBST and incubated overnight with the respective primary antibody diluted in PBST at 4°C. Following 3 x 5 min washing with PBST, membranes were incubated with HRP-conjugated secondary antibody for 1 h at room temperature. After washing, the signal was visualized using chemiluminescent HRP substrate (Immobilon Western, WBKLS0500, Merck Millipore). For semi-quantification, signal intensities were analyzed by ImageJ software.

2.3.3 Immunoprecipitation (IP)

Endogenous ubiquitination of ERK3 protein

For immunoprecipitation of endogenous ERK3, HT-29 and HCPECs cells were seeded in 10 cm dishes at an initial density of $2x10^6$ cells per dish. Next day, medium was exchanged for medium without FBS and supplements and cells were treated with MG-132 inhibitor for 6 h prior to LPS (200 ng/ml) stimulation for 0 or 4 h. Afterwards, medium was aspirated, cells were washed with ice-cold PBS and lysed with ice cold IP buffer (10 mM HEPES pH 7.4; 150 mM NaCl, 1% Triton X-100, plus protease inhibitor cocktail set I-Calbiochem 1:100 (Cat# 539131, Merck Millipore), 1 mM Na_3VO_4 and 1mM NaF. After 30 min on ice, samples were centrifuged at 15000 rpm for 10 min, followed by protein concentration measurement using the 660 nm Protein Assay (Cat# 22660, ThermoFisher). Antibody-protein complexes were precipitated by Protein A/G-Agarose beads (Cat# 11 134 515 001/ 11 243 233 001, Roche). Beads were washed twice with 200 µl of IP buffer and between 200 and 500 µg of total protein containing lysates were added along with the ERK3 antibody. The mixture was incubated for 2 h at 4°C while rotating. After the incubation, beads were washed three times with 500 µl of IP buffer, centrifuged each time for 30 s at 1000 rpm, sample buffer was added and samples were boiled for 5 min at 95°C.

Pull down of endogenous c-Jun

HT-29 cells were stimulated with LPS (200 ng/ml) for 4 h in medium without FBS. After the stimulation, cells were washed with ice-cold PBS and lysed with ice cold IP buffer (10 mM HEPES pH 7,4; 150 mM NaCl, 1% Triton X-100, plus protease inhibitor cocktail Set I-Calbiochem 1:100 (Cat# 539131, Merck Millipore), 1 mM Na_3VO_4 and 1mM NaF. After 30 min on ice, samples were centrifuged at 14000 rpm for 10 min. Protein A/G-Agarose beads (Cat# 11 134 515 001/ 11 243 233 001, Roche), lysates and c-Jun antibody were incubated for 2 h at 4°C with rotating. After the incubation beads were washed with IP buffer and analysed by immunoblot.

2.3.4 Antibodies

Antibody	Type	Source and Catalog number
Anti-phospho-ERK3 (pSer189)	Primary	Sigma #SAB4504175
Anti-ERK3	Primary	Cell Signaling Technology #4067
Anti-MK5/MAPKAPK5	Primary	Cell Signaling Technology #7419
anti-c-Jun (60A8)	Primary	Cell Signaling Technology #9165
Anti-V5-Tag	Primary	Cell Signaling Technology #13202
Anti-p44/42 MAPK (ERK1/2)	Primary	Cell Signaling Technology # 9102
Anti-phospho-p44/42 MAPK (Thr202/Tyr204)	Primary	Cell Signaling Technology #9101L
Anti-phosphor-p38 MAPK (Thr180/Tyr182)	Primary	Cell Signaling Technology #9215
Anti-p38 MAPK	Primary	Cell Signaling Technology #9212
Anti-I kappa B α	Primary	Cell Signaling Technology #4812
Anti-phospho-SAPK/JNK (183/Y185)	Primary	Cell Signaling Technology #9251
Anti-phospho-MEK1/2 (Ser217/221)	Primary	Cell Signaling Technology # 9154

Anti-MEK1	Primary	Cell Signaling Technology #2352
Normal Rabbit IgG	Primary	Cell Signaling Technology #2729
Anti-ERK4	Primary	Abcam, ab211501
Anti-phospho-MK5 (phospho T182)	Primary	Abcam, ab138668
Anti-β-actin	HRP conjugated	Abcam, ab49900
Mono-and poly-ubiqutin	HRP-conjugated	Enzo #BML-PW8810-0100
Anti-GAPDH antibody	Primary	GeneTex, GTX627408
Anti-alpha tubulin	Primary	GeneTex, GTX628802
(HRP)-conjugated secondary for rabbit IgG	Secondary	Novex, A16096
(HRP)-conjugated secondary for rabbit IgG	Secondary	ThermoFisher Scientiffic, #32460

2.4 *In vitro* and *in vivo* migration assays

2.4.1 Isolation of Human Neutrophils

Neutrophils were prepared from heparinized peripheral blood obtained from healthy volunteers. For dextran sedimentation blood was mixed at a 1:1 ratio with 3% dextran 500 (Cat# 9219.1, Carl Roth) in 0.9% NaCl, in 1:1 ratio (7.5 ml blood in 7.5 ml dextran solution) by gentle inverting prior to 20-30 min incubation at room temperature. The layers containing neutrophils were harvested; 6 ml of leukocyte-rich layer was gently pipetted onto 7.5 ml of Histopaque-1077 (Cat# 10771, Sigma) and low-density gradient

centrifugation was performed at 1700 rpm at room temperature for 30 min. Supernatants were then removed and pellets were gently resuspended in 7.5 ml of ACK lysing buffer, samples were incubated for 10 min at room temperature protected from light, followed by 2 min centrifugation at 1700 rpm. To maintain clean populations of leukocytes with no residual erythrocytes, samples were washed with phosphate buffered saline (PBS), pH 7,2. Neutrophils cell pellets were resuspended in Minimum Essential Media (MEM), viability and cell number was assessed using trypan blue (Cat# 1450021, Bio-Rad) and Neubauer chamber.

2.4.2 Neutrophils and THP1 *in vitro* chemotaxis -Transwell migration Assay

To test the effects of the ERK3-dependent IL-8 production in HCPECs/HT-29 cells, chemokine-containing supernatants were used in Transwell migration assays and effects on the chemotaxis of neutrophils and THP1 cells were assessed. Transwell plate with 6.5 mm diameter polycarbonate membranes, with 5.0 µm (neutrophils)/ 8 µm (THP1) pore size (Cat# 3421/3422 respectively, Corning) were used. In the lower chamber of the Transwell plate HCPECs were seeded and transiently infected with either a control vector (shCo) or shRNA targeting ERK3. After the migration, HCPECs seeded in the lower chamber were lysed and subjected to Western Blot analysis in order to assess the knockdown efficiency. Alternatively, supernatants obtained from HCPECs transfected with either a negative control shRNA (shCo)/siRNA (siCo) or shRNA/siRNA targeting ERK3 were placed in the lower chamber. Freshly isolated neutrophils obtained from peripheral blood of healthy volunteers were pre-stained with 5 µM CellTracker Green CMFDA (Cat# C7025, Thermo Fisher) for 15 min prior migration, followed by 30 min stimulation with LPS (200 ng/ml). Neutrophils were added to the inserts (5 µm pore size) at a final concentration of $3x10^5$cells per insert. To assess chemotaxis of THP1 cells, HT-29 cells carrying a stable knockdown of ERK3 or empty vector control cells (shCo) were seeded into the lower chamber. Alternatively, supernatants obtained from genetically modified HCPECs (control vector (shCo)/negative control siRNA (siCo) or shRNA/siRNA targeting ERK3) were used. THP1 cells were counted and stained with 5 µM of CellTracker Green CMFDA for 15 min, cells were then resuspended in 200 µl of RPMI medium with no FBS and $1.2x10^5$ cell was added into each insert (8 µm pore size). To determine the role of IL-8 in the observed chemotaxis, human CXCL8/IL-8 neutralizing antibody (R&D, MAB208) was used in the lower compartment at a

concentration of 2.8 ng/µl. Following 2 h incubation at 37°C, migration of neutrophils or THP1 to the lower chambers was measured using fluorescence (excitation wavelength 480 nm, emission wavelength 535 nm). Fold change of Relative Fluorescence Units (RFU) was then calculated for each condition. Medium control was incorporated into each experiment to determine background rate RFU, which were then subtracted from all the tested conditions.

2.4.3 *In vivo* studies of murine leukocytes chemotaxis

To assess physiological impact of ERK3-depletion from human intestine epithelial cells (HCPECs) *in vivo* chemotaxis experiments were performed. All animal experiments were approved by local authorities and conducted according to the German Animal Protection Law.

Mice

Eight-week-old female C57BL/6J mice were purchased from Janvier Labs.

Supernatants production: HCPECs were seeded in 6-well plate at initial density of $3x10^5$ cells/well. After 24 h cells were transfected with either a negative control siRNA (siCo) or siRNA specific to ERK3 (siERK3) in the presence of Saint-sRNA transfection reagent. Twenty-eight hours post-transfection medium was exchanged for 10 ml of MEM without FBS, L-glutamine and sodium pyruvate. After 24 h supernatants were harvested for HCPECs siCo/siERK3. Collected supernatants were further concentrated using Amicon Ultra-15 Centrifugal Filter (3 kDa, UFC900324, Merck Millipore) and IL-8 concentration was determined by ELISA.

Intraperitoneal injections: Groups of 5 eight-week-old C57BL/6J female mice were injected intraperitoneally (i.p) with one of the following: 1 ml of MEM without any supplements (MEM control), 1 ml of MEM containing 900 ng of Human Recombinant CXCL8/IL-8 (Peprotech, 200-08) (rhCXCL8/IL-8), 1 ml of HCPECs siCo concentrated supernatant (siCo supernatant) or 1 ml of HCPECs siERK3 concentrated supernatant (siERK3 supernatant). Four hours post-injections mice were sacrificed and peritoneal white blood cells populations were harvested by peritoneal lavage with 10 ml of cold PBS pH 7,2, supplemented with 1% heat-inactivated FBS. Cell suspensions were

centrifuged at 1300 rpm for 5 min. Pellets were resuspended in 100 µl of PBS and transfered into 1.5 ml Eppendorf tube. Absolute cell number per mm^3 was measured with scil Vet abc hematology counter.

2.5 RNA isolation, cDNA synthesis and real-time-PCR analyses

For gene expression analysis, cells were washed with cold PBS and total RNA was extracted using Trizol (Cat# 15596018, Ambion) according to the manufacturer's instructions. Quality of the RNA was evaluated by NanoDrop (ThermoFisher): absorbance at 260/280 was measured and samples within range of 2.0±0.3 were used. Isolated RNA (500 ng) was then used as a template for cDNA synthesis with the RevertAid First Strand cDNA synthesis kit using random hexamer primers (Cat# K1621, ThemroFisher Scientific) according to the supplier's protocol.
Real-time PCR was performed using EvaGreen qPCR master mix (5 x Hot Start Taq EvaGreen® qPCR Mix (No ROX), Cat# 27490, Axon) and following primers:

ERK3 Frw_5' ATGGATGAGCCAATTTCAAG, Rv_5' CTGACAATCATGATACCTTTCC;
ERK4 Frw_5'AAGGGTTATCTGTCAGAAGG, Rv_5' CTTTGGTGTAGTTATTGGGG;
IL-8 Frw_5' GAGCACTCCATAAGGCACAAA, Rv_5' ATGGTTCCTTCCGGTGGT,
IL-8 #3 Frw_5' TGTAAACATGACTTCCAAGC, Rv_5' AAAACTGCACCTTCACAC;
IL-16 Frw_5' CAGTGTTAATCCCTATTGCAC, Rv_5' ATTGTTGAGAGAGGGACTTC;
CXCL6 Frw_5' CCTCTCTTGACCACTATGAG, Rv_5' GTTTTGGGGTTTACTCTCAG.

The housekeeping genes 18s or GAPDH were used for normalization:

18s Frw_5' AGAAACGGCTACCACATCCA, Rv_5' CACCAGACTTGCCCTCCA;
GAPDH Frw_5' CGACAGTCAGCCGCATCTT, Rv_5' CCCCATGGTGTCTGAGCG.

Relative expression levels were calculated as ΔΔCt.

2.6 Secretome analysis and TF arrays

2.6.1 Secretome analysis

HCPECs were seeded in 12-well plates at an initial density of $2x10^5$ cells/well. Twenty-

four hours later, cells were transiently transfected with either control siRNA (siCo) or siRNA targeting ERK3 (siERK3). Forty-eight hours post-transfection medium was exchanged for MEM–FBS and other supplements. Twenty-four hours later supernatants were harvested from each well for secretome analysis. Cells were lysed in RIPA buffer and total protein concentrations were measured using 660 nm Protein Assay (Cat# 22660, ThermoFisher Scientific). Cells were subjected for immunoblot analysis to determine knockdown efficiency.

Antibody Array

The RayBiotech human L-Series biotin-based antibody array was purchased from Tebu-Bio and performed according to the manufacturer's instructions. Briefly, supernatants were dialyzed prior biotin labeling. Labeled proteins were then incubated on blocked glass slides at room temperature. Two slides were provided: L-507 and L-493 coated with 507 and 493 different capture antibodies, respectively. Array slides were subsequently washed and fluorescence (Cy3) label-conjugated Streptavidin was added. Slides were then dried and send for fluorescence detection and analysis by RayBio. Normalized data were then further analyzed for specific targets. Either fold change in signal intensity was calculated between siERK3 and siCo samples or relative amount in µg/ml of each secreted factor was determined by dividing normalized fluorescence signals by total protein concentrations measured in total cell lysates.

2.6.2 TF Activation Arrays

TF Activation Profiling Plate Array-I

HCPECs were seeded in 10 cm dishes at an initial density of $2x10^6$ cells. After 24 h cells were transfected with either negative control siRNA (siCo) or siRNA targeting ERK3, using Saint-sRNA transfection reagent according to the manufacturer's instructions. Twenty-four hours post-transfection medium was exchanged for MEM minus FBS and other supplements and cells were stimulated with LPS (200 ng/ml) for 0 or 24 h. After stimulation part of the cells was lysed in RIPA buffer for further Western Blot analysis and knockdown verification. Residual cells were subjected to nuclear extraction according to instructions provided with Nuclear Extraction Kit (Cat# SK-0001, Signosis, Inc.).

TFs profiling array was performed following the instructions in the user manual provided by the manufacturer (Signosis, Inc.). Briefly, 5 µg of nuclear extract was incubated with biotin-labeled probes. TF/probe complexes were then purified from the unbound probes and hybridized with the plate pre-coated with complementary sequences for each probe. Captured DNA probes were then incubated with Streptavidin-HRP conjugate, followed by substrate solution. Luminescence was measured (integration time 1s) and Relative Luminescence Units (RLU) are presented.

Transcription factor Filter Plate Assay

HCPECs were seeded in 6-well plates at initial density of $3x10^5$ cells per well. After 24 h cells were transfected with either negative control siRNA (siCo) or siRNA targeting ERK3, using Saint-siRNA transfection reagent. Twenty-four hours post-transfection cells were stimulated with LPS (200 ng/ml) for 24 h in medium without any supplements.

Control (CrispR Co/shCo) and ERK3 knockout (CrispR ERK3) or knockdown (shERK3) HT-29 cells were seeded in 6-well plates. Once the cells reach 70%-80% confluence, medium was exchanged to FBS-free medium and cells were stimulated with LPS (200 ng/ml) for 24 h.

After stimulation, cells were subjected to nuclear extraction according to instructions provided with Nuclear Extraction Kit (Cat# SK-0001, Signosis and nuclear extracts were subjected to Filter Plate Assay (#FA-0004, Signosis).

Assay was performed according to the manufacturer's instructions. Briefly, nuclear extracts were incubated with biotin labelled AP-1/CREB DNA binding sequences in order to allow TF-DNA complex formation. AP-1/CREB bound probes were then retained with the filter plate. Pre-labeled AP-1/CREB probes were eluted from the filter, followed by hybridization to 96-well hybridization plate. Captured AP-1/CREB probes were further detected with streptavidin-HRP and luminescence was measured as Relative lights Units (RLU). Data for single biological replicate are presented as RLU and for three biological replicates, fold change in RLU was calculated in respect to the control cells.

2.7 Immunofluorescence

Control (shCo) and ERK3 knockdown (shERK3) HT-29 cells were seeded in 6-well plates on coverslips. Next day, medium was exchanged to FBS-free medium and cells were stimulated with LPS (200 ng/ml) for 1.5 h. After the treatment, cells were fixed in 3.7% formaldehyde (Roth) for 15 min, followed by washing with PBS and 3 min permeabilisation using 0.1% Triton X-100 (AppliChem). After washing twice with PBS, cells were blocked with 1% BSA (Sigma) in PBS for 15 min and washed once with PBS. Staining was performed with anti-ERK3 antibody (MAB3196, R&D) (dilution 1:400) and anti-c-Jun (60A8) (#9165, Cell Signaling) antibody in blocking solution for 1 h at RT. Afterwards, cells were washed with PBS and incubated with secondary antibodies: anti-rabbit IgG-Alexa 488 (A11008, ThermoFisher), secondary anti-mouse IgG-Cyanine3 (A10521, ThermoFisher) at 5 µg/ml and Hoechst at 10 µg/ml in blocking solution for 1 h at RT in the dark. Samples were washed twice with PBS and cells were mounted onto glass slides using Moviol (+DABCO) (Sigma). Cells were imaged using a Leica SP8 confocal microscope (63X, oil immersion objective).

2.8 RNA sequencing and bioinformatic analyses

For transcriptome analysis three biological replicates of HCPEC were seeded in 12-well plates at initial density of $2x10^5$ cells/well. Twenty-four hours later cells were transiently transfected with either control siRNA (siCo) or siRNA targeting ERK3 (siERK3). Twenty-four hours post-transfection medium was exchanged for MEM-FBS and other supplements and cells were stimulated with LPS (200 ng/ml) for 24 h. After the stimulation cells were washed with cold PBS and lysed with Trizol (Cat# 15596018, Ambion) according to the manufacturer's instructions. Total RNA was quantified by a Qubit 2.0 fluorometer (Invitrogen). Quality was assessed using Agilent's bioanalyzer 2100 and a RNA 6000 Nano chip (Agilent). Samples with RNA integrity number (RIN) > 8 were further subjected to RNA library preparation. Barcoded cDNA libraries were prepared from 300 ng of total RNA using the NEBnext Poly(A) mRNA Magnetic Isolation Module and NEBNext Ultra RNA Library Prep Kit for Illumina (NEB) according to the provided instruction. Library quantity was assessed on a Qubit 2.0 fluorometer using Invitrogen's Qubit HS assay kit. Library size was determined using Agilent's Bioanalyzer 2100 and a HS DNA assay chip. Barcoded RNA-Seq libraries were onboard clustered

using HiSeq Rapid SR Cluster Kit v2 using 8pM and 59 bps were sequenced on an Illumina HiSeq2500 using a HiSeq Rapid SBS kit v2. Quality control on the sequencing data (59 base pairs, single end) was performed with the FastQC tool (available at http://www.bioinformatics.babraham.ac.uk/projects/fastqc/), as well as the comprehensive Qorts suite. By inspecting the produced reports, all samples were deemed of good quality and were further processed. Short reads alignment was performed with the ENSEMBL Homo_sapiens. GRCh38 was chosen as the reference genome. The corresponding annotation (ENSEMBL v79) was retrieved from the ENSEMBL FTP website (http://www.ensembl.org/info/data/ftp/index.html). The STAR aligner (version 2.4.0b) was used to perform mapping to the reference genome [124]. Subsequent analyses were performed with R statistical software (version 3.5.0), leveraging core packages of the Bioconductor project. Alignments were processed with the "featureCounts" function of the Rsubread package, using the annotation file also used for supporting the alignment. Exploratory data analysis and functional annotation to Gene Ontology terms was performed with the pcaExplorer package (version 2.6.0, Marini and Binder 2018: pcaExplorer: an R/Bioconductor package for interacting with RNA-seq principal components. BioRxiv. https://doi.org/10.1101/493551). Differential expression analysis was performed with the DESeq2 package (version 1.20.0), limiting the false discovery rate to 0.05 [125]. The apeglm (package version 1.2.1) shrinkage estimator was used to calculate the effect size for the contrasts of interest [126]. MA-plots were generated with the ideal package (version 1.4.0). Log2FC profiles for the different contrasts were plotted as heatmaps with the pheatmap package (version 1.0.12). Intersections between different sets are displayed in Venn diagrams, generated with the gplots package (version 3.0.1). Expression plots for selected genes display the individual values for the normalized counts, with a bar to show the median in each group.

2.9 Appendix-material

Chemicals

Acrylamide/Bis solution 40%	Bio Rad
APS	Applichem
Bromophenol blue	Roth
DTT	MP biomedicals
Ethanol	Roth
HEPES	Roth
Hydrochloric acid (HCl)	Roth
Glycerol	Applichem
Glycine	Applichem
Protease inhibitor cocktail	Calbiochem, Merck Millipore
SDS sodium chloride (NaCl)	Roth
Sodium orthovanadate (NaVO3)	Sigma
Sodium fluoride (NaF)	Sigma
Sodium hydroxide (NaOH)	Riedel-de-Haën
T-EDTA	Sigma
Temed	Sigma
Tris-base	Applichem
Trypsin/EDTA	Sigma

Triton X-100	Applichem

All the other chemicals, buffers and reagents used are described in the respective method section.

3. Results

3.1 LPS-mediated regulation of ERK3 expression

3.1.1 LPS stimulation leads to upregulation of ERK3 protein expression in HT-29 cells

Human intestinal epithelium remains in constant contact with bacteria-derived microbial products. Component of the Gram-negative bacteria cell wall-lipopolysaccharide (LPS) is one of the most potent stimuli of the innate immune response [127, 128]. The role of classical MAPKs in the PAMPs-mediated inflammatory response is very well established and was described in the introduction. To investigate the role of atypical MAPK ERK3 in the LPS–mediated TLR4 cascade, HT-29 colon adenocarcinoma cells were stimulated with 200 ng/ml LPS at indicated time points **(Figure 3.1)**. ERK3 phosphorylation at S189 as well as the total protein levels were determined by Western Blot analysis **(Figure 3.1 A)** and quantified using imageJ software **(Figure 3.1 B)**. These data revealed that LPS stimulation subsequently enhances ERK3 phosphorylation at S189 as well as its total protein levels. Further, expression levels of ERK3 mRNA were determined with quantitative RT-PCR **(Figure 3.1 C)** with no significant increase detected. These findings suggested that LPS might have a stabilizing effect on ERK3 protein. Thus, cycloheximide (CHX) chase experiments were performed in the presence or absence of LPS and ERK3 half-life was determined under both conditions. Results confirmed a very short half-life of the protein, ranging between 30 and 60 min, which increased to around 2 h after stimulation with LPS **(Figure 3.1 D and E)**. In conclusion, LPS did not lead to a significant increase in the mRNA levels of ERK3 and CHX chase experiments confirmed that LPS triggered an increase in the half-life of ERK3 protein.

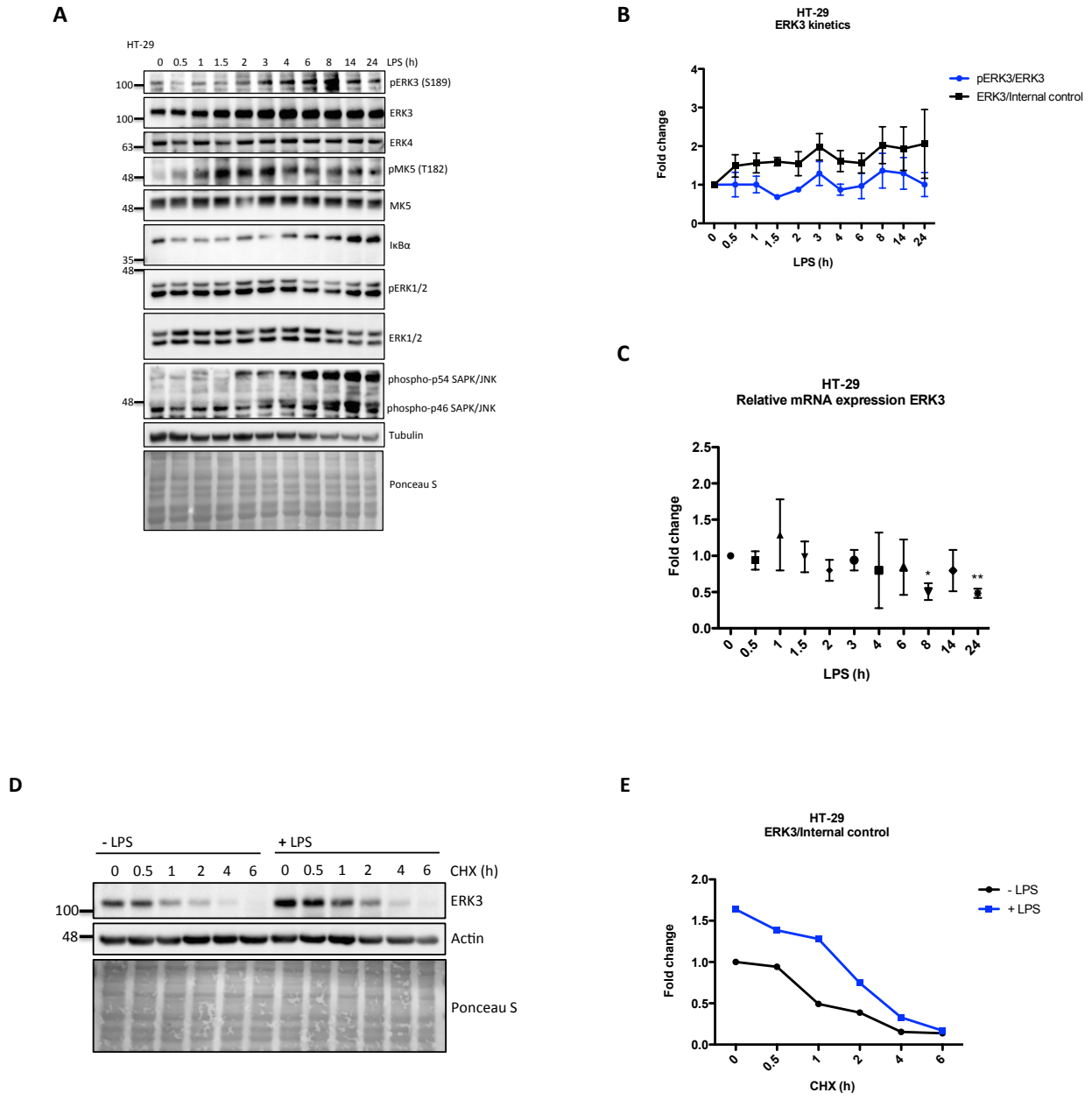

Figure 3.1 LPS stimulation of HT-29 cells leads to upregulation of ERK3 protein. (A). Representative Western Blot analysis of HT-29 cells. Phosphorylation and/or total protein levels of ERK3, MK5, JNK, ERK1/2, ERK4 and IkBα were monitored, α-tubulin and Ponceau S staining were used as an internal control. **(B)** Changes in expression and phosphorylation of ERK3 are shown as a fold change after normalization to the levels of internal loading control (tubulin or actin). Each time point was normalized with respect to time point 0 (unstimulated cells). Data are a representative of at least three independent experiments with similar results. Fold change values are represented as mean ± SEM (n=3). **p<0.01, ***p<0.001; paired t-test. **(C)** Quantitative RT-PCR of ERK3. Each biological replicate was measured in triplicates. Log2 fold change in gene expression is presented as mean ± SEM of three independent experiments. *p<0.05, **p<0.01, ***p<0.001, paired t-test. **(D)** ERK3 protein stability in the presence and absence of LPS. HT-29 cells were divided into two sets, one was pre-stimulated with LPS for 30 min. After

the pre-stimulation, both sets of cells were subjected to CHX chase for 0 h, 0.5 h, 1 h, 2 h, 4 h and 6 h. Western Blot analysis was performed. Fold change in **(E)** ERK3 expression in respect to untreated (0 h) cells. Ratios of ERK3 and internal control (Ponceau S) are presented.

3.1.2 LPS stimulation of Human Colonic Primary Epithelial Cells (HCPECs) leads to a decrease in ERK3 protein expression

Due to the interesting observations of LPS-dependent ERK3 regulation in HT-29 colon cancer cells, HCPECs (Human Colonic Primary Epithelial cells) were tested. In contrast to HT-29 cells, LPS stimulation attenuated ERK3 expression in those cells **(Figure 3.2 A-B)**. Interestingly, a stimulating effect of LPS was observed on p38, ERK1/2 and MK5 activity **(Figure 3.2 A).** ERK3 mRNA expression levels were monitored, but no significant downregulating effect was detected on ERK3 transcript levels upon LPS stimulation **(Figure 3.2 C)**. CHX chase was performed like in case of HT-29 cells and ERK3 half-life was determined in HCPECs **(Figure 3.2 D and E)**. Results further confirmed the labile nature of ERK3 protein, but the effect of LPS on the ERK3 stability in those cells was not assessed as ERK3 protein levels are reduced upon LPS stimulation **(Figure 3.2 A and B)**. Taken together, these results indicate that LPS regulates ERK3 protein levels rather than its transcription.

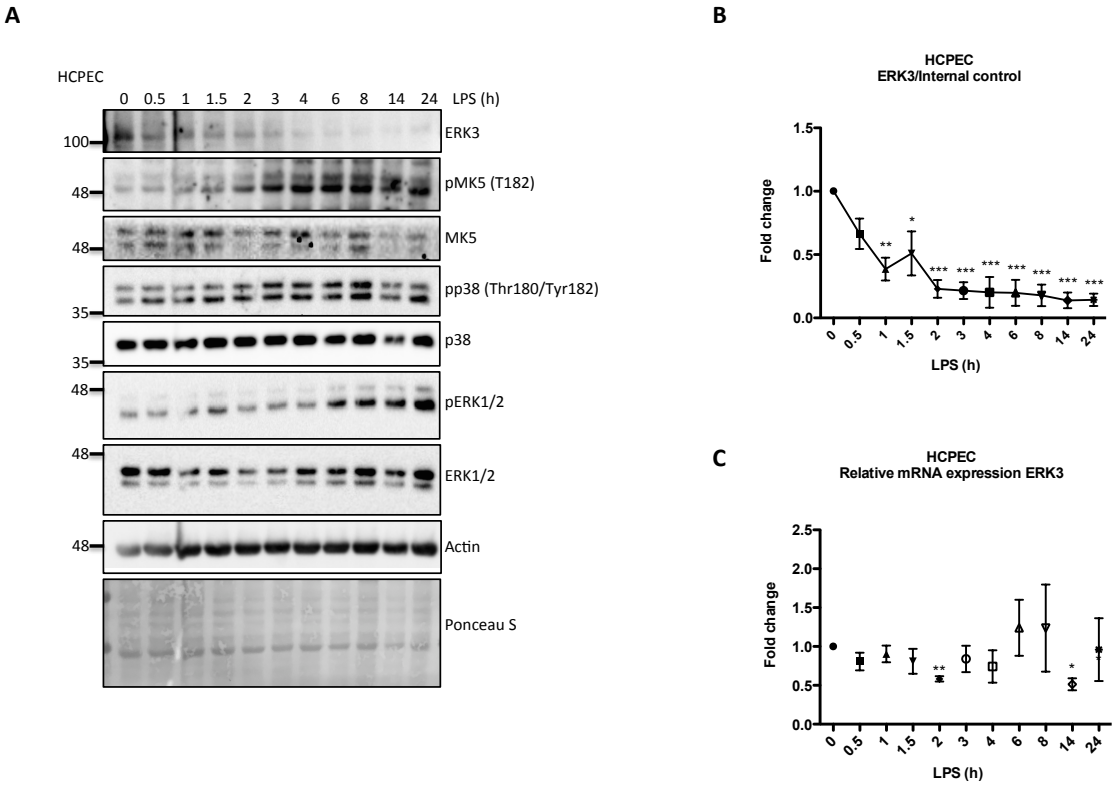

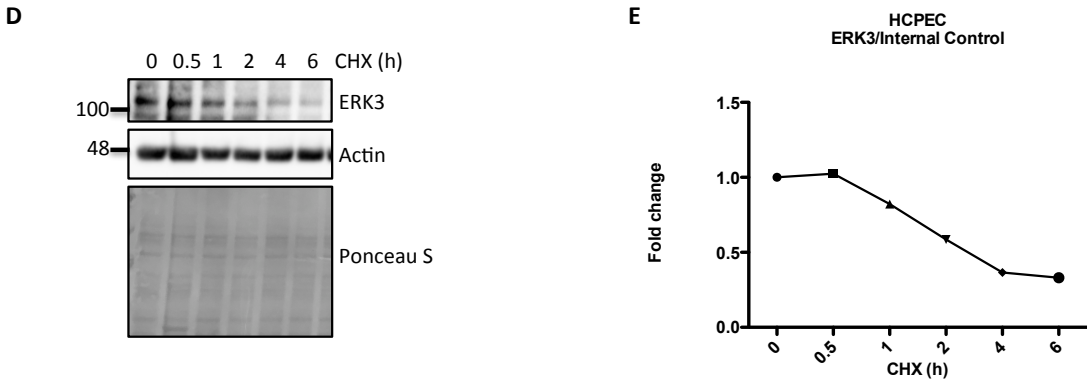

Figure 3.2 LPS leads to a decrease in ERK3 protein expression in HCPECs (A) HCPECs were stimulated with LPS at indicated time points and analyzed by immunoblot for the expression and/or phosphorylation levels of ERK3, ERK4, MK5, ERK1/2 and p38. β-actin and Ponceau S staining were used as a loading control. **(B)** Shown here are fold changes in expression levels of ERK3 protein. Results are shown as mean ± SEM fold change after normalization with the levels of an internal loading control gene expression (tubulin or actin). Each time point was normalized with respect to time point 0 (unstimulated HCPECs). Data are a representative of three independent experiments with similar results (n=3); ** p<0.01, ***p<0.001; paired t-test. **(C)** Quantitative RT-PCR of ERK3 mRNA expression levels. Log2 fold change in gene expression is presented as mean ± SEM of three independent experiments (n=3); *p<0.05, **p<0.01, paired t-test. **(D-E)** Data present ERK3 protein stability in HCPECs. Cells were treated with CHX at indicated time points and were subjected to immunobloting analysis. ERK3 protein levels were monitored and actin was used as a loading control for normalization. Fold change in comparison to untreated control cells is presented.

3.2 ERK3 as a novel regulator of IL-8

3.2.1 ERK3 regulates IL-8 transcription in HCPECs

Results so far revealed that upon LPS treatment ERK3 expression was decreased in HCPECs cells, while all the other tested MAPKs remained active. These data suggested that ERK3 might play a significant role in mediating innate immune responses in primary epithelial cells. To determine genes regulated by ERK3, RNA sequencing was employed for control (siCo) and siERK3 knockdown cells in the presence or absence of LPS (24 h). A heat map was generated that depicts all differentially expressed (DE) genes in tested conditions **(Figure 3.3 A)**. **Figure 3.3 B** shows a plot representation of log2fold change of DE genes in ERK3-depleted cells as compared to the control (siCo) in resting (t=0 h, t0 shown on the left) and LPS stimulated cells (t=24 h, t24 shown on the right). These results are further visually presented by a Venn diagram in **Figure 3.3 C**.

Analysis revealed a multitude of genes, which are downregulated upon ERK3 depletion. One of the transcripts that brought the attention was potent chemotactic factor-CXCL8/IL-8. Moreover, RNAseq data determined the expression profile of TLRs in HCPECs **(Figure 3.3 E)**. Interestingly, ERK3 depletion leads to a downregulation of all these TLRs, including TLR3, which is highly expressed in HCPECs **(Figure 3.3 F)**.

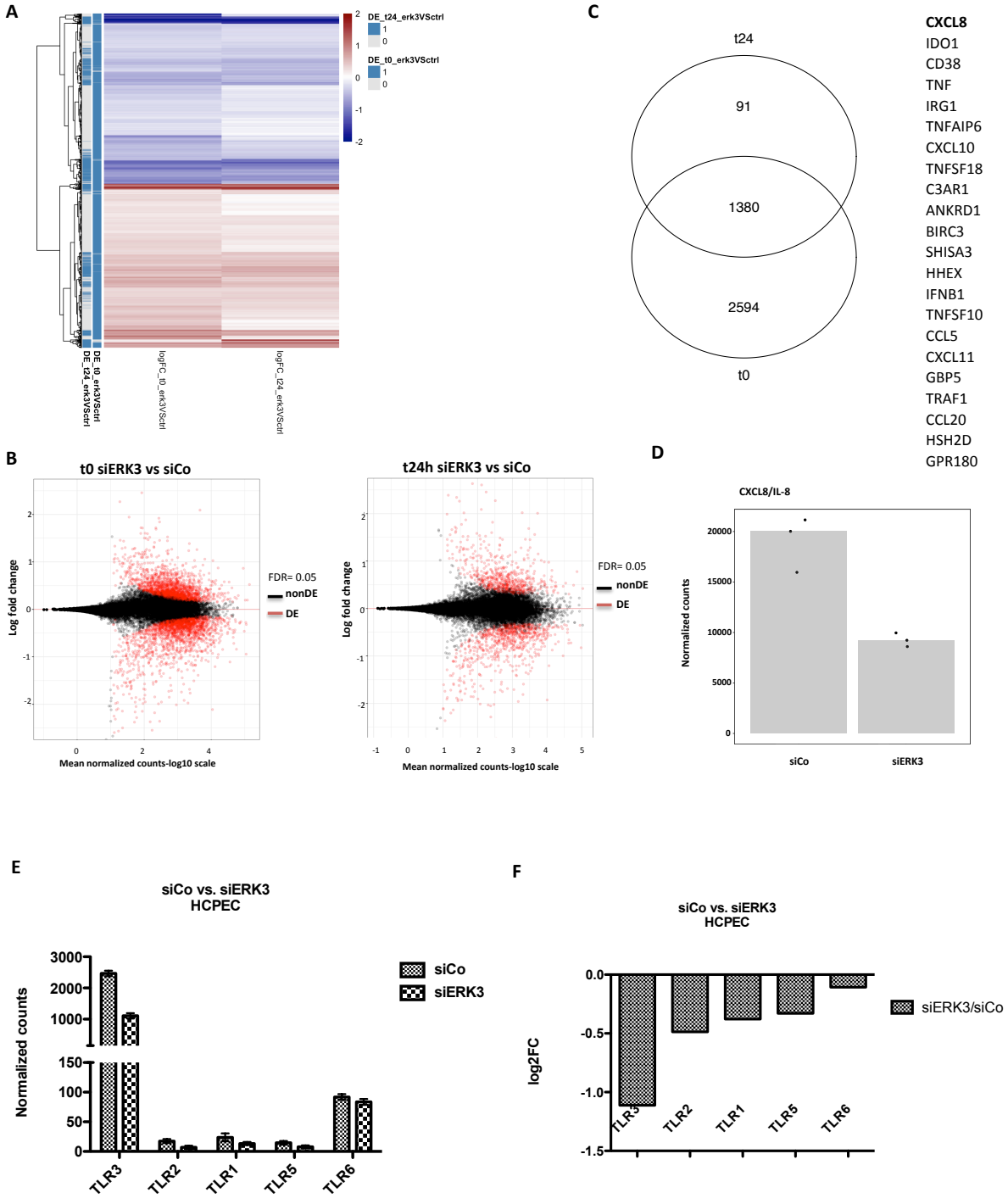

Figure 3.3 RNA sequencing results of genes regulated by ERK3 in primary epithelial cells. Three biological replicates of HCPECs were subjected to ERK3 silencing using specific siRNA. 24 h post-

transfection medium was changed for MEM without FBS and other supplements and 24 h LPS stimulation was started. The RNA isolated from the cells was subjected to RNAseq analysis. **(A)** A heat map representing differentially expressed (DE) genes. **(B)** Plots representing DE genes in resting and LPS stimulated siERK3 cells as compared to siCo. **(C)** Visual representation of DE genes. **(D)** RNA-seq derived box plot analysis of CXCL8/IL-8 expression levels in siCo and siERK3 HCPECs, represented as normalized counts**. (E-F)** Expression levels of TLRs detected in RNAseq data. **(E)** Represents normalized counts in siCo and siERK3 samples. **(F)** Log2fold change in expression of TLRs in ERK3-depleted HCPECs as compared to the control (siCo).

3.2.2 Epithelial secretome analysis - ERK3 depletion leads to a decrease in IL-8 secretion

Supernatants obtained from one of the biological replicates used for RNAseq **(Figure 3.3)** were analyzed using a biotin-based antibody array (L-Series Human Antibody Array 1000) to determine the secretome of control and ERK3-depleted HCPECs **(Figure 3.4).** Obtained data revealed distinct groups of up and downregulated factors. A decrease in CXCL8/IL-8 protein was observed in the supernatant obtained from ERK3-depleted HCPECs **(Figure 3.4 A, B),** further confirming the observed phenotype**.** Secretome-derived data were then further compared with the transcriptome (txome) analysis **(Figure 3.4 C)** revealing a significant overlap for 702 factors.

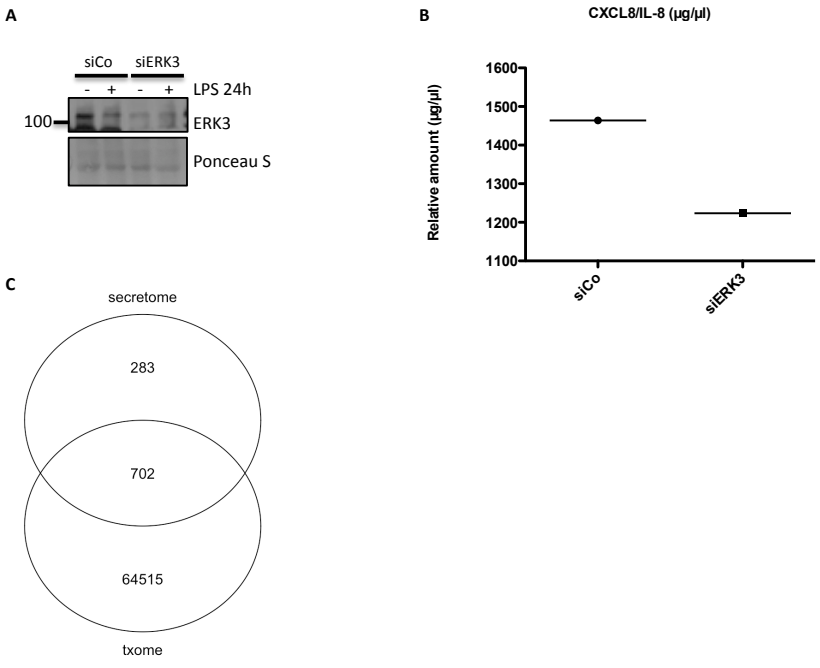

Figure 3.4 ERK3 regulates secretion of IL-8 by epithelial cells. HCPECs were transfected with either control siRNA (siCo) or RNA targeting ERK3 (siERK3). 24 h post-transfection medium was exchanged (MEM-FBS and supplements), cells were further cultured for 24 h and supernatants were harvested. Secreted factors were then detected using human biotin-based antibody array (L-Series Human Antibody Array 1000). **(A)** Western blot analysis of one of the HCPECs replicates used for secretome studies. ERK3 knockdown verification, ERK4 levels and Ponceau S staining as loading control are presented. **(B)** Relative amount of IL-8 in µg/µl was calculated as described in materials and methods section. **(C)** Visual representation of differentially expressed genes determined by RNAseq and secretome analysis.

3.2.3 Role for ERK3 in mediating IL-8 secretion in multiple cell types

Data presented thus far revealed that ERK3 regulates CXCL8/IL-8 production in HCPECs. Further experiments were performed to elucidate whether the observed phenotype is universal and can be seen in other cell types. Knockdown of ERK3 was established in HCPECs, HT-29, MDA-MB231 or HeLa cells and levels of secreted IL-8 were determined by ELISA **(Figure 3.5)**. Results confirmed universality of the observed phenotype across multiple cell lines, proving that indeed decrease in ERK3 expression leads to downregulation of IL-8 secretion.

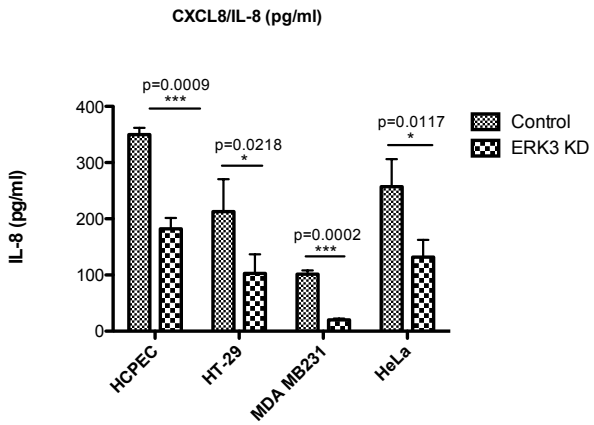

Figure 3.5 ERK3 knockdown downregulates IL-8 secretion in multiple cell lines. Secretion of CXCL8/IL-8 was measured in supernatants obtained from different cell lines. Each cancer cell line was stably transfected with either shRNA control empty vector or with shRNA targeting ERK3. HCPECs were transiently transfected with either control siRNA or siRNA targeting ERK3. After 24 h medium was exchanged with FBS free medium. Cells were cultured for additional 24 h, supernatants were collected and IL-8 levels were measured by ELISA. Results are representing mean ± SEM concentration in pg/ml from three biological replicates. *p<0.05, **p<0.01, ***p<0.001; t-test.

3.2.4 IL-8 protein levels reflect ERK3 expression status in LPS-stimulated HCPECs and HT-29 cells

As ERK3 regulates IL-8 production in both HCPECs and HT-29 cells **(Figure 3.5)** and as LPS treatment led to opposing effects on ERK3 protein **(Figure 3.6 A, B),** levels of CXCL8/IL-8 were determined in both cell lines in response to LPS. These results confirmed that the concentrations of IL-8 secreted reflect the expression levels of ERK3 in HT-29 **(Figure 3.6 C)** and HCPECs **(Figure 3.6 D)**. In comparison to the cancer cell lines, HCPECs displayed an extremely high basal level of secreted IL-8 **(Figure 3.6 D).** LPS stimulation induced a decrease in ERK3 levels, but activated all the classical MAPKs in primary epithelial cells. Despite MAPK activation upon LPS stimulation, IL-8 levels are decreasing in HCPECs during the time frame of the experiment **(Figure 3.6 E).** The decrease in CXCL8/IL-8 secretion in response to LPS stimulation is proportional to the ERK3 levels in the stimulated cells.

Considering that LPS did not have any stimulatory effect on IL-8 production in HCPECs, other stimuli were tested. As shown in **Figure 3.6 F-G**, TNFα and IL-1β exhibited more pronounced stimulatory effect on IL-8 levels and on ERK3. Both stimuli enhanced phosphorylation of ERK3 at S189. All stimuli induced ERK1/2 and/or p38 activation within 30 min **(Figure 3.6 F-H)**, but the activation of classical MAPKs did not correlate with an increase in CXCL8/IL-8 expression **(Figure 3.6 I-K).** However, levels of IL-8 increased after 2 h, which was concomitant with an increase in ERK3 phosphorylation and expression **(Figure 3.6 F-K)**. Treatment with TLR 7/8 agonist R848 **(Figure 3.6 H)** resulted in a time-dependent decrease of ERK3 expression, which was very similar to the results obtained by LPS treatment. Nevertheless, 0.5 h treatment with the TLR 7/8 agonist R848 led to an increase in ERK3 protein expression and ERK1/2 phosphorylation, which seems to be translated into a slight increase in IL-8 levels **(Figure 3.6 K).**

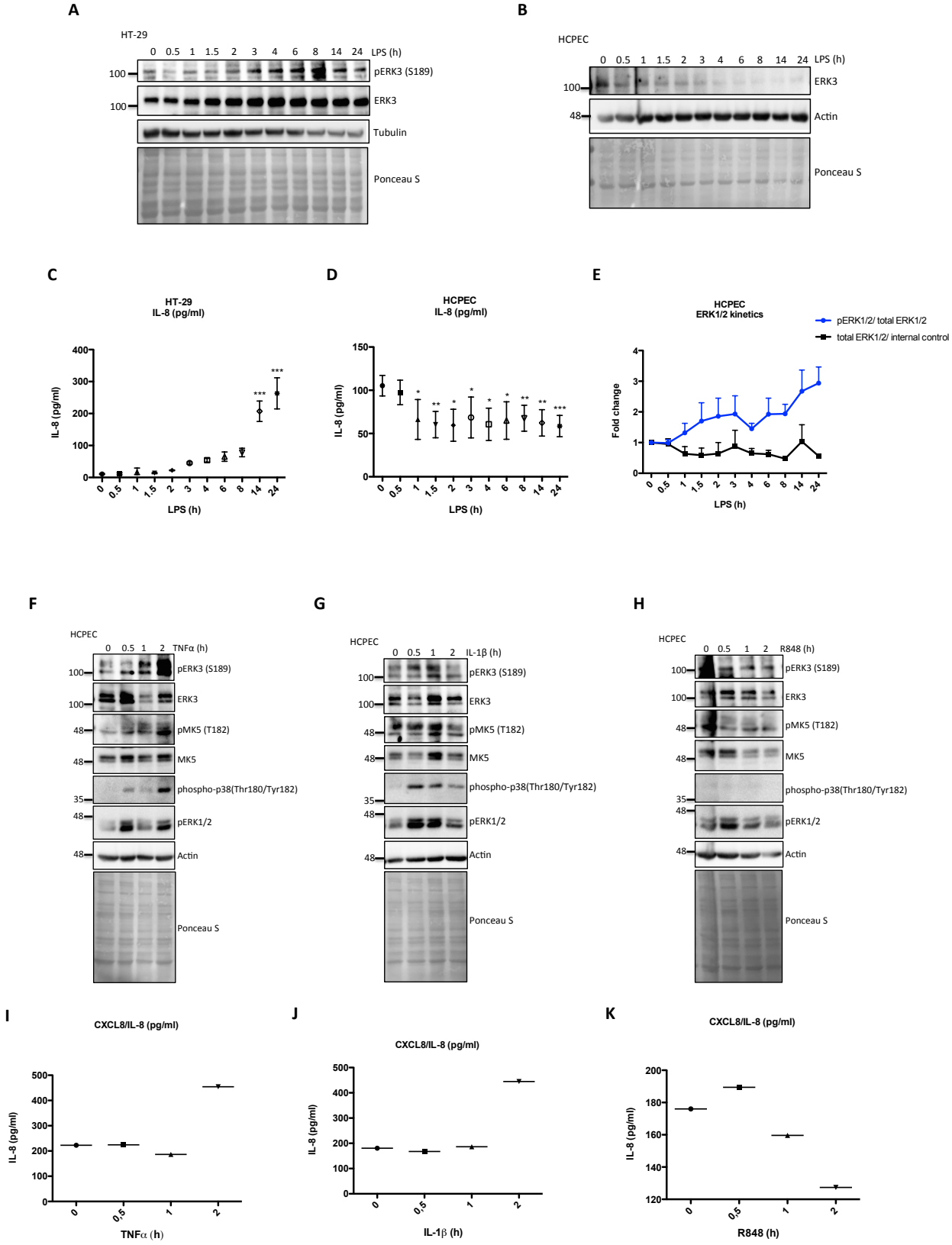

Figure 3.6 LPS stimulation leads to two different phenotypes in cancer and primary epithelial cells. HT-29 cells and HCPECs were stimulated with LPS at indicated time points in the absence of FBS, supernatants were harvested for each time point and cells were analyzed by immunoblotting **(A-B)** Representative Western blots depicting ERK3 expression levels in HT-29 and HCPECs. **(C-D)** ELISA

analyses of CXCL8/IL-8 levels are presented as mean ± SEM obtained from three independent experiments (n=3). *p<0.05, **p<0.01, ***p<0.001; t-test. **(F-K)** HCPECs were stimulated for 0, 0.5 h, 1 h and 2 h with TNFα (10 ng/ml), IL-1β (10 ng/µl) and R848 (2.5 µg/ml). Supernatants were harvested and cells were lysed for Western Blot analysis. **(F-H)** Phosphorylation levels of ERK3 (S189), MK5 (T182), p38 and ERK1/2 were monitored as well as a total protein levels for ERK3 and MK5, actin and Ponceau S loading controls are presented. **(I-K)** IL-8 concentration in pg/ml measured by ELISA.

3.2.5 IL-8 transcription in cancer and primary epithelial cells in response to LPS

Given that LPS stimulation enhances IL-8 secretion in HT-29 cell while proved to have an inhibiting effect on that cytokine in HCPECs, mRNA expression was evaluated in both cell types. LPS showed to have a stimulatory effect on IL-8 mRNA expression in HT-29 cells, resulting in a 2 to 5-fold increase **(Figure 3.7 A)**. Interestingly, highest mRNA levels were detected after 1.5 h, which reflects the time slot for the highest expression of ERK3 protein **(Figure 3.7 C).** As for the HCPECs, no significant differences in IL-8 transcript levels were observed during the course of treatment **(Figure 3.7 B)**.

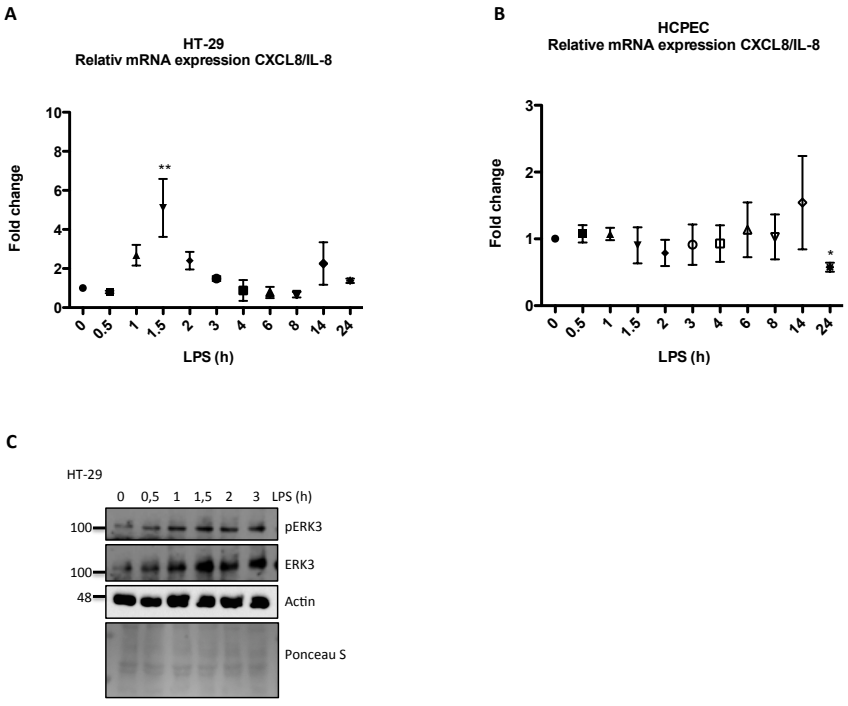

Figure 3.7 LPS stimulation alters IL-8 mRNA levels in HT-29 cells, but has no significant effect on the chemokine transcription in HCPECs. Expression profile of CXCL8/IL-8 gene evaluated by quantitative RT-PCR in **(A)** HT-29 cells and **(B)** HCPECs upon LPS treatment. Each sample was measured in triplicates and log2 fold change in gene expression is presented as mean ± SEM of three independent

experiments (n=3); *p<0.05, **p<0.01, paired t-test. **(C)** Short-time LPS stimulaiton of HT-29 cells and Western blot analysis of ERK3 phosphorylation and total protein levels. Actin and Ponceau S staining are provided as a loading control.

3.2.6 Loss of function studies to evaluate the role of ERK3 in IL-8 secretion

3.2.6.1 shRNA - and siRNA - mediated knockdown of ERK3 leads to a decrease in IL-8 production

Different gene depleting methods were implemented to evaluate and further reaffirm the on-target effect of ERK3-mediated IL-8 phenotype. Three different short hairpin RNAs (shRNA) constructs were expressed stably with lentiviruses as mentioned in methods in HT-29 cells to determine the efficiency and to compare IL-8 secretion phenotype **(Figure 3.8 A)**. In parallel, small interfering RNAs (siRNAs) targeted to two different regions of ERK3 gene were tested in HCPECs using the same readout **(Figure 3.8 B)**. Consistently, all these methods confirmed the role of ERK3 in IL-8 production.

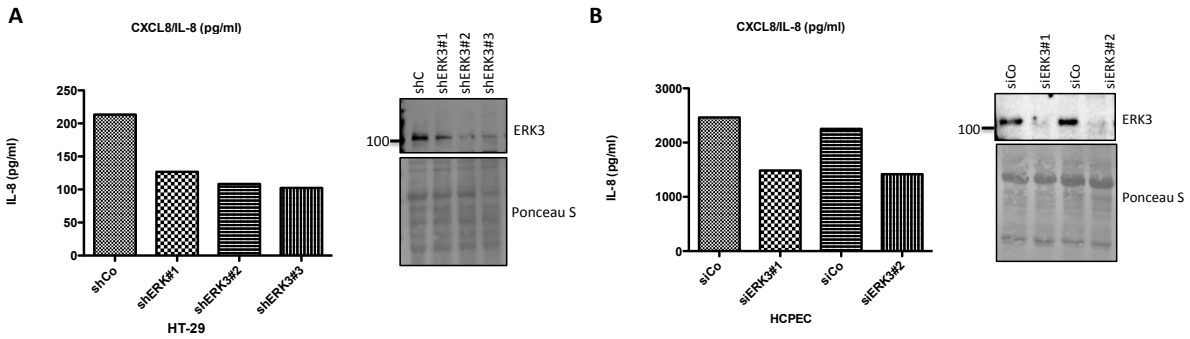

Figure 3.8 shRNA and siRNA-mediated knockdown of ERK3 leads to similar if not identical IL-8 phenotype. (A) HT-29 cells were stably transfected with three different shRNAs targeting ERK3 (shERK3 #1, shERK3 #2, shERK3 #3), shRNA empty vector (shCo) was used as a control. After puromycin selection, cells were seeded in 12-well plate at an initial density of $2x10^5$ cells/well. Next day medium was exchanged for McCoy's FBS free medium. 24 h later supernatants were harvested for each cell type for IL-8 ELISA measurement. Cells were lysed in RIPA buffer and analyzed by SDS-Page to determine ERK3 knockdown efficiency, Ponceau S staining was used as a loading control. **(B)** HCPECs were transiently transfected with either control siRNA (siCo) or with two different siRNAs targeting ERK3. 24 h post-transfection medium was exchanged for MEM-FBS. 48 h post-transfection supernatants were harvested and IL-8 levels were measured by ELISA. Cells were analyzed by Western Blot and levels of ERK3 were determined in each sample to verify knock down efficiency, Ponceau S staining is presented as a loading control.

3.2.6.2 ERK3 depletion suppresses LPS-induced secretion of IL-8

Previous data showed that ERK3 regulates basal IL-8 levels **(Figure 3.5)** and that LPS stimulation induced production of this cytokine in HT-29 cells **(Figure 3.6 C).** To investigate whether it is ERK3 that potentiates CXCL8/IL-8 levels in an LPS-dependent manner, knockdown of ERK3 was generated by expressing shRNA or CRISPR/Cas constructs in HT-29 cells.

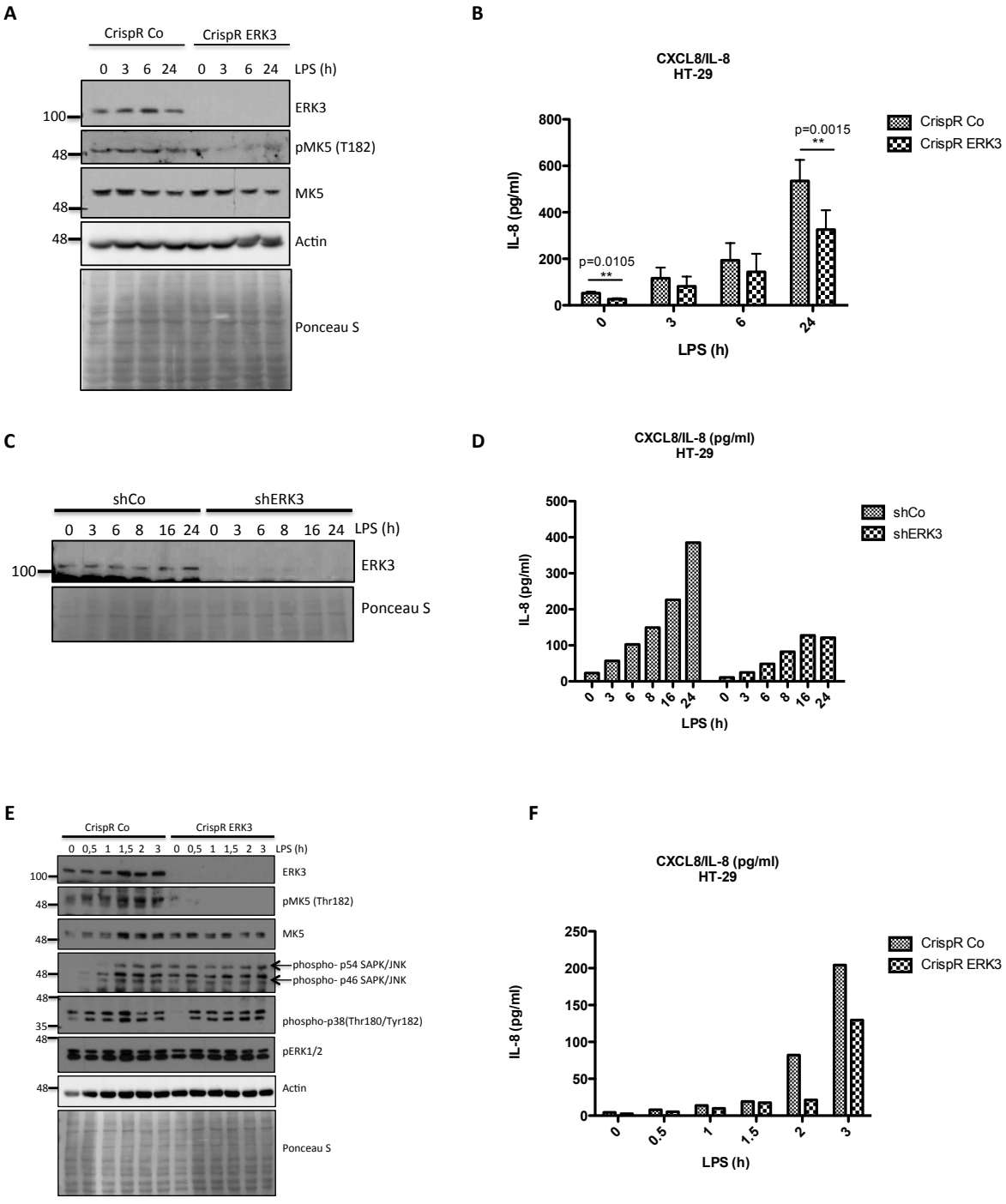

Figure 3.9 ERK3 regulates LPS-induced levels of IL-8. Control (CrispR Co) and ERK3 depleted (CrispR ERK3) HT-29 cells were stimulated with LPS for 0, 3 h, 6 h and 24 h, supernatants were harvested and IL-8 ELISA was performed. **(A)** Concentrations in pg/ml are represented as mean ± SEM obtained from three independent experiments (n=3). *p<0.05, **p<0.01, ***p<0.001; t-test. **(B).** Western Blot analysis of ERK3 and MK5 phosphorylation/expression levels. Actin and Ponceau S staining were included as a loading control. **(C-D)** Control (shCo) and ERK3 knockdown (shERK3) cells were stimulated with LPS at indicated time points. **(C)** Western Blot analysis of ERK3 levels and Ponceau S staining control. **(D)** IL-8 ELISA **(E)** Short-time LPS stimulation of CrispR Co and CripsR ERK3 cells at 0 0.5 h, 1 h, 1.5 h, 2 h and 3 h was performed. Subsequently, immunoblot analyses of ERK3, MK5, ERK4, JNK, ERK1/2 and p38 phosphorylation and/or total protein levels, β-actin and Ponceau S were used as loading control. **(F)** IL-8 ELISA analysis of the supernatants from cells shown in (E).

HT-29 cells with both, shRNA **(Figure 3.9 C-D)** and CRISPR **(Figure 3.9 A-B)** based knockdowns of ERK3 showed an induction of CXCL8/IL-8 production upon LPS stimulation, but the IL-8 expression never reached the levels attained in the control cells. In both cell models ERK3 proved to be crucial for full induction of the LPS-mediated IL-8 production. Moreover, decrease of CXCL8/IL-8 levels was observed in CRISPR ERK3 cells despite the activation of p38, JNK and ERK1/2 **(Figure 3.9 E and F)**.

3.2.7 Regulation of IL-8 by ERK3 is kinase independent

To further confirm the observed phenotype and to exclude any off-target effects of the siRNAs/shRNAs and CRISPR used, complementation experiments were performed. ERK3 was depleted in MDA MB231 and HeLa cells with an shRNA targeting the 3' untranslated region (3'UTR). After stable knockdown of the endogenous expression of ERK3, ERK3 WT carrying a V5 tag was reintroduced. As demonstrated in **Figures 3.10 A and C,** reconstitution with the wild type ERK3 rescued IL-8 levels decreased upon the ERK3 knockdown.

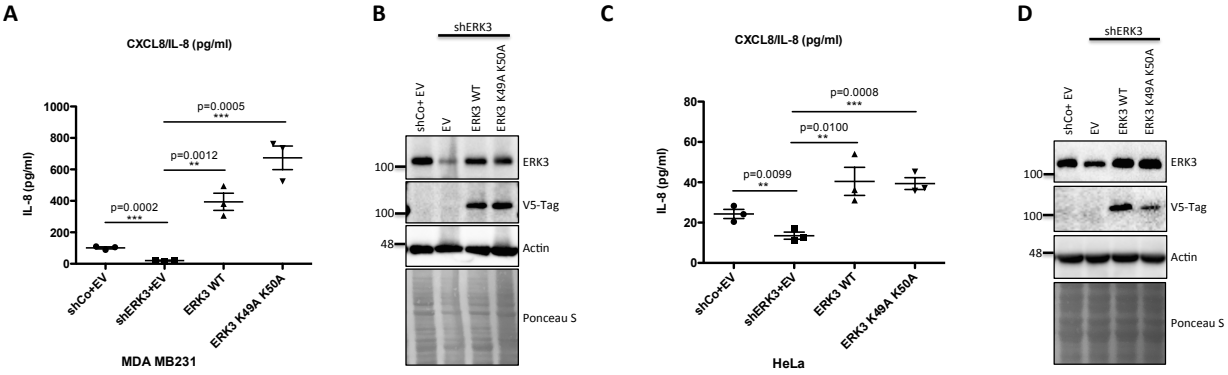

Figure 3.10 ERK3 regulates IL-8 production in kinase independent manner. MDA MB231 and HeLa cells were stably transfected with either control shRNA (shCo) or shRNA targeting ERK3 at 3'UTR. **(A-B)** MDA MB231 ERK3 knockdown (shERK3) cells were reconstituted with either ERK3 WT, ERK3 kinase dead mutant (ERK3 K49A K50A) or with an empty vector control (EV). IL-8 levels were determined in obtained supernatants. **(A)** ELISA measurement representing mean ± SEM concentration in pg/ml from three biological replicates (n=3). *p<0.05, **p<0.01, ***p<0.001; t-test. **(B)** Immunoblot analyses were performed: Levels of ERK3 protein were monitored to determine ERK3 knockdown efficiency and V5-tag expression levels were assessed to determine mutant overexpression efficiency. Actin and Ponceau S staining were used as a loading control **(C-D)** HeLa control and ERK3-depleted cells were transiently transfected with wild type ERK3, kinase dead mutant K49A K50A and EV control. **(C)** IL-8 levels were measured as described previously and are represented as mean ± SEM concentration from three biological replicates (n=3). *p<0.05, **p<0.01, ***p<0.001; t-test. **(D)** Knockdown and overexpression efficiency was verified by immunoblot analysis, actin and Ponceau S staining were used as a loading control.

As a kinase, ERK3 would be expected to rely on its kinase activity to regulate biological processes. To test whether it is the case, ERK3 kinase dead mutant was generated by introducing two point mutations at lysine 49 and 50. The kinase dead mutant (K49A K50A ERK3) was then expressed in ERK3-depleted MDA MB231 and HeLa cells.

Intriguingly, no decrease in IL-8 levels was observed in cells expressing a kinase inactive mutant of ERK3 when compared to the ERK3 WT **(Figure 3.10 A-D)**, leading to the conclusion that ERK3 kinase activity is not required to regulate IL-8 levels.

3.2.8 ERK3 positively regulates IL-8 promoter activity

Using a secreted Gaussia luciferase (GLuc) as a reporter, the activity of the IL-8 promoter was measured. To determine role of ERK3 in regulating CXCL8/IL-8 promoter activity, siRNA-mediated depletion of ERK3 gene was implemented in MDA MB231 cells that were lentivirally transduced to stably express GLuc under the control of the IL-8 promoter. As shown in **Figure 3.11 B**, loss of ERK3 significantly downregulated IL-8 promoter activity. At the same time, IL-8 secretion was measured in obtained supernatants, further proving a correlation between this atypical kinase and chemokine levels **(Figure 3.11 C)**. It is worth mentioning that no substantial changes can be observed in ERK1/2 phosphorylation levels or activity of NF-κB pathway **(Figure 3.11 A)**, indicating that IL-8 promoter inhibition is mediated through ERK3 depletion.

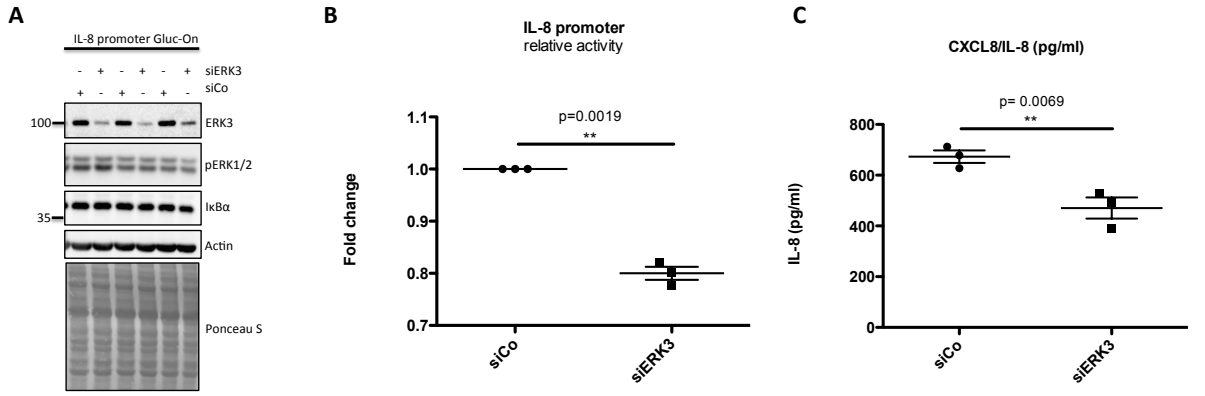

Figure 3.11 ERK3 knockdown leads to a decrease in IL-8 promoter activity. MDA MB231 cells were stably transduced with CXCL8/IL-8 Gaussia Luciferase construct (Gluc-On Promoter Reporter Clones) (IL-8 promoter Gluc) or with the internal vector control (PEZX-LvPG02). Cells were then transfected with siRNA targeting ERK3 (siERK3) or control siRNA (siCo). 24 h post-transfection medium was exchanged for FBS free medium and cells were cultured for 24 additional hours. Supernatants were harvested and luciferase activity as well as IL-8 concentration were measured. Cells were subjected to Western Blot analysis. **(A)** SDS-PAGE analysis was used to verify knock down efficiency as well as levels of pERK1/2 and IkBα. Actin and Ponceau S are provided as a loading controls. **(B)** Luciferase activity was monitored. Relative Luminescence Units (RLU) from the negative control were subtracted from IL-8 promoter expressing samples. Values are presented as mean ± SEM fold change in RLU of siERK3 samples normalized to the siCo (n=3). *p<0.05, **p<0.01, ***p<0.001; paired t-test. **(C)** IL-8 concentration was measured by ELISA and mean ± SEM concentrations in pg/ml are presented from three biological replicates (n=3). *p<0.05, **p<0.01, ***p<0.001; t-test. ERK3 knockdown efficiency was monitored by immunoblotting analysis. Activity of ERK1/2 as well as IkBα total protein levels were assessed. Actin control and Ponceau S staining was used. Western Blot analysis is presented for all three biological replicates.

3.3 ERK3-dependent regulation of the epithelial secretome and leukocytes chemotaxis

3.3.1 ERK3 regulates IL-8-mediated migration of neutrophils and monocytes *in vitro*

After establishing ERK3 as a novel, potent regulator of CXCL8/IL-8 in epithelial cells, we investigated the physiological relevance of this observed phenotype. Previous studies have shown that IL-8 is the most potent chemotactic factor for neutrophils activation, migration and degranulation [129-132]. To evaluate the role of ERK3 in IL-8-mediated chemotaxis, *in vitro* transwell migration assays were performed, using either freshly

isolated neutrophils obtained from peripheral blood of healthy volunteers or THP-1 monocytic cells. The supernatants from control of ERK3 depleted cells were added to the lower chamber of the transwell and served as a chemoattractant. In some experiments the control or ERK3 depleted epithelial cells are directly cultured in the lower chamber. After 2 h, migration rate through the polycarbonate membranes was evaluated by fluorescence measurement of pre-stained (CellTracker Green) THP1 cells and neutrophils. IL-8 neutralizing antibody was used to elucidate the role of IL-8 in the observed chemotaxis.

As presented in **Figure 3.12**, ERK3 depletion leads to a significant decrease in the *in vitro* migration rate of both, THP-1 cells and neutrophils. Neutralization antibody incubation revealed that indeed the observed effect is mediated by CXCL8/IL-8, as there is an additive effect between untreated and treated variant within each condition (Control-Control+IL-8 Ab and ERK3 KD-ERK3 KD+IL-8 Ab). However, IL-8 neutralization did not entirely inhibit chemotaxis of monocytes or neutrophils under these experimental settings. .

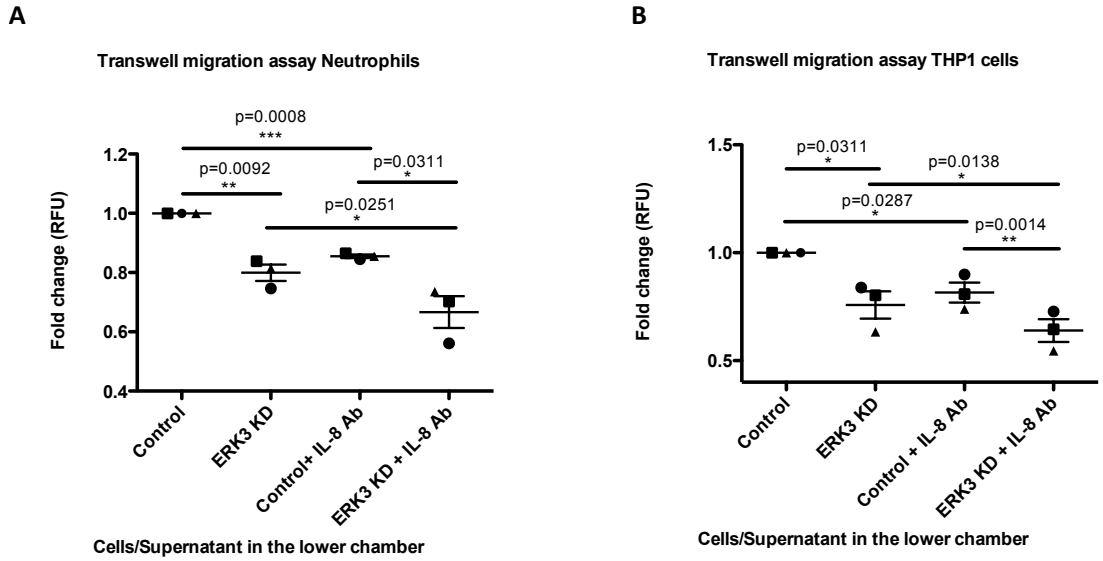

Figure 3.12 ERK3 depletion leads to a decrease in IL-8 secretion by epithelial cells and negatively affects neutrophils and monocytes chemotaxis. (A) LPS-activated neutrophils or **(B)** THP-1 cells were stained with 5 μM CellTracker Green CMFDA for 15 min. Afterwards, cells were added to the inserts (5 μm/8 μm pore size respectively) at a final concentration of $3x10^5$ /$1.2x10^5$ cells per insert. Conditioned media obtained from control and ERK3-depleted HCPECs or cells transfected with either control or siRNA/shRNA targeting ERK3 were placed in the lower chamber. IL-8 neutralizing antibody at 2.8 ng/μl was used in each condition as a control. Following 2 h incubation at 37°C, migration of neutrophils or

THP1 cells to the lower chambers was measured, using fluorescence (excitation wavelength 480 nm, emission wavelength 535 nm). Fold change of Relative Fluorescence Units (RFU) was then calculated for each condition. Data represent mean ± SEM of three biological replicates (n=3). *p<0.05, paired t-test.

3.3.2 ERK3 maintains transcriptional regulation of epithelial secretome

The ability of chemokines to promote leukocyte chemotaxis is one of the well-established and important biological functions [133]. However, multiple chemokines are involved in regulation of this process. Apart from IL-8, there is a group of factors such as GCP-1/CXCL6, MCP, CXCL10, NAP-2 or IL-16, which as mentioned in the introduction are important for efficient chemotaxis of leukocytes. Therefore, we investigated the expression levels of other chemotactic factors upon ERK3 depletion. Transcriptome data revealed that besides IL-8, also MCP1, CXCL10 and GCP-1/CXCL6 chemokines were significantly downregulated in ERK3-depleted cells **(Figure 3.13 A)**. Further evaluation of the secretome-derived data of primary epithelial cells **(Figure 3.13 B)** confirmed that ERK3 is a potent factor, maintaining proper balance of epithelial secretome and proper chemotaxis of leukocytes. Some of the chemotactic factors, including IL-8, CXCL6 and IL-16 were then validated by RT-PCR in control and ERK3 knockdown HCPECs, in the presence or absence of LPS **(Figure 3.13 C-E).**

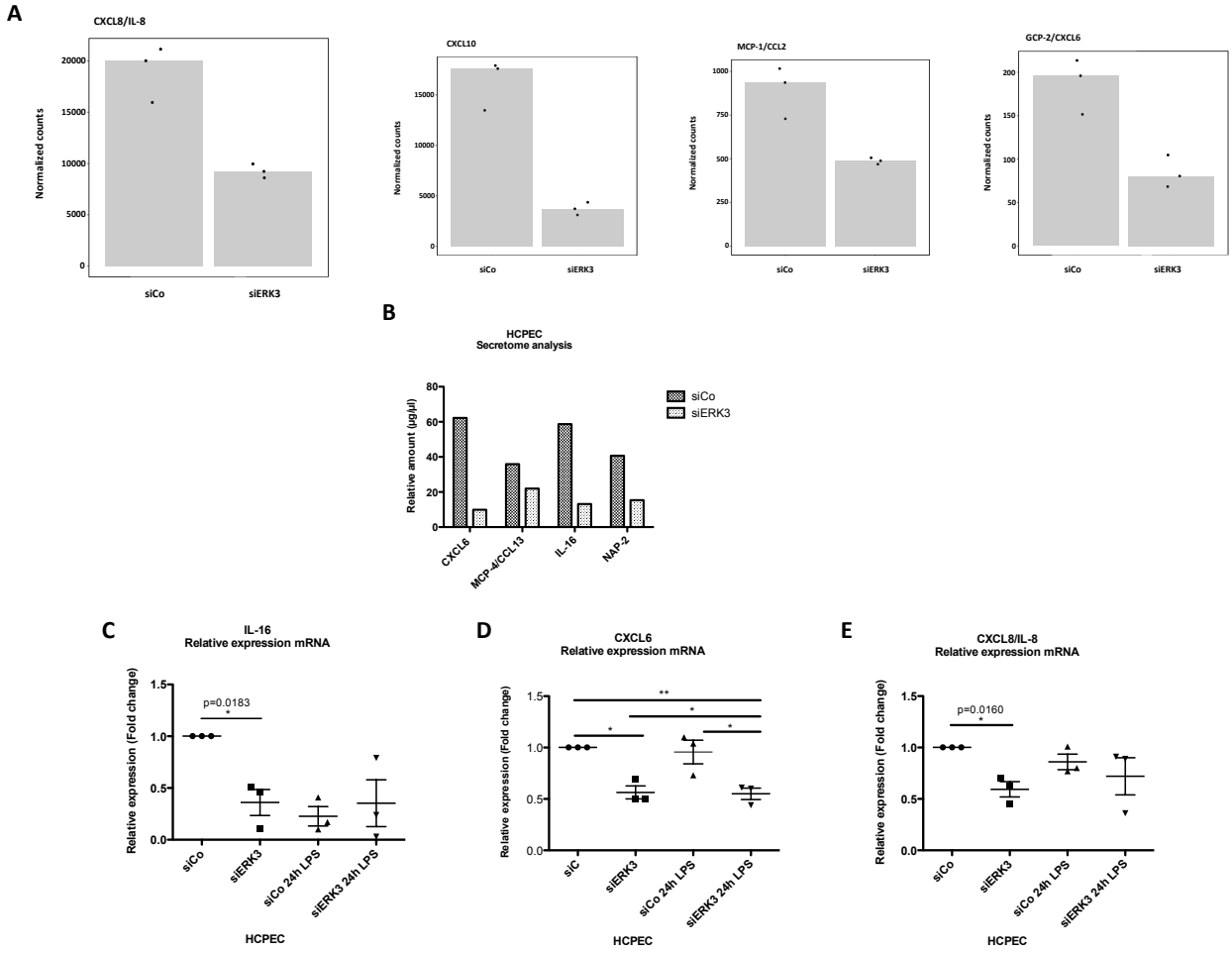

Figure 3.13 ERK3 regulates production of most potent chemotactic factors (A) RNAseq-derived analyses of several chemokine regulated by ERK3. Graphs represent normalized counts comparing siCo samples and siERK3 samples from three biological replicates of HCPECs. **(B)** Label based (L-series) Human Antibody Array 1000-derived factors from supernatants obtained from one of the biological replicates analyzed by RNA sequencing. Presented graph depicts CXCL6, CCL13 and IL-16 chemokines levels in µg/µl. **(C-E)** RT-PCR validation of CXCL8/IL-8, CXCL6 and IL-16 mRNA expression levels in control (siCo) and ERK3 depleted (siERK3) HCPECs presented as mean ± SEM log2 fold change in untreated and LPS stimulated cells (n=3). *p<0.05, **p<0.01, paired t-test.

3.3.3 Effect of ERK3-depleted epithelial supernatants on intraperitoneal leukocyte migration *in vivo*

To elucidate the physiological implications *in vivo,* leukocyte chemotaxis was studied in a mouse model. Supernatants of control and ERK3-knockdown primary epithelial cells **(Figure 3.14 D)** were injected into the peritoneal cavity of C75BL/6J female mice and leukocytic infiltration was assessed by peritoneal lavage and subsequent analyses. A

decreased number of all checked leukocyte populations was observed in lavage samples derived from animals injected with supernatants obtained from ERK3 knockdown cells as compared to the control supernatants. Significant inhibition of chemotaxis of granulocytes was detected **(Figure 3.14 A)** as well as of monocytes **(Figure 3.14 B)** and an obvious decrease was recognized in case of lymphocytes **(Figure 3.14 C).** As IL-8 is a key chemokine regulating neutrophil recruitment, human recombinant CXCL8/IL-8 was used as a positive control. Mice, despite the lack of IL-8 encoding gene, express receptor analogous to human CXCR2, which in response to human IL-8 mediates neutrophil chemotaxis [134].

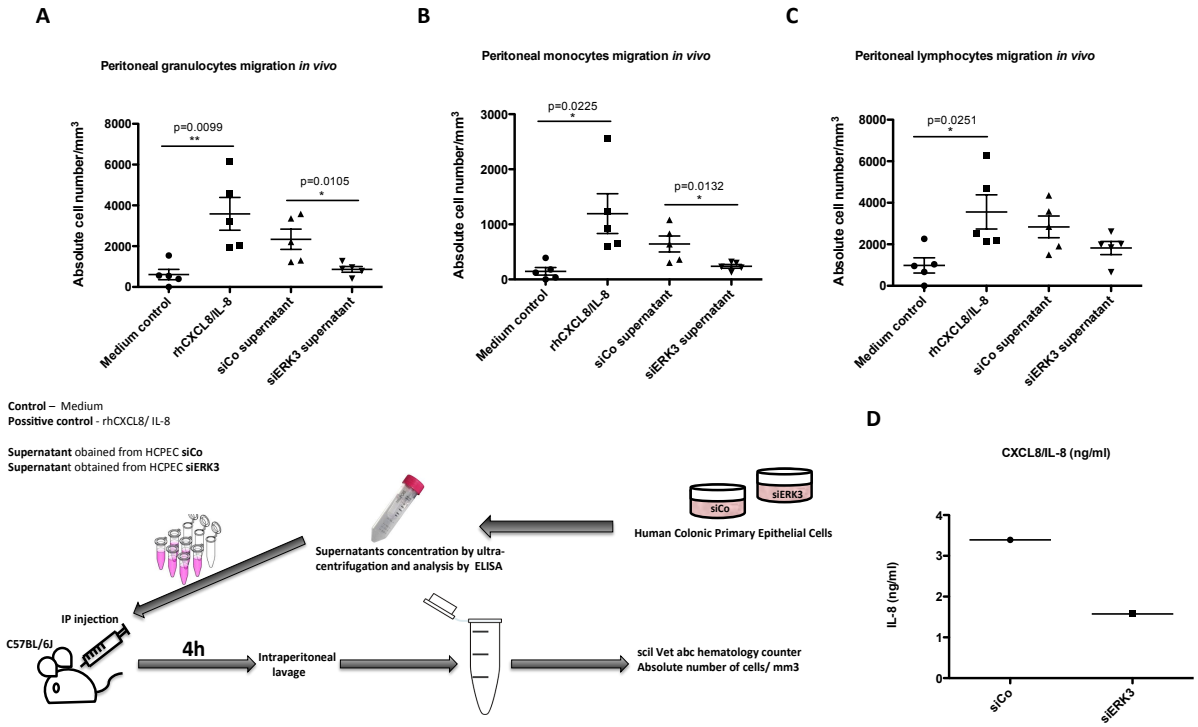

Figure 3.14 Supernatants obtained from ERK3-depleted HCPECs caused attenuation of leukocytes chemotaxis *in vivo.* Experimental procedure is explained in detail in Material and Methods section. Briefly, Groups of 5 8-week-old C57BL/6J female mice were injected intraperitoneally (i.p) with either 1 ml of MEM medium without supplements (MEM control), 1 ml of MEM containing 900 ng human recombinant CXCL8/IL-8 (rhCXCL8/IL-8) or 1 ml of HCPECs siCo/siERK3 concentrated supernatants. Four hours post-injections mice were sacrificed and intraperitoneal lavage was performed **(A-C)** Scatter plots representing absolute number of **(A)** granulocytes **(B)** monocytes and **(C)** lymphocytes. Data are represented as mean ± SEM. *p<0.05, **p<0.01, ***p<0.001, t-test. **(D)** IL-8 ELISA of supernatants used for the experiment.

3.4 Opposing effect of MK5 and ERK4 knockdown on ERK3 expression

3.4.1 Endogenous MK5 is a positive regulator of ERK3 expression

As MK5 has been shown to be a substrate of ERK3, it became interesting to verify whether MK5 plays any role in ERK3-mediated IL-8 phenotype. Loss of MK5 led to a decrease in ERK3 total protein levels in HT-29 cells **(Figure 3.15 A and B).** Concomitantly, IL-8 levels were also found to be reduced in MK5 KD cells **(Figure 3.15 C)**. Interestingly, reduction of CXCL8/IL-8 production is sustained in MK5 knockdown cells despite the hyperactivation of the canonical pathways like MEK1/2-ERK1/2 **(Figure 3.15 D)** and active NF-κB pathway **(Figure 3.15 A).** Consequently, a decrease in ERK3 protein levels upon MK5 knockdown, generated with three different shRNAs was observed in HCPECs **(Figure 3.15 E)**.

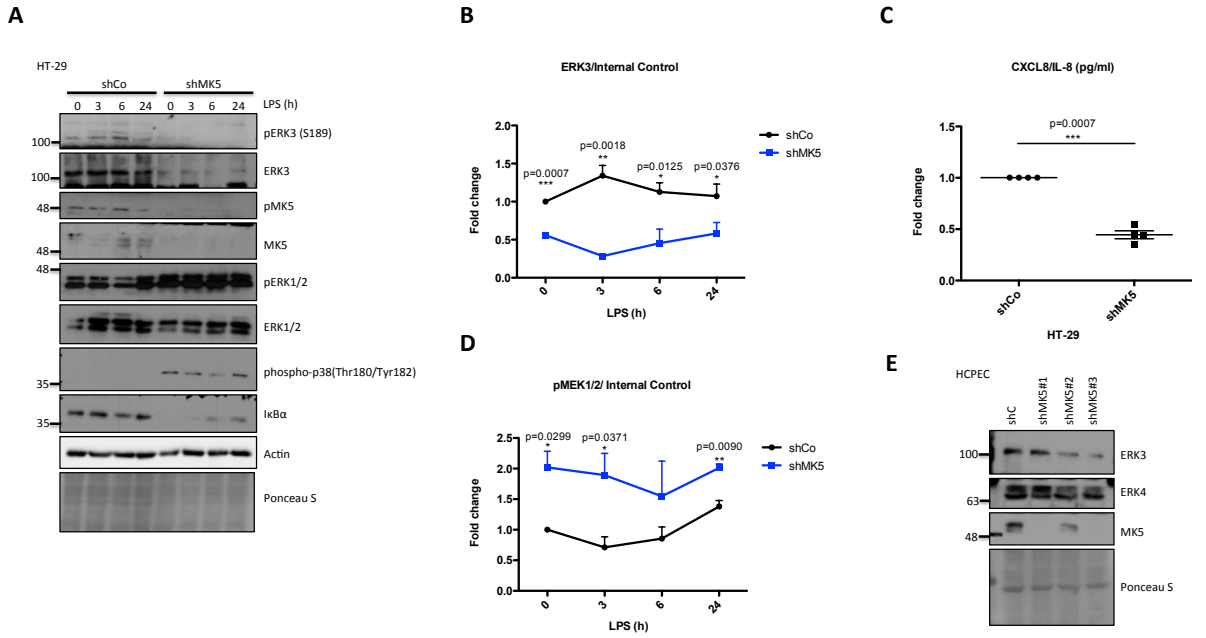

Figure 3.15 MK5 depletion leads to a downregulation of ERK3 expression, resulting in LPS-independent decrease of IL-8 levels. (A) Representative Western Blot analysis of HT-29 control (shCo) and MK5 knockdown (shMK5) cells, stimulated with LPS for 0 h, 3 h, 6 h and 24 h. Activation status of ERK3, MK5, ERK1/2, and p38, as well as total protein levels of mentioned proteins and IκBα were monitored. β-actin and Ponceau S were used as an internal loading control. **(B)** ERK3 protein expression levels in resting cells (0 h) as well as in LPS treated control (shCo) and MK5-depleted cells (shMK5) were quantified in comparison to the internal controls. Fold change values are represented as mean ± SEM (n=3). *p<0.05 **p<0.01, ***p<0.001; paired t-test. **(C)** ELISA measurement of IL-8 concentration in pg/ml is represented as mean ± SEM obtained from four independent experiments (n=4). *p<0.05 **p<0.01,

***p<0.001; t-test. **(D)** Phosphorylation levels of MEK1/2 in respect to the internal controls were monitored in shCo and shMK5 HT-29 cells stimulated with LPS at indicated time point. Fold change values are presented as mean ± SEM (n=3). *p<0.05 **p<0.01, ***p<0.001; paired t-test **(E)** Western blot analysis of control (shCo) and MK5 knockdown (shMK5) HCPECs. ERK3, ERK4 and MK5 total protein levels were assessed and Ponceau S was used as a loading control.

To verify previously published data suggesting that MK5 might function as an ERK3 stabilizing partner [31], CHX chase experiments were performed in control and shMK5 cells. As presented in **Figure 3.16 A and B,** no effect on ERK3 protein stability was observed upon MK5 knockdown in neither HT-29 nor CaCo2 colon adenocarcinoma cells. To determine whether MK5 regulates ERK3 transcription, expression levels of ERK3 mRNA were monitored in control and MK5 knockdown cells. Results shown that indeed, MK5 depletion leads to a significant downregulation of ERK3 transcript **(Figure 3.16 C)**. As it was demonstrated previously in **Figure 3.15 C,** decreased levels of ERK3 in MK5 knockdown cells led to a drastic downregulation of IL-8 protein levels. Taking into account that ERK3 mRNA levels are reduced in MK5-depleted cells, CXCL8/IL-8 transcription was assessed **(Figure 3.16 D)**. Data revealed a strong correlation between IL-8 transcription and ERK3 mRNA expression levels **(Figure 3.16 C and D)**. These studies are extended to three different cancer cell lines: Calu1, MDA-MB231 and CaCo2 **(Figure 3.16 E, F)** and we detected consistent effects.

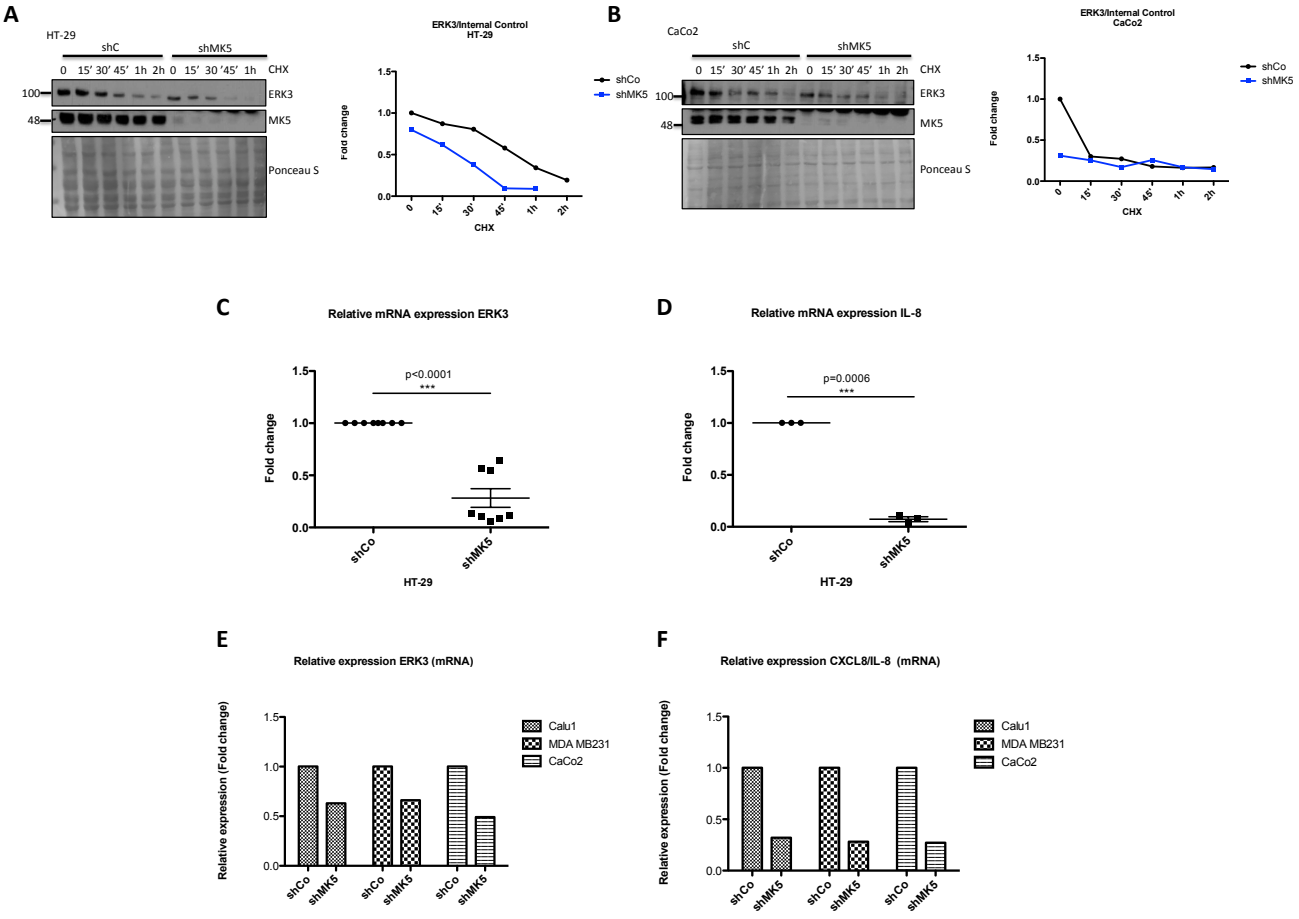

Figure 3.16 MK5 regulates ERK3 mRNA expression and its depletion leads to a decrease in IL-8 transcription. (A-B) Western blot analysis and quantification of CHX chase assessing ERK3 protein stability in control and MK5-depleted **(G)** HT-29 and **(H)** CaCo2 cells. **(C)** RT-PCR analysis of ERK3 mRNA levels in MK5 knockdown HT-29 cells in comparison to the control cells (shCo). **(D)** Expression levels of IL-8 mRNA in MK5 depleted (shMK5) and control (shCo) HT-29 cells. Log2 fold change in genes expression is presented as mean ± SEM of n=8 (ERK3) and n=3 (IL-8) biological replicates. *p<0.05, **p<0.01, paired t-test. **(E-F)** Presents relative mRNA expression levels of **(E)** ERK3 and **(F)** IL-8 in Calu1, MDA MB231 and HeLa MK5-depleted and control cells.

3.4.2 ERK4 negatively regulates endogenous levels of ERK3 protein

There are already few reports indicating that both ERK3 and ERK4 can interact with MK5 and are required for the phosphorylation of this kinase at T182 [31, 50, 135]. However, no direct interaction between ERK3 and its ortholog ERK4 has been described so far.

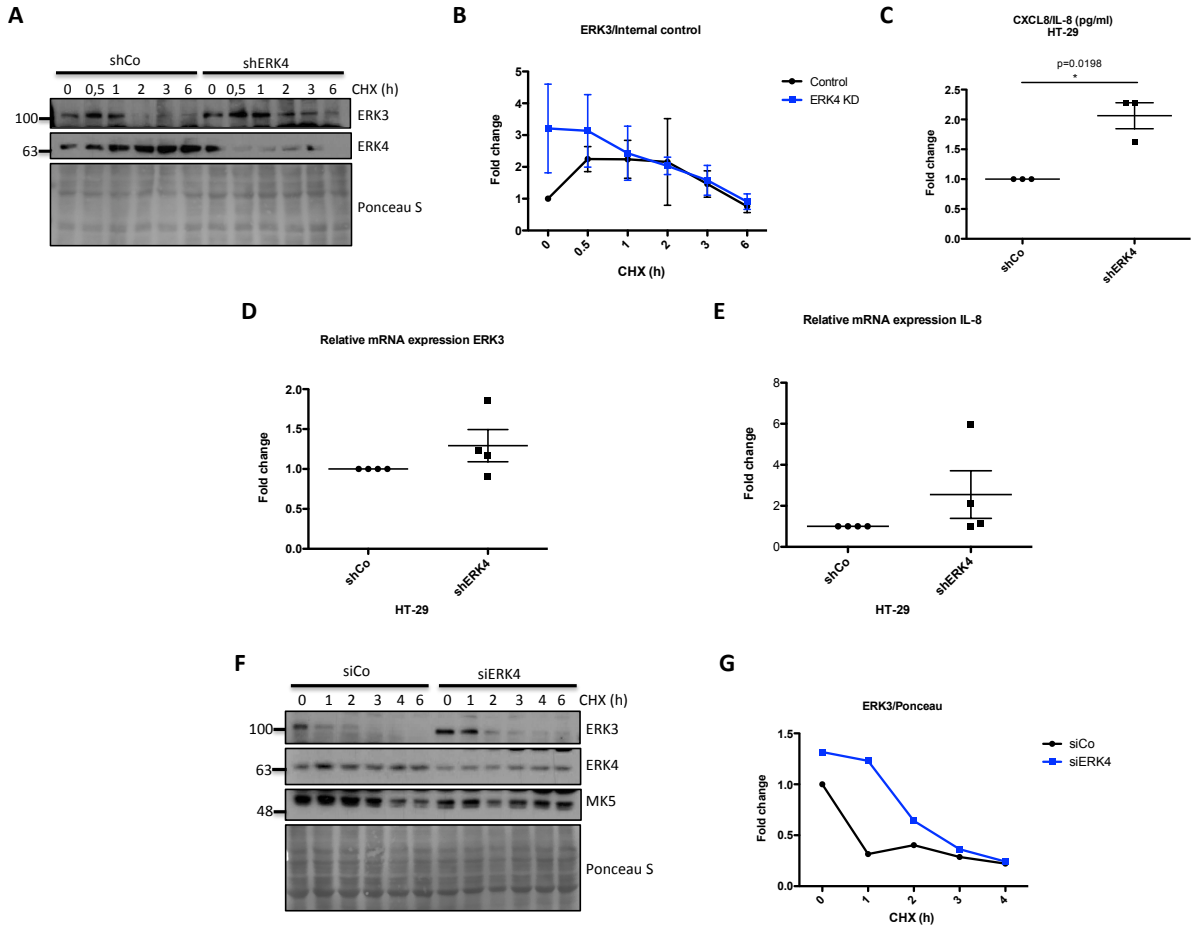

Figure 3.17 Depletion of ERK4 leads to an upregulation of ERK3 and IL-8 protein levels. (A) Representative Western Blot analysis of HT-29 control (shCo) and ERK4 knockdown (shERK4) cells treated with CHX for 0 h, 0.5 h, 1 h, 2 h, 3 h and 6 h. ERK3 protein levels were monitored and Ponceau S was used as an internal control. **(B)** Ratios of ERK3 protein levels to the internal loading control are presented as mean fold change ± SEM from three independent experiments (n=3). *p<0.05 **p<0.01, ***p<0.001; paired t-test. **(C)** IL-8 ELISA of shCo and shERK4 HT-29 cells. Results are presented as mean ± SEM concentration in pg/ml, measured in three biological replicates (n=3). *p<0.05 **p<0.01, ***p<0.001; paired t-test. **(D-E)** Log2 fold change in gene expression of ERK3 and IL-8 in ERK4-depleted HT-29 cell is shown in comparison to the control as mean ± SEM for four biological replicates (n=4). *p<0.05 **p<0.01, ***p<0.001; paired t-test. **(F)** Western blot analysis of control (siCo) and ERK4 knockdown (siERK4) HCPECs treated with CHX for 0 h, 1 h, 2 h, 3 h, 4 h and 6 h. ERK3, ERK4 and MK5 protein levels as well as Ponceau S staining are shown. **(G)** Western Blot quantification of ERK3 levels normalized with respect to the control cells.

In contrast to the MK5-mediated phenotype, knockdown of ERK4 regulated ERK3 levels in a positive way, leading to an increase in its protein expression in both, cancer HT-29 cells **(Figure 3.17 A and B)** and in HCPECs **(Figure 3.17 F and G),** without significant alterations in ERK3 protein stability. The mRNA expression level of ERK3 was then

assessed upon ERK4 knockdown, revealing no significant differences in expression when compared to the control HT-29 cells **(Figure 3.17 D)**. Interestingly, increase in IL-8 secretion was observed in ERK4-depleted cells **(Figure 3.17 C)**, but similarly to ERK3 expression, no effect was detected on mRNA levels **(Figure 3.17 E)**. Taken together, these results suggest that ERK4 might be involved in post translational regulation of ERK3 and thereby IL-8 levels.

3.4.3 Knockdown of ERK3 in ERK4-depleted cells leads to a decrease in IL-8 secretion, reflecting ERK3-knockdown phenotype

ERK3 and ERK4 showed opposite effects regarding IL-8 protein regulation, but only ERK3 affects transcription of the chemokine. Considering the effect of ERK4 depletion on the ERK3 protein levels, question rose whether the phenotypic effect leading to an increase in IL-8 levels was induced by ERK4 depletion itself or if intermediate upregulation of ERK3 protein caused the rise of chemokine levels. To determine which kinase controls observed IL-8 phenotype, ERK3 knockdown was generated in ERK4-depleted cells.

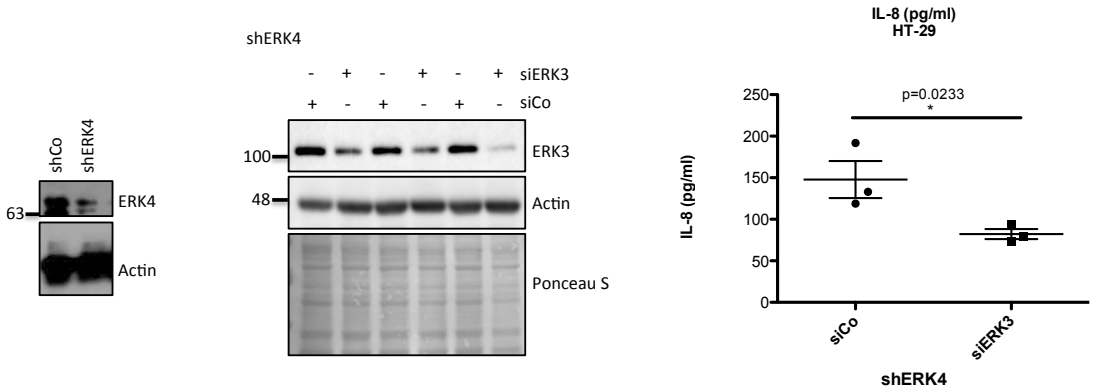

Figure 3.18 Knockdown of ERK3 in ERK4-depleted cells leads to a decrease in IL-8 levels, presenting ERK3 knockdown phenotype. ERK4-depleted HT-29 cells (shERK4) were transiently transfected with either control siRNA (siCo) or with siRNA targeting ERK3. 24 h post-transfection medium was exchanged for McCoy's-FBS and cells were stimulated with LPS at indicated time points. 48 h post-transfection supernatants were harvested and IL-8 levels were measured by ELISA. Results are presented as mean ± SEM concentration in pg/ml, measured in three biological replicates (n=3). *p<0.05 **p<0.01, ***p<0.001; t-test. Cells were analyzed by immunoblot and levels of ERK3 are presented as well as ERK4 knockdown efficiency, Ponceau S staining was used as a loading control.

As shown in **Figure 3.18,** depletion of ERK3 in ERK4 knockdown cells led to a decrease in IL-8 levels, reflecting ERK3-mediated phenotype and further proving that it was ERK3 upregulation that caused an increase in IL-8 levels upon ERK4 knockdown.

3.5 ERK3-dependent transcriptional regulation of IL-8 - transcription factors profiling

As demonstrated above, depletion of ERK3 downregulated IL-8 transcription in HCPECs. To obtain more insight into the mechanisms leading to the observed phenotype, the activity of 48 different transcription factors (TFs) was monitored in control and ERK3 knockdown HCPECs, in the presence or absence of LPS. TFs activation profiling assay revealed that ERK3 positively regulates activity of majority of the verified transcription factors, as the knockdown of ERK3 led to a downregulation of most of the TFs **(Figure 3.19 A)**.

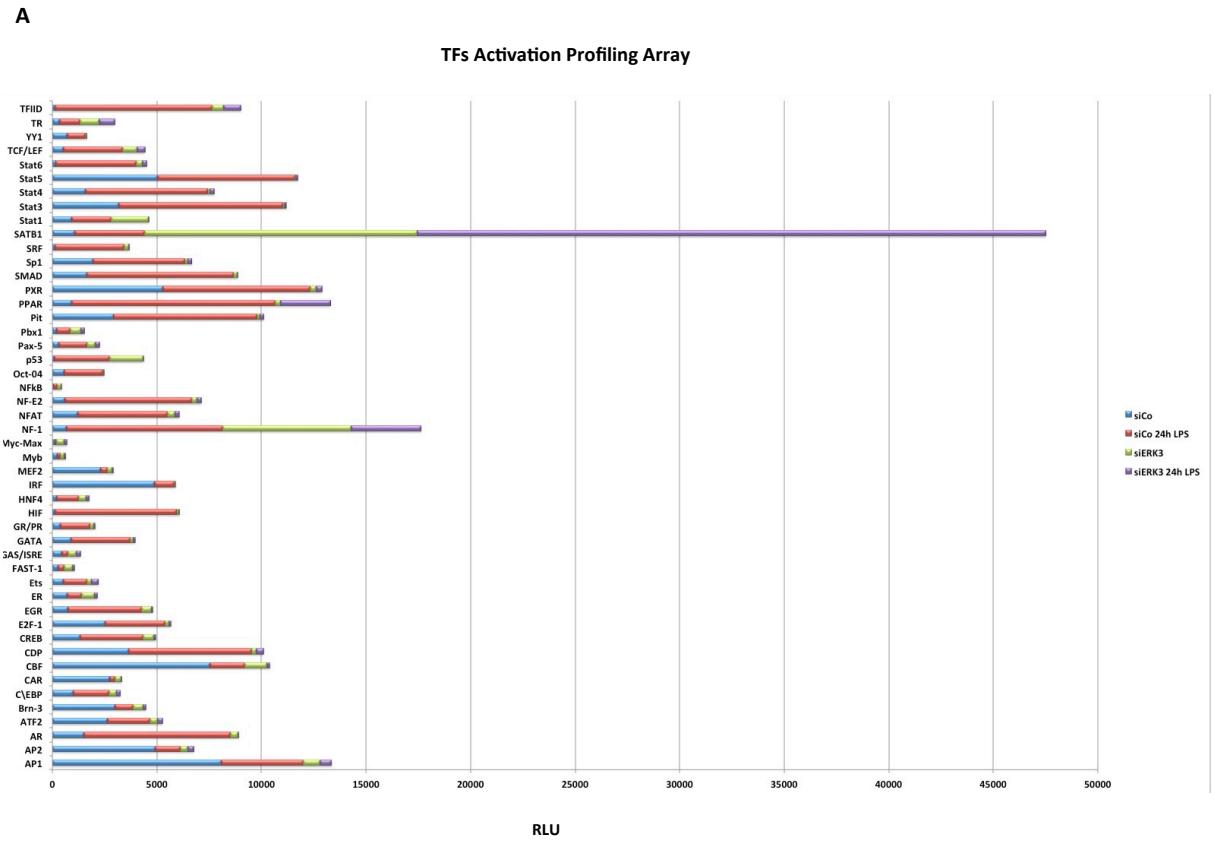

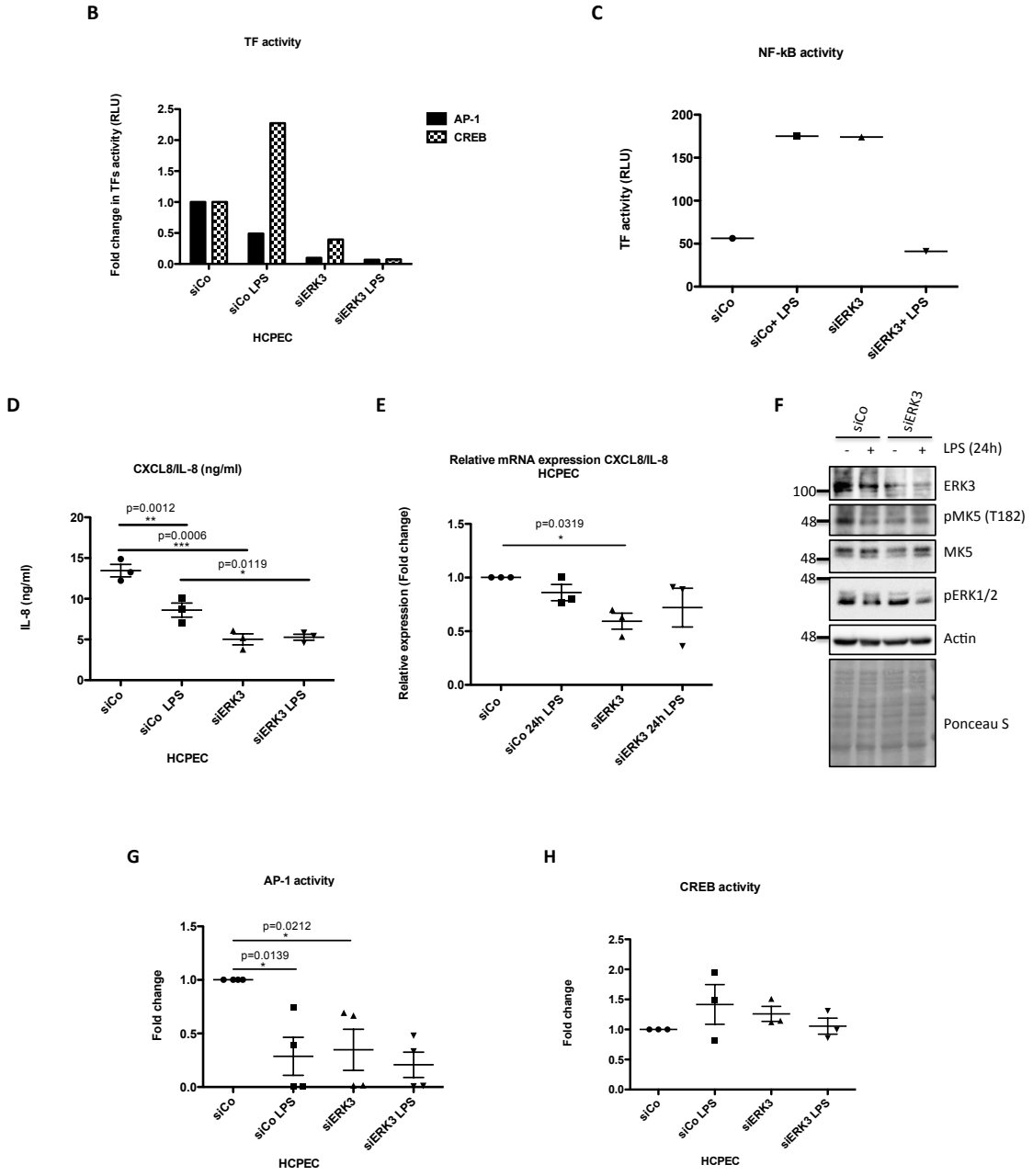

Figure 3.19 ERK3 regulates multitude of potent TFs. HCPECs were seeded in 10 cm dishes at initial density of $2x10^6$ cells. After 24 h cells were transfected either with negative control siRNA (siCo) or siRNA targeting ERK3. 24 h post-transfection medium was changed for MEM minus FBS and other supplements and cells were stimulated with LPS for 0 h/24 h. After stimulation, cell culture supernatants were harvested from each dish and part of the cells was lysed in RIPA buffer for further Western Blot analysis and knockdown verification, the rest of the cells was subjected to nuclear extraction and further TFs activation plate profiling. **(A)** Analysis of 48 TFs in control and ERK3-depleted HCPECs in the presence and absence of LPS. Relative Luminescence Units (RLU) are presented. **(B)** Graph representing transcriptional activity of AP-1 and CREB depicted as RLU. **(C)** Graph depicting activity of NF-κB in control and ERK3 knockdown cells in the presence and absence of LPS. **(D)** ELISA of IL-8 levels measured in control and LPS stimulated siCo/siERK3 HCPECs. Results are depicted for each

sample as mean concentrations (pg/ml) ± SEM from three (n=3) biological replicates per condition; *p<0.05, **p<0.01, ***p<0.001, t-test. **E)** RT-PCR validation of CXCL8/IL-8 mRNA expression levels in control (siCo) and ERK3 depleted (siERK3) HCPECs, presented as mean ± SEM log2 fold change in untreated and LPS stimulated cells (n=3). *p<0.05, **p<0.01, paired t-test. **(F)** Immunoblot analysis of ERK3, MK5 and ERK1/2 protein phosphorylation and/or expression. Actin and Ponceau S staining were used as a loading control. **(G-H)** Graphical representation of **(G)** AP-1 **(H)** CREB activity measured with Filter Plate Assay according to the manufacturer's instructions. Twenty-four hours post-transfection, control (siCo) and ERK3 knockdown (siERK3) HCPECs were stimulated with LPS for 24 h in medium without any supplement. Afterwards, cells were subjected to either Western Blot analysis or nuclear extraction and Filter Plate Assay analysis. Results are represented as mean fold change in activity measured in RLU ± SEM from three independent experiments (n=3); *p<0.05, **p<0.01, ***p<0.001, paired t-test.

Interestingly, ERK3 depletion led to a decrease in activity of AP-1 and CREB **(Figure 3.19 B)**, all three TFs, which were previously indicated as highly involved in transcriptional regulation of CXCL8/IL-8 [63, 72]. Surprisingly, NF-κB activity was increased upon ERK3 knockdown **(Figure 3.19 C),** which is contradictory to the observed decrease in IL-8 production **(Figure 3.19 D)**. Moreover, considering the integral role of NF-κB in regulation of CXCL8/IL-8 it was surprising to see that LPS-induced activation of NF-κB in HCPECs cells is inversely correlated with IL-8 secretion **(Figure 3.19 C and D)**. Another observation worth mentioning is that LPS stimulation led to a downregulation of NF-κB activity in ERK3-depleted cells **(Figure 3.19 C)**, which surprisingly had no additive effects on neither protein **(Figure 3.19 D)** nor mRNA **(Figure 3.19 E)** levels of IL-8. Taken together, these data showed that ERK3 regulates IL-8 gene transcription by controlling the activity of its most potent regulators AP-1 and CREB.

Filter plate activity assay validation of DNA binding activity of AP-1 and CREB confirmed the initial results, highlighting AP-1 as the TF regulated by ERK3 protein abundance and maintaining ERK3 mediated IL-8 levels in HCPECs **(Figure 3.19 G and 3.19 H)**.

3.5.1 ERK3 interacts with c-Jun and regulates DNA binding activity of AP-1

In order to better understand mechanisms, by which ERK3 contributes to AP-1 regulation observed in HCPECs **(Figure 3.19 G and 3.19 H)** we tested ERK3 and c-Jun binding properties in transformed HT-29 epithelial cells. Considering that LPS has been shown here to be a potent stimulus, regulating ERK3 protein and triggering IL-8

production in HT-29 cells, pull down of endogenous c-Jun protein from resting and LPS stimulated cells was performed.

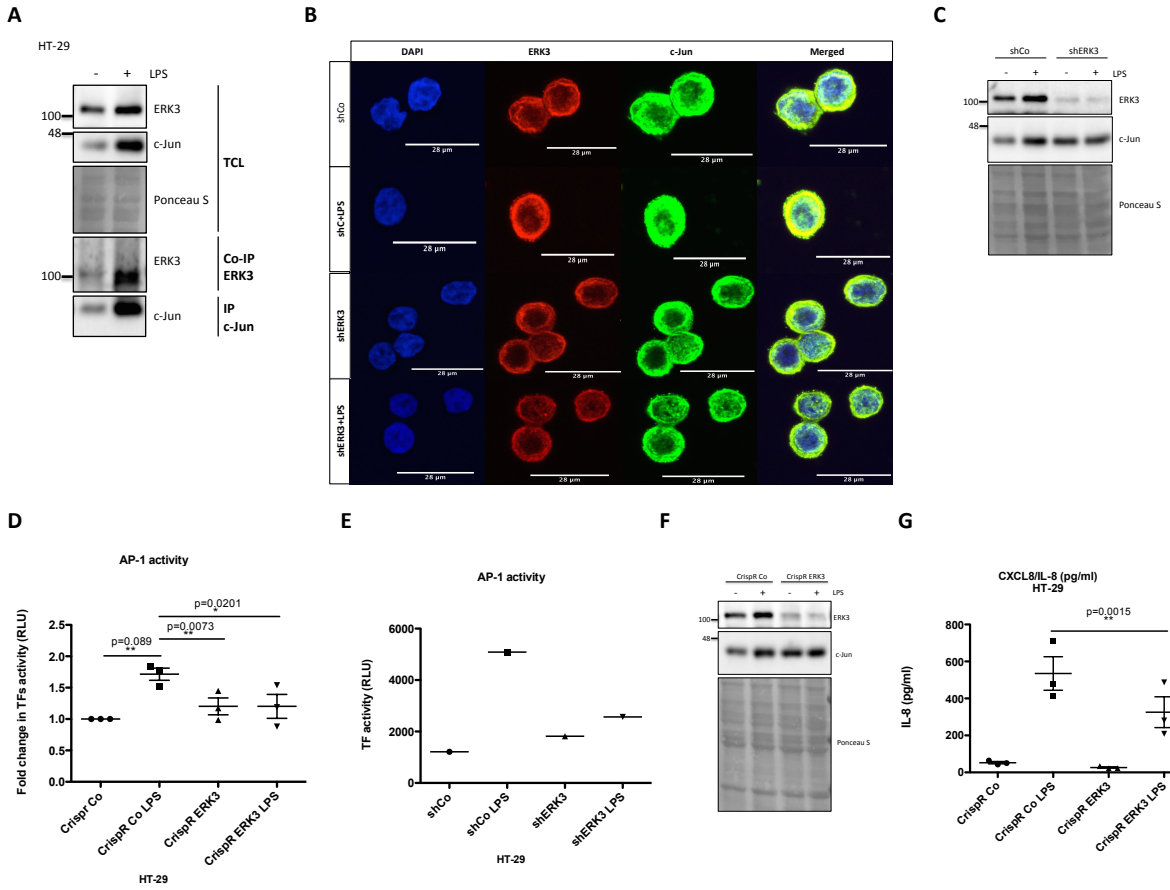

Figure 3.20 ERK3 interacts with c-Jun, regulates its nuclear localization and DNA binding activity. **(A)** Co-immunoprecipitation of ERK3 and c-Jun in unstimulated and LPS stimulated HT-29 cells, using an anti c-Jun antibody. Levels of c-Jun and ERK3 were monitored. Ponceau S staining was used as a loading control for TCL Western Blot analysis. **(B)** Confocal analysis of immunofluorescence staining of control (shCo) and ERK3 knockdown (shERK3) HT-29 cells in the presence and absence of LPS. Cells were stained with c-Jun primary antibody followed by rabbit Alexa488 (green), with ERK3 antibody followed by Cy3 mouse secondary (red) and Hoechst for the nucleus. Scale bars 28 µm. **(C)** Western blot analysis of control (shCo) and ERK3 depleted (shERK3) HT-29 cells -/+ LPS used for immunofluorescence staining in (B). Levels of ERK3 and c-Jun are presented as well as Ponceau S staining. **(D-E)** LPS-induced AP-1 activity is impaired by ERK3 knockout (CrispR ERK3) and shRNA generated knockdown (shERK3). **(D)** Graph represents AP-1 binding activity analysis by filter plate assay in control (CrispR Co) and ERK3 knockout (CrispR ERK3) cells in the presence and absence of LPS. Data are presented as mean fold change in RLU ± SEM from three independent experiments (n=3); *p<0.05, **p<0.01, ***p<0.001, paired t-test. **(E)** Depicts AP-1 activity measured in one biological replicate of control (shCo) and ERK3 knockdown (shERK3) HT-29 cells in the presence and absence of LPS. Results are represented as RLU. **(F)** Western blot analysis of unstimulated and LPS stimulated CrispR Co and CrispR ERK3 HT-29 cells. Levels of ERK3 and c-Jun are presented. Ponceau S staining was used as a loading control. **(G)** IL-8 concentration in pg/ml is

represented as mean ± SEM obtained from three independent experiments (n=3) of CrispR Co and CrispR ERK3 HT-29 cells cultured in the presence and absence of LPS; *p<0.05, **p<0.01, ***p<0.001, t-test.

Results shown that ERK3 co-immunoprecipitates with c-Jun and we could observe a strong complex formation between the two proteins upon LPS stimulation **(Figure 3.20 A)**. Furthermore, to verify cellular localization of ERK3 and c-Jun and to determine a role of ERK3 in LPS mediated regulation of c-Jun, immunofluorescence staining was performed in control (shCo) and ERK3 knockkdown (shERK3) HT-29 cells. Obtained results not only confirmed that LPS triggers expression of ERK3 protein, but also revealed that stimulation triggers nuclear translocation of ERK3 and that atypical MAPK is localized in both, nuclear and cytosolic compartment of the cell **(Figure 3.20 B and C)**. Regarding c-Jun and ERK3 interaction, staining presented co-localization of both proteins, which is enhanced upon LPS stimulation and decreased in ERK3 depleted (shERK3) cells. Moreover, knockdown of ERK3 seems to alter the nuclear abundance of c-Jun, regardless of LPS stimulation (Figure 7B). Western Blot analysis further shown that knockdown of ERK3 does not alter c-Jun protein expression **(Figure 3.20 C)**. We further verified whether the observed interaction and co-localization of ERK3 and c-Jun protein has any regulatory effect on AP-1 activity. TF filter plate assay revealed not only that LPS induced IL-8 production in HT-29 cells is regulated through an increase in AP-1 binding activity, but also further suggested that LPS triggered upregulation in chemokine level is ERK3 dependent **(Figure 3.20 D-G)**.

3.6 Cross-talk between atypical and canonical MAPKs

3.6.1 Inhibition of MEK1/2-ERK1/2 pathway leads to a downregulation of ERK3 protein expression

Throughout the course of the experiments studying the role of ERK3 in IL-8 production a striking correlation between ERK3 protein levels and activation of canonical MAPKs was observed. It was also reported previously that BRAF depletion as well as ERK1/2 inhibition leads to a significant downregulation of ERK3 protein expression [56]. Recently, it was shown that inhibition of either BRAFV600E or ERK1/2 activity leads to a downregulation of IL-8 transcription [136]. Worth mentioning is that both studies were performed in BRAFV600E-driven melanoma cells. Considering the observed direct (ERK3-depleted cells) and intermediate (shMK5 knockdown, LPS stimulated HCPECs)

effects of ERK3 downregulation on IL-8 production and no compensatory mechanisms from the other MAPKs, we further investigated the correlation between the atypical and canonical MAP kinases in regulation of IL-8. Levels of CXCL8/IL-8 as well as ERK3 protein expression were monitored upon inhibition of MEK1/2-ERK1/2 pathway by trametinib. Taking into account that previously published data indicated BRAFV600E as a regulator of ERK3 expression, two colonic cell lines were tested: HT-29, carrying BRAFV600E mutation and CaCo2, expressing wild type BRAF. As shown in **Figure 3.22 A,** trametinib (putative MEK1/2 inhibitor) treatment leads to a decrease in ERK3 protein expression in HT-29 cells, but the same effect was observed in CaCo2 cells **(Figure 3.22 B),** indicating that the negative effect of ERK1/2 inhibition on ERK3 protein can be observed regardless of BRAF mutations. Moreover, trametinib treatment inhibited LPS-induced IL-8 levels in HT-29 cells **(Figure 3.22 C)**. Interestingly, activation of NF-kB upon LPS stimulation is not compromised upon tramatenib treatment despite the decrease in IL-8 levels in these cells **(Figure 3.22 D)**. Moreover, treatment with trametinib did not cause any alterations in ERK3 mRNA levels **(Figure 3.22 E)**. Considering published information on BRAF regulating ERK3 expression [56] and the very recent report on BRAF (vemurafenib) and MEK inhibitor (trametinib) role in downregulating IL-8 production, it was tested whether treatment with PLX4720 (vemurafenib progenitor) or GDC-0879 Raf inhibitor affects ERK3 protein expression and phosphorylation. As shown in **Figure 3.22 F**, blocking MEK1/2-ERK1/2 pathway by inhibition of BRAF led to a decrease in both, ERK3 phosphorylation and protein expression.

To further verify functional synergism between ERK1/2 and ERK3, control (shCo) and ERK3 knockdown (shERK3) HT-29 cells were treated with trametinib and stimulated with LPS in order to induce IL-8 production. Results shown that treatment with tremetinib leads to an additive decrease of IL-8 levels in ERK3 depleted cells **(Figure 3.22 G and H)**.

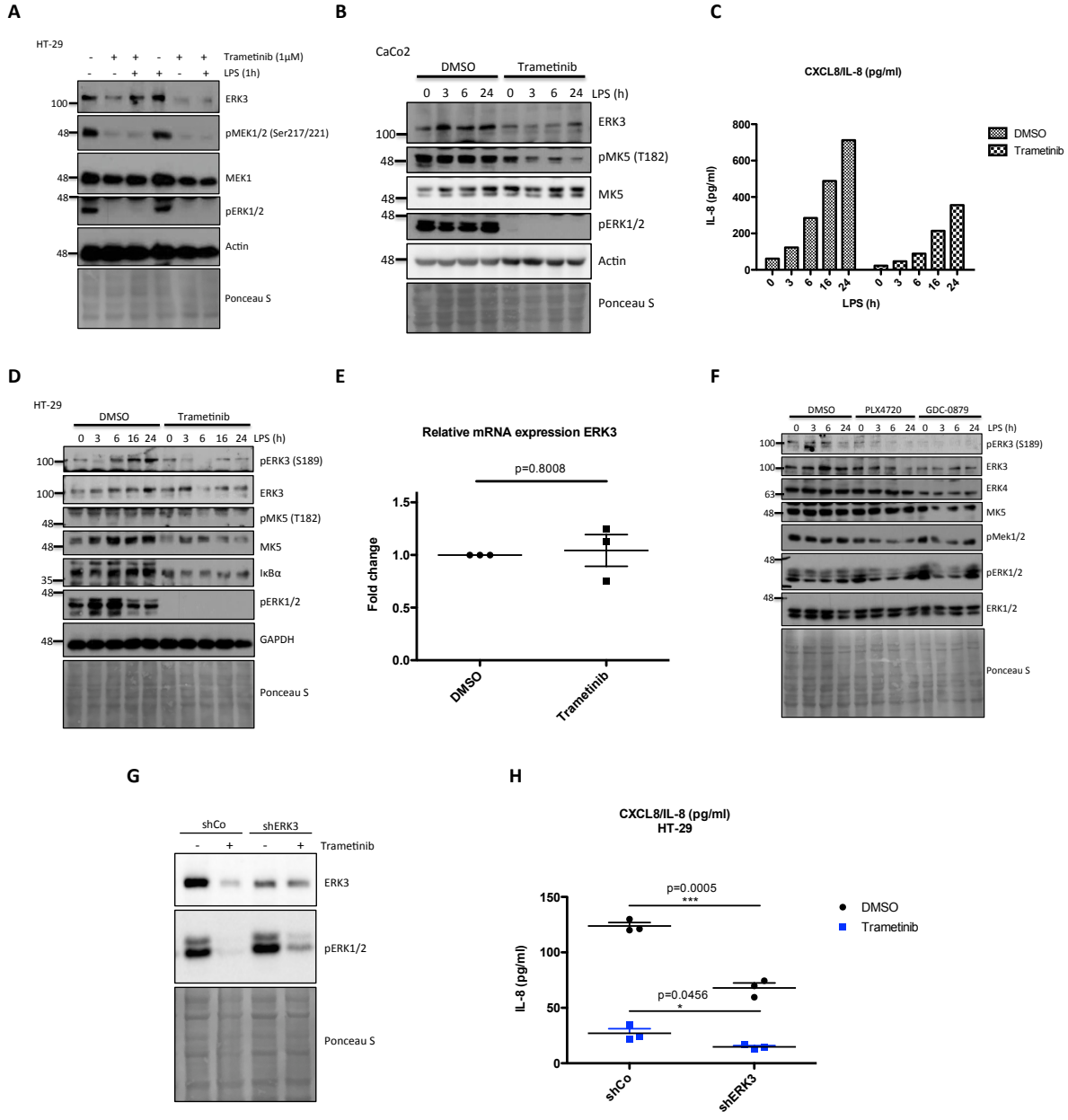

Figure 3.22 Inhibition of MEK1/2-ERK1/2 pathway leads to a downregulation of ERK3 protein expression. (A) Western Blot analysis of HT-29 cells pre-treated for 1 h with either DMSO or trametinib, followed by 1 h stimulation with LPS. SDS-PAGE analysis of ERK1/2, MEK1/2 and ERK3 was performed. As internal control, the membrane was probed for actin and stained with Ponceau S. **(B)** Immunoblot analysis of CaCo2 cells treated with trametinib and stimulated with LPS at indicated time points. Phosphorylation or/and total protein levels of ERK3 and MK5 were monitored. Phosphorylation of ERK1/2 was detected as a positive control for the inhibitor treatment. β-actin and Ponceau S staining were used as a loading control. **(C)** ELISA analysis of IL-8 levels measured in supernatans obtained from control and trametinib/LPS treated HT-29 cells. **(D)** Western Blot analysis of HT-29 cells. Levels of ERK3 and ERK3 phosphorylation, as well as ERK1/2, MK5 and IkBα proteins were monitored in response to trametinib and LPS. GAPDH and Ponceau S staining were used as a loading control. **(E)** Log2 fold change in gene expression of ERK3 upon trametinib treatment in HT-29 cells presented as mean ± SEM for three

biological replicates (n=3); *p<0.05, **p<0,01, ***p<0.001, paired t-test. **(F)** Western Blot analysis of HT-29 cells pre-treated with Raf inhibitors PLX4720 or GDC-0879 and further stimulated with LPS to determine phosphorylation and/or total levels of ERK3, MEK1/2, ERK1/2, ERK4 and MK5 proteins. Ponceau S staining was performed as a control. **(G-H)** Control (shCo) and ERK3 knockdown (shERK3) HT-29 cells were treated with trametinib for 1 h followed by 24 h LPS stimulation in order to induce IL-8 production. Supernatants were harvested and IL-8 levels were analysed by ELISA, cells were subjected to immunoblot analysis. **(G)** Representative Western Blot analysis. Levels of ERK3 are presented and phosphorylation of ERK1/2 to validate inhibitor efficiency, Ponceau S staining is provided as a loading control. **(H)** ELISA analysis of IL-8 levels measured in pg/ml, depicted for each sample as mean concentrations (pg/ml) ± SEM from three (n=3) biological replicates per condition; *p<0.05, **p<0.01, ***p<0.001, t-test.

3.6.2. Blocking proteasomal degradation rescues ERK3 and IL-8 levels decreased by trametinib treatment

Previously shown data proved that ERK3 is an extremely labile protein with a half-life of approximately 45 min. Surprisingly, a newly discovered biological function of ERK3 in controlling IL-8 gene seems to be regulated by its protein abundance rather than its kinase activity. Furthermore, considering observed trametinib-induced downregulation of ERK3 protein levels, it was tested whether the IL-8 decrease observed upon ERK1/2 inhibition in **Figure 3.22** was induced by blocked activity of MEK1/2-ERK1/2 module or by the intermediate attenuation of the ERK3 protein abundance caused by the treatment. To determine potency of ERK3 role in the observed phenotype, HT-29 cells were pre-treated with MG-132 inhibitor to prevent proteasomal degradation, prior the trametinib treatment further followed by LPS stimulation to induce IL-8 production in the tested cells.

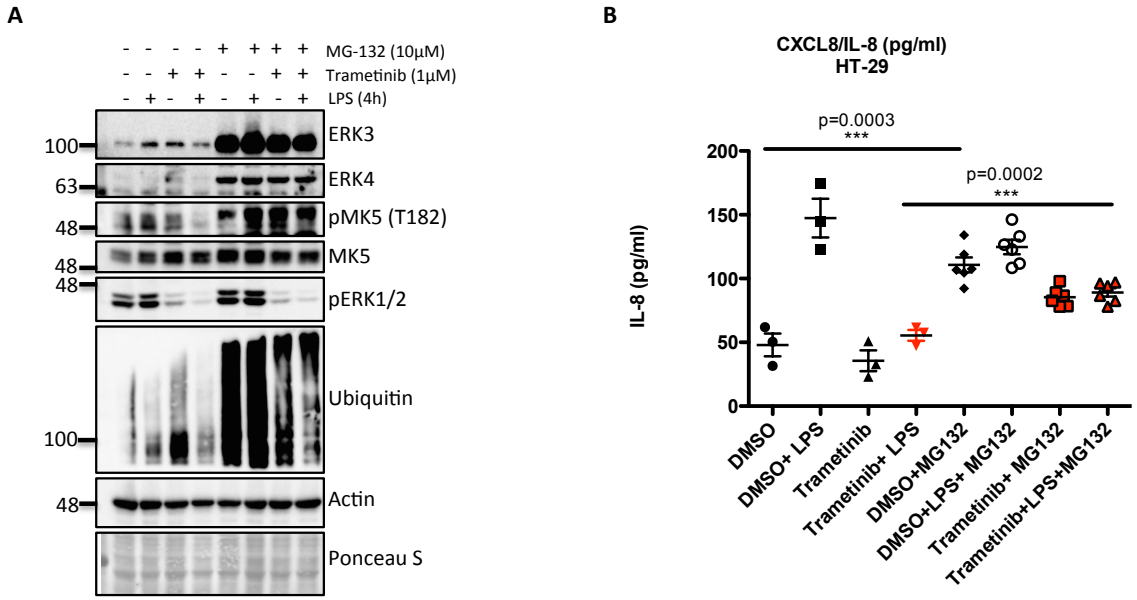

Figure 3.23 Blocking the proteasomal degradation of ERK3 in trametinib-treated cells restores IL-8 production. HT-29 cells were seeded in 12-well plate at initial density of $2x10^5$ cells. Next day, medium was exchanged for FBS free medium and cells were pre-treated with MG-132 for 6 h prior to 1 h incubation with DMSO/trametinib. Further, cells were stimulated with LPS for 4 h. **(A)** Western Blot analysis. Levels of ERK3, ERK4 and phosphorylation status of MK5 (T182) and ERK1/2 were monitored, membranes were probed for ubiquitin to determine MG-132 treatment efficiency. Actin was used as a loading control. **(B)** IL-8 protein levels quantified by ELISA. Results represent mean ± SEM concentration in pg/ml obtained from at least three biological replicates per condition. *p<0.05, **p<0.01, ***p<0.001; t-test.

As shown in **Figure 3.23 A**, MG-132 treatment led to a strong accumulation of ubiquitin conjugated ERK3 in both DMSO and trametinib treated cells. Furthermore, blocking the proteasomal degradation of ERK3 rescued IL-8 levels decreased by trametinib treatment in both, resting and LPS stimulated cells, despite no activation of ERK1/2 **(Figure 3.23 A and B)**. Interestingly, MG-132 treatment itself caused an increase in IL-8 levels comparable with the one obtained by LPS stimulation, further proving a potent effect of ERK3 on this chemokine production. Interestingly, accumulation of ERK3 upon MG-132 treatment led to an increase in ERK4 expression, which shows consistency with previously shown data **(Figure 3.17)**, further indicating that ERK4 controls ERK3 protein abundance.

3.7 Role of the proteasome in ERK3 expression and its biological activity

3.7.1 Blocking proteasomal degradation of ERK3 in HCPECs restores LPS-mediated decrease in IL-8 secretion

LPS stimulation of HCPECs always leads to a decrease of ERK3 protein levels, which correlates directly with attenuation of IL-8 secretion and with no significant alterations on mRNA levels of both proteins. Considering these results and the labile nature of the atypical MAPK ERK3 protein, experiments were performed to determine the role of the ubiquitin-proteasome system in regulating ERK3 and by extension, IL-8 protein in HCPECs. First of all, treatment of HCPECs with the proteasome inhibitor MG-132 led to an accumulation of ERK3 protein, indicating a possible role of the proteasome in ERK3 regulation **(Figure 3.24 A).** Moreover, blocking the ERK3 degradation restored IL-8 levels decreased by LPS stimulation **(Figure 3.24 B).**

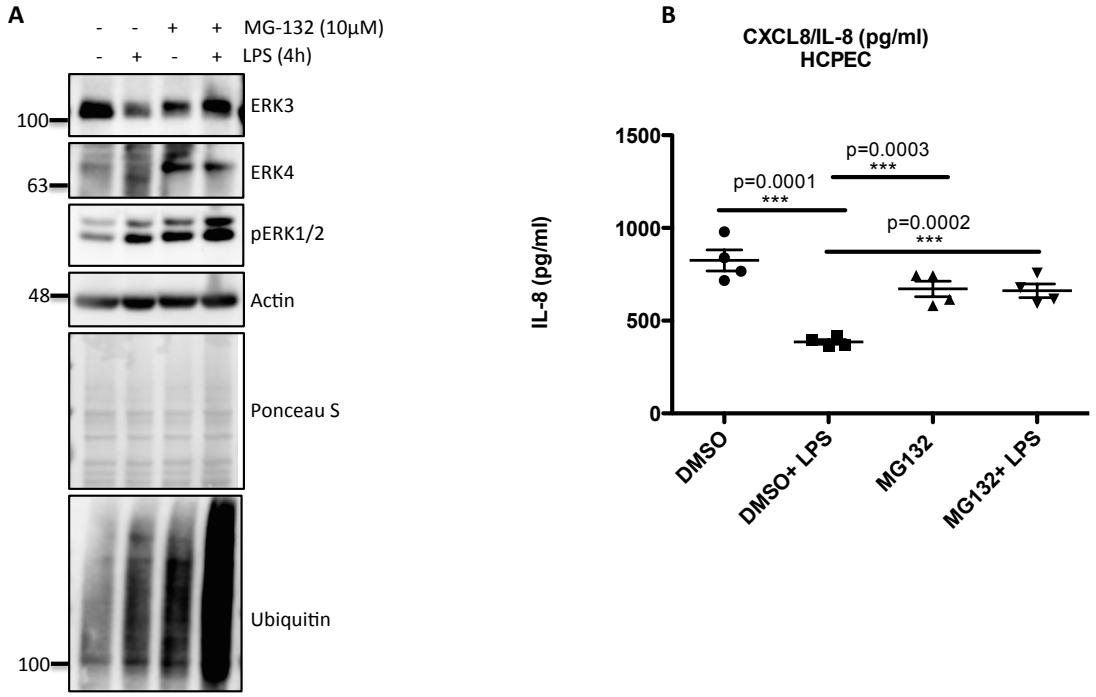

Figure 3.24 LPS-mediated decrease of IL-8 levels in HCPECs can be rescued by blocking the proteasomal degradation of ERK3. (A-B) HCPECs were seeded at an initial density of $2x10^5$ cells/well in 12-well plate. Next day medium was exchanged for MEM basal medium without supplements and cells

were pre-treated with either DMSO or MG-132 proteasome inhibitor, followed by 4 h stimulation with LPS. After the stimulation supernatants were harvested and cells were subjected to immunoblot analysis. **(A)** Western Blot analysis of total protein levels of ERK3 and ERK4 and phosphorylation of ERK1/2. MG-132 treatment was verified by probing with Ubiquitin antibody. Actin and Ponceau S are shown as loading control. **(B)** IL-8 concentration measured by ELISA. Results are represented as mean concentration (pg/ml) ± SEM from four (n=4) biological replicates per condition. *p<0.05, **p<0.01, ***p<0.001, t-test.

3.7.2 Opposing effects of LPS on ERK3 proteostasis in HT-29 and HCPECs

Considering the opposite effect of LPS stimulation on ERK3 in HT-29 and primary epithelial cells **(Figure 3.6 A-B)**, the ubiquitination status of the protein was evaluated in LPS-treated cell lines.

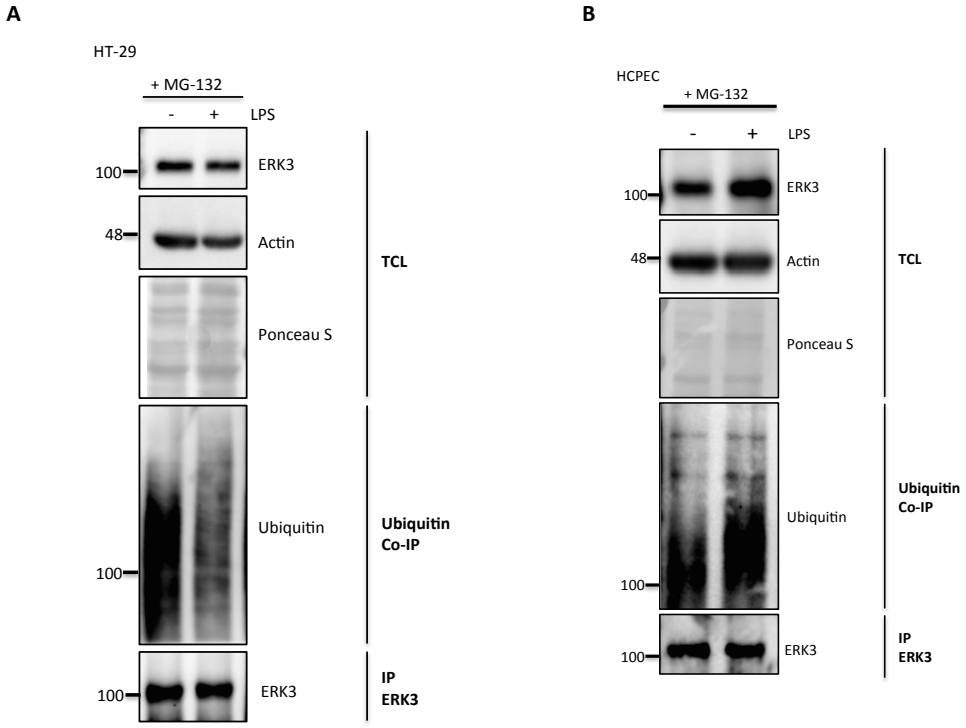

Figure 3.25 Contrasting effects of LPS stimulation on ERK3 poly ubiquitination in HT-29 and HCPECs. HT-29 and HCPECs cells were seeded in 10 cm dishes at an initial density of $2x10^6$ cells per dish. Next day medium was exchanged for medium with no supplements and cells were treated with MG-132 inhibitor for 6 h, followed by 4 h LPS stimulation. Cells were subjected to co-immunoprecipitation (Co-IP) with ERK3 antibody. Total cell lysates (TCL) and immunoprecipitates (IP) were analyzed by immunoblotting. Levels of ERK3 and the ubiquitination status of pulled down protein were monitored. Actin and Ponceau S staining were used as loading controls for TCL immunoblotting.

Results showed exactly opposite effects of LPS treatment on ERK3 ubiquitination in the cancer cell line HT-29 and in HCPECs **(Figure 3.25)**. Taken together, these data suggest

a role of the ubiquitin-proteasome pathway in LPS-dependent regulation of ERK3 protein levels in cancer derived and primary epithelial cells.

3.8 ERK3 controls epithelial architecture by controlling TFAP2A/AP-2 and ICAM-1

3.8.1 ERK3 regulates TFAP2A/AP-2 transcription factor

Recently, it was reported that ERK3 regulates transcription factor TFAP2A, commonly known as AP-2α, which regulates genes crucial for proper epithelial architecture development ([137], 2018). The results of this work presented thus far were showing the role of ERK3 in intestinal epithelial cell function, therefore transcriptome and TFs array derived data were screened and levels of AP-2 were analyzed in control and ERK3 depleted HCPECs.

As shown in **Figure 3.26,** knockdown of ERK3 led to a significant downregulation in AP-2 transcription factor activity **(Figure 3.26 A)** and its gene expression **(Figure 3.26 B)**. These data taken together with the recently published observations suggest a crucial role of ERK3 in maintaining epithelial architecture.

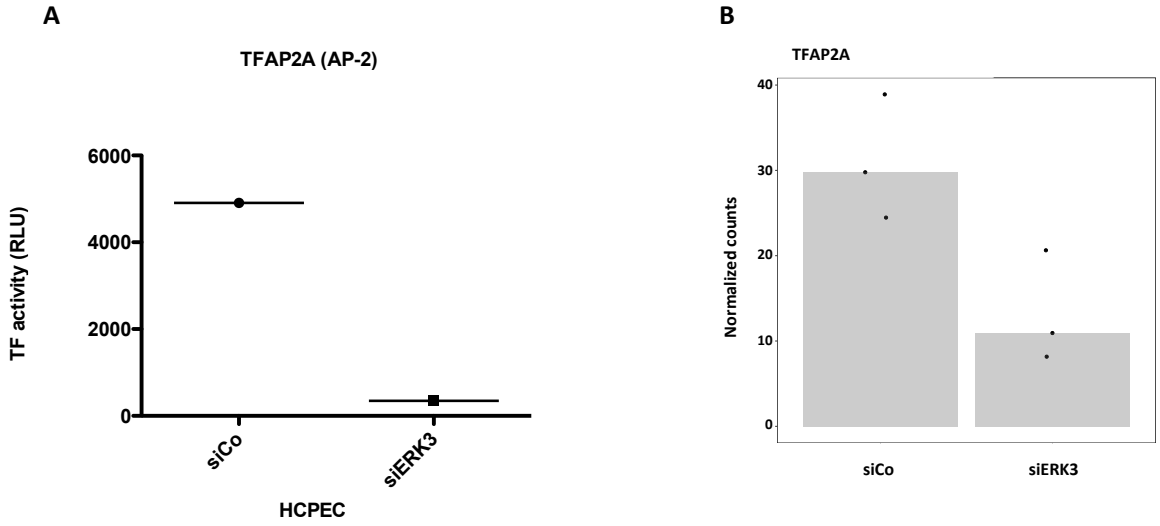

Figure 3.26 ERK3 regulates expression of AP-2 transcription factor. Control and ERK3 knockdown HCPECs were analyzed by TF-activating array (n=1 biological replicate) **(A)**, RNAseq (n=3 biological replicates) **(B)** and expression levels of TFAP2A were determined. A detailed description of the experiments and the evaluation can be found in the methods section.

3.8.2 ERK3 regulates expression of cell adhesion proteins, ICAM-1 and VCAM-1

Regulation of IL-8 expression grants ERK3 an enormous potential in regulating neutrophils chemotaxis to the site of injury, which is pivotal for wound healing as well as to evoke a proper immune response. LPS, TNF and IL-1β signaling in endothelial cells was reported to lead to an upregulation of transmembrane proteins involved in cell-cell adhesion, such as intercellular adhesion molecule-1 (ICAM-1) or vascular cell adhesion molecule 1 (VCAM-1) and triggers facilitation of leukocyte migration through the vessels and across the endothelium to the surrounding tissues [58]. ICAM-1 was reported to play a significant role in lymphocyte and neutrophil adhesion to the HT-29 colonic epithelial cells [138, 139]. Moreover, studies on epithelial cells revealed that secreted IL-8 enhances the expression of CD11/CD18 adhesion receptors by neutrophils, which enables the migration by promoting the interaction of the receptors with the adhesion molecules like ICAM-1 [139]. At the same time previous studies showed that CXCL8/IL-8 upregulates expression of ICAM-1 in HT-29 cells, thus promoting neutrophil-epithelium cell adhesion [139]. Infiltration by neutrophils requires a combination of chemotaxis and adhesion of the activated neutrophils to the epithelium, thus it became interesting to verify whether in addition to the IL-8 regulation, ERK3 can alter expression of ICAM-1 and VCAM-1 in HCPECs. As shown in **Figure 3.27 A and B,** RNAseq analysis revealed that indeed, ERK3 depletion leads to a significant transcriptional downregulation of two important cell adhesion proteins, ICAM-1 and VCAM-1.

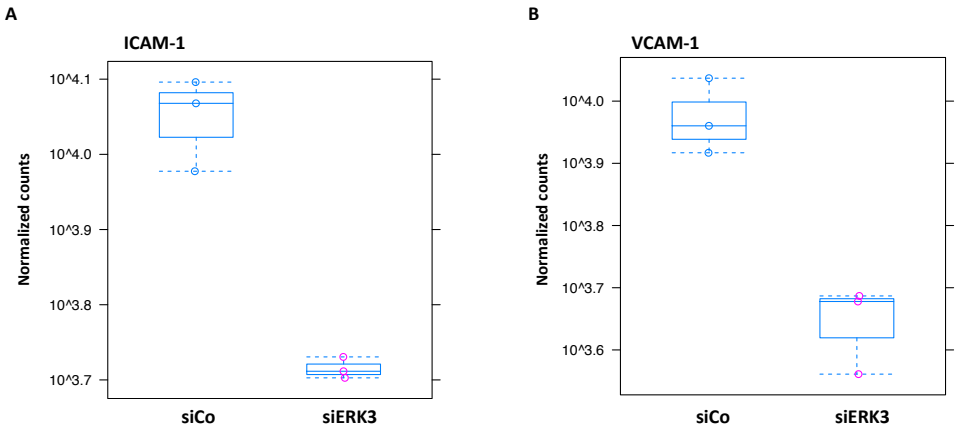

Figure 3.27 ERK3 regulates expression of cell adhesion molecules ICAM-1 and VCAM-1. RNAseq analysis of three biological replicates (n=3), representing differential expression in normalized counts of **(A)** ICAM-1 and **(B)** VCAM-1 levels in control and ERK3-depleted HCPECs**.**

Taken together, these data suggest an obligatory role for ERK3 in the regulation of epithelial secretome and neutrophil chemotaxis. We identifed a novel non-canonical pathway where ERK3 is critically required for basal as well as LPS induced IL-8 levels in both primary and tumor cells. Intriguingly, observed phenotype is kinase independent and despite the activation of classical MAPKs and NF-κB, ERK3 is critically required in multiple cell types for IL-8 production. Our data further suggest that inhibition of MEK1/2-ERK1/2 pathway with trametinib also reduced the protein stability of ERK3, uncovering thus far unknown obligatory and synergistic role for ERK3 in IL-8 regulation. Presented results describe how LPS triggers an opposing effect on ERK3 protein stability in primary epithelium and oncogenic cells. Finally, we could show that ERK3 is a new interacting partner of c-Jun and thus regulator of AP-1 activity. We were also able to uncover the physiological role of MK5 and ERK4 and shown that both regulate IL-8 levels in ERK3 dependent manner.

4. Discussion

4.1 LPS exerts opposing effects on ERK3 expression in primary epithelial cells and colon carcinoma cell lines

MAP kinases over the years emerged as one of the most versatile members within the kinome. Human genome encodes 566 kinases and most of the classical MAPKs have been reported to be ubiquitously expressed and engaged in regulation of the innate immune responses [57, 58]. Epithelial monolayer serves as the first line of defense against pathogens in the gastrointestinal tract. Emerging studies confer a direct role for the intestinal microbiome in regulating the immune responses [140, 141]. Epithelium creates a border between the luminal flora and the very sterile subepithelial immune system, therefore maintains mucosal homeostasis [142]. Similar to the immune cells like macrophages and dendritic cells (DCs), the intestinal epithelium expresses PRRs like TLRs. As described in the introduction, these transmembrane receptors recognize their ligand, which in turn contributes to the activation of signaling cascades to impinge on a specific phenotype. Bacterial-derived products like LPS induce the production of chemokines and initiate immune cells infiltration to the site of infection. LPS has been shown to evoke immediate inflammatory responses in intestinal epithelial cell lines *in vitro* by modulating cytokine secretion [128].

While the role of classical MAPKs in the regulation of immune responses is relatively well established, comparatively less is understood on the contribution of atypical MAPKs. Despite the discovery nearly 30 years ago, ERK3 remains understudied kinase. Majority of the published studies strongly suggest that ERK3 may exhibit oncogenic properties as it was reported to promote tumor cell migration, invasion and chemoresistance [39, 40, 43, 44, 143-145]. Given the potential role of ERK3 in mediating tumorigenesis it is crucial to characterize its immunomodulatory properties.

As described in the introduction, anti-tumor immune responses, angiogenesis and tumor immune microenvironment are modulated through the proper balance of pro and antiinflammatory cytokines. Discovering the role of ERK3 in modulating immune response would be an important step in deciphering its role in driving physiological and pathophysiological processes.

ERK3 has been reported to be highly expressed in the gastrointestinal tract, nevertheless, its physiological role in the gut remains elusive [25, 146]. Therefore, we first tested basal expression levels and kinetics of ERK3 activation in response to LPS in HT-29 cells a colon cancer derived cell line. Subsequent stimulation of the colon adenocarcinoma cells resulted in gradual increase of ERK3 total protein levels (Fig. 3.1 A-B). Further analyses of the ERK3 mRNA levels showed no significant alterations in relative expression of ERK3 upon LPS (Fig. 3.1 C) and CHX chase experiments further confirmed that LPS triggered an increase in the half-life of ERK3 protein (Fig. 3.1 D-E). Nevertheless, considering that HT-29 is a tumor derived cell line, it was essential to evaluate the role of ERK3 in normal, untransformed human colonic epithelial cells. Stimulation of HCPECs with LPS provoked drastic decrease in ERK3 protein levels, resulting in the completely opposite effect to the one observed in the cancer cells (Fig. 3.2 A-B). Healthy colonic epithelial layer can tolerate significant quantities of lumenal LPS, which can be explained by the fact that primary intestinal epithelial cells express very low levels of TLR4. Downregulation of TLR4 expression in IECs was reported previously [128, 142] and was confirmed by RNAseq of HCPECs in this study. Interestingly, upregulation of TLR4 is always associated with inflammatory bowel diseases like ulcerative colitis [128, 147, 148]. As shown in Fig. 3.3 E-F, among all detected TLRs, TLR3 seems to be highly expressed by primary epithelium, which confirms already published reports [128, 142], but the role of this receptor in mediating immune response in epithelial cells remains unexplored. Observed discrepancies in responsiveness to LPS between colon carcinoma and primary epithelial cells can be further confirmed by multiple reports describing upregulation of the TLR4 in colorectal cancer, including HT-29 cells [127, 149]. Data suggest that LPS-TLR4 activates multiple pathways resulting in tumor progression and metastasis [147, 150, 151].

4.2 ERK3 is indispensable for basal and LPS-induced levels of IL-8

IL-8 was first discovered as leukocyte chemotactic factor and since then this cytokine has emerged as a double-edged sword of inflammation [67]. The physiological role of CXCL8/IL-8 is mainly to regulate neutrophil chemotaxis, which is maintained by multitude of different mechanisms as introduced in section 1.4.1. Over the past 20 years, IL-8 was reported to play a crucial role in the pathogenesis of cancers. It has been shown to induce angiogenesis, EMT or protect tumor cells from apoptosis. Taken together, IL-8

was strongly suggested to promote progression of multiple human cancers [67, 78, 82, 83, 103, 117, 152-154]. Tumor cells can use the same signaling mechanisms as the immune cells and physiological tissue to activate autocrine feedback loops and maintain constant activity of IL-8/IL-8R module.

It is well established that upon infection, IL-8 secretion by the intestinal epithelium rises drastically [155]. Also, freshly isolated primary epithelial cells maintain basal physiological expression levels of IL-8 [119, 156]. Very interesting kinetics of ERK3 and canonical MAPKs observed in HCPECs upon LPS stimulation (Figure 3.2 A) encourage further analysis of these cells.

RNA sequencing and secretome analyses revealed that several crucial cytokines and chemokines regulating epithelial function and immune responses were altered at the steady state in ERK3 depleted HCPECs, suggesting that this atypical MAPK is required for the maintenance of epithelial secretome (Fig. 3.3 and 3.4). Transcriptome and secretome analyses revealed that ERK3 is indispensable for basal IL-8 levels (Fig. 3.3 D and 3.4 B). Multiple loss of function analyses confirmed the correlation between ERK3 expression and IL-8 levels in both, primary and tumor cells (Fig. 3.5, 3.8 and 3.9). Apart from regulating basal expression levels of IL-8, ERK3 was shown to play a key role in LPS-dependent alterations of the chemokine production, which suggests that ERK3 evokes expression levels of inflammatory modulators such as IL-8 in response to immune stimuli (Fig. 3.9). Interestingly, discrepancies in LPS-mediated ERK3 protein regulations in HCPECs and cancer-derived HT-29 cells were directly reflected in the IL-8 protein levels (Fig. 3.6 A and C and 3.6 B and D). Intriguingly, although HCPECs and HT-29 cells respond differently to LPS, mechanisms regulating IL-8 in both cell types are ERK3 dependent and the decrease in expression of ERK3 directly correlates with lower chemokine levels. Moreover, decrease in IL-8 levels was detected despite the fully activated canonical MAPKs, which as described in sections 1.3.1 and 1.4.2 along with NF-κB are the main regulators of chemokines production. Taken together, this data uncovers an atypical MAPK as an indispensable regulator of IL-8 production. However, these data also suggest synergism between ERK3 and canonical MAPKs in regulation of IL-8 levels.

4.3 Cross-talk between canonical MAPKs and ERK3 in regulating IL-8

As mentioned before, canonical MAPKs are major regulators of cytokines production. The p38 kinase was shown to stabilize CXCL8/IL-8 mRNA and together with JNK and ERK1/2 modules, to regulate AP-1 complex formation [63]. Our data consistently showed that despite the activation of the classical MAPKs and NF-κB, loss of ERK3 leads to a reduction of IL-8 levels. Furthermore, treatment with trametinib led to an additive decrease in IL-8 production in ERK3 deficient cells (Fig 3.22 G-H). These data suggest functional synergism between the classical MEK1/2-ERK1/2 pathway and ERK3 in controlling IL-8 levels. However, cross-talk between the MAPKs is rarely explored in case of the cytokine production and relation between canonical and poorly understood atypical MAP kinases seems to be crucial to truly understand the mechanism of action regulating IL-8.

Previous studies have shown that ERK1/2 inhibition and BRAF depletion leads to a downregulation of ERK3 protein levels [56]. Recently ([136], 2017), it was shown that inhibiting MEK1/2-ERK1/2 module by inhibiting either BRAF (PLX4720) or MEK (trametinib) leads to a decrease in IL-8 levels [136]. Our data demonstrated that MEK inhibitor treatment leads to a decrease in ERK3 expression in both: BRAFV600E mutated HT-29 cells as well as in CaCo2 cells, expressing wild type BRAF (Fig. 3.22 A and B). Likewise, blocking of BRAF with PLX4720 and GDC-0879 inhibitors led to a decrease in ERK3 protein expression (Fig. 3.22 F). Interestingly, the observed correlation between lower expression of ERK3 and CXCL8/IL-8 production was not shown previously, thus the observed downregulation in chemokine production was alluded to the inhibition in the activation of the MEK1/2-ERK1/2 module [136]. No significant effect of trametinib on the ERK3 mRNA levels (Fig. 3.22 E) further suggested that MEK1/2 kinases and the classical MAPK cascade seem to play a critical role in the regulation of ERK3 protein levels. Interestingly, treatment with proteasomal inhibitor rescued ERK3 levels in trametinib treated cells and as a consequence, restored IL-8 levels (Fig. 3.23). These data indicate that the classical MAPK is probably involved in the regulation of the ubiquitin signaling machinery that contributes to the ubiquitin-dependent turnover of ERK3 protein levels. Ubiquitin-proteasome system regulates major processes, including innate immune responses, exemplified by NF-κB signaling pathway described in section 1.3.2. Recently, ERK3 has been shown to be regulated by

USP20 deubiquitinase [37]. Deubiqutinases (DUBs) play a critical role in regulating protein abundance as they control removal of ubiquitin moieties from their substrate, thus maintaining proper protein quality and homeostasis [157]. It is also known that multiple DUBs can regulate the same substrate and apart from USP20, authors suggested two more USPs that might regulate ERK3 protein stability: USP13 and USP16 [37]. Considering that rapid protein turnover of ERK3 plays an important role in regulating its physiological outcome, it is crucial to identify E3 ligases regulating its ubiquitination and further evaluate role of MEK1/2-ERK1/2 signaling in regulation of the putative DUBs and E3 ubiquitin ligases controlling ERK3 protein abundance. Protein kinases, including MAPKs have already been reported to control protein stability by regulation of ubiquitin-proteasome system [158, 159]. It has been reported that enhanced phosphorylation of p38 MAPK in response to the osmotic stress negatively regulates 26 S proteasome activity [159]. Furthermore, MAPK and PI3K have been shown to phosphorylate and influence the ubiquitination and stability of RING finger E3 ubiquitin ligase RNF157 (Really interesting new gene (RING) finger protein 157) during the cell cycle [158]. Protein phosphorylation and its ubiquitination are not separate mechanisms and protein stability is linked to the phosphorylation status of the degradation signal, degron [160, 161]. Phosphodegron is a short amino acid sequence that when phosphorylated binds to the ubiquitin ligase, leading to protein degradation [161]. The main ubiquitin ligase that binds to phosphodegron is the Skp1-Cullin1-F-box ligase (SCF), which consists of a core (Skp1, Cullin1 and RING-box protein 1) and F-box protein that recognizes phosphorylated motifs of the substrate and recruits them to the SCF ubiquitin-ligase complex leading to the substrate ubiquitination [161, 162].

Considering that LPS triggers downregulation of ERK3 and thus IL-8 in HCPECs, we tested ERK3 kinetics in response to other innate immune stimuli like IL-1β and TNFα. We could readily detect an increase in the phosphorylation of ERK3 (S189) in response to both stimuli (Fig. 3.6 F-H). Moreover, IL-8 secretion can be elevated in primary epithelial cells by IL-1β and TNFα (Fig. 3.6 I-K), but further analyses are required to validate the possible role of ERK3 in regulating IL-1β and TNFα-mediated upregulation of IL-8 levels and on the cellular phenotypes.

4.4 ERK3 regulates IL-8 transcription and promoter activity in a kinase independent manner

ERK3-dependent regulation of IL-8 is maintained by transcriptional regulation of CXCL8/IL-8 gene by the atypical MAPK. More interestingly, reconstitution of ERK3 expression with kinase inactive mutant (K49A K50A) recovered IL-8 levels in ERK3 depleted cells to the same extent as wild type ERK3, suggesting a kinase independent role in this process (Fig. 3.10). Rapid turnover of ERK3 protein was already reported to be independent of its activation loop phosphorylation at S189 and kinase activity [32]. Here, we provide first physiological role for ERK3, which is kinase independent, but where ERK3 protein abundance maintains IL-8 levels.

All fundamental biological processes are regulated by protein phosphorylation and therefore protein kinases such as MAPKs have been intensively studied. Nevertheless, apart from their catalytic activities, increasing evidence, including presented here data suggest that non-catalytic roles of protein kinases can be not only substantial, but even sufficient to maintain their biological function [163]. The classical example is kinase-independent role of CRAF in the regulation of Rho-associated kinase alpha (ROK-α) [164]. It has been shown that CRAF physically interacts with ROK-α and knockdown of CRAF disrupts actin cytoskeleton in fibroblasts and keratinocytes leading to an attenuation of cell migration. Interestingly, reintroduction of kinase dead mutant of CRAF in knockout fibroblasts rescued observed defects in cell shape and migration [164].

ERK3 depletion attenuates IL-8 promoter activity in MDA MB231 cells (Fig. 3.11). As mentioned in section 1.4.1, to maintain promoter activity and thus IL-8 transcription, functional cooperativity of different TFs and their binding sites is crucial [63, 72]. Expression of CXCL8/IL-8 is mediated by binding of the transcription factors such as AP-1, NF-κB and CREB to the promoter sequence [63, 72]. Regulation of IL-8 promoter activity grants ERK3 an enormous potential. Furthermore, we were able to show that ERK3 controls activity of AP-1 in both, HCPECs (Fig. 3.19) and HT-29 cells (Fig. 3.20 D-E). The AP-1 activity was significantly downregulated in ERK3 knockdown cells, regardless of LPS stimulation. Interestingly, NF-κB activity was increased in the ERK3 depleted HCPECs with levels equivalent to those generated by LPS (Fig. 3.19 C). Moreover, elevated activity of NF-κB upon LPS stimulation did not have any effects on

reduced IL-8 levels (Fig. 3.19 D and E), in ERK3-depleted cells. Taking all the observations into account, it appears that NF-κB alone is not able to control IL-8 promoter activity and that ERK3 has a critical role in the process.

AP-1 is a transcription factor, which in most cells is composed of c-Fos and c-Jun heterodimeric complexes and its activity is regulated by MAPKs [63, 165]. c-Jun is a transcription factor, which is predominantly regulated by JNK [166, 167]. Interestingly, nuclear translocation of c-Jun has been proven to be independent of its phosphorylation by and interaction with JNK [168]. One of the potential non-catalytic roles of protein kinases is to function as a scaffold for interacting partners. Interestingly, this study provides evidence that ERK3 and c-Jun are present in the same complex (Fig. 3.20 A). Moreover, immunofluorescence based intra-cellular localization studies revealed that ERK3 is also required for c-Jun translocation to the nucleus, as ERK3 knockdown cells shown less c-Jun localization in the nuclear compartments (Fig. 3.20 B). Together with the finding that kinase activity of ERK3 is dispensable for IL-8 regulation, these data indicate scaffolding and translocating function of ERK3 for c-Jun. Activated JNK translocates to the nucleus where it can phosphorylate c-Jun at S63/73 and T91/93, which in turn enables c-Jun homodimerization or heterodimerization with c-Fos [169, 170]. Nevertheless, the capacity of JNK to regulate c-Jun activity is controlled by sub-nuclear localization of AP-1 proteins [170]. Therefore, it is tempting to hypothesize that ERK3 is required for the nuclear abundance of c-Jun and thus AP-1 activity.

4.5 Depletion of ERK3 in epithelial cells causes attenuation of leukocytes chemotaxis

As described in section 1.4.3, regulation of neutrophil chemotaxis is one of the main properties of IL-8. In the presented study, the main attribute of ERK3 was identified: maintaining proper physiological levels of IL-8, which in turn regulates epithelium-mediated leukocytes chemotaxis. While studying the *in vitro* migration of neutrophils and monocytes, the significant decrease was observed in chemotaxis mediated by secretome of ERK3-depleted HT-29 and HCPECs (Fig. 3.12). IL-8 neutralization led to a further decrease in chemotaxis within the control and ERK3 knockdown cells/supernatants, however, it was noticeable that the migration was not abolished completely. Considering that CXCL8/IL-8 is not the only chemokine modulating leukocytes migration to the site of infection, closer look into RNAseq and secretome data

revealed that knockdown of ERK3 leads to a downregulation of several potent chemotactic factors (Fig. 3.13). Taken together with the *in vitro* migration results it suggests that presence of MCP-1/CCL2, GCP-2/CXCL6 and NAP-2 might still control the migration, but not to the same extend as IL-8. It was already suggested that all other factors are there to boost IL-8-mediated chemotaxis [89, 93, 96, 133] and indication that ERK3 is able to control transcription of all of these chemokines, suggests a potent proinflammatory role for ERK3. To strengthen the results obtained by *in vitro* transwell migration, *in vivo* animal model of chemotaxis was studied. Diminished potential of supernatants obtained from ERK3-depleted HCPECs in promoting IL-8-mediated chemotaxis was further proved, most significantly in granulocytes and monocytes populations (Fig. 3.14).

Further, transcriptome analysis of the primary epithelial cells revealed that apart from controlling IL-8-mediated chemotaxis, ERK3 also regulates expression of adhesion molecules like ICAM-1 (Fig. 3.27). It was already reported that colonic carcinoma cells like CaCo2 and HT-29 express ICAM-1 molecules [171]. It has been suggested that ICAM-1 might be a prognostic factor for colon cancer [172, 173]. Previous reports indicated that ICAM-1 expression correlates with the progression of melanoma and breast cancer and should be considered as a new target in cancer treatment [174, 175]. As mentioned before, IL-8 upregulation contributes to the angiogenesis and EMT. *In vivo* and *in vitro* data in our study further confirmed that IL-8 plays a crucial role in regulating leukocyte chemotaxis and by all means can contribute to tumor microenvironment and metastasis. Taking into account that both, IL-8 and ICAM-1 are considered bad prognostic markers of cancer only confirms that ERK3 is a potential druggable target in cancer and inflammatory disorders.

There is only a small group of transcription factors regulating EMT during development and wound healing, but all of them can be altered into progressing tumor development for example by oncogenic Ras [176]. AP-2α (TFAP2A) was reported as an oncogenic factor in gastric, breast, lung and prostate cancer as well as in melanoma [177-185]. It was also related to neuroblastoma progression, as it seems to maintain highly proliferative phenotype in these tumors [186]. Furthermore, TFAP2A was labeled a conserved component of the network regulating EMT [186]. Nonetheless, mechanisms of its regulation remain largely unknown. Given the potential of EMT in tumor pathophysiology and latest publication about ERK3-dependent regulations of epithelial

architecture [121], it was even more exciting to observe that depletion of ERK3 from HCPECs resulted in downregulation of both, expression and activity of TFAP2A transcription factor (Fig. 3.26 A and B). ERK3 has been shown to maintain epithelial architecture. This study confirms that the transcriptional regulation of not only IL-8 and other chemotactic factors, but also of TFAP2A/AP-2 and its activity depends on ERK3 expression, provides yet another evidence that ERK3 has a critical physiological role in the regulation of epithelial function and homeostasis.

4.6 Functional interplay among ERK3, ERK4 and MK5

Considering all the published studies about ERK3-ERK4-MK5 signaling modules, it became interesting to verify physiological relevance of their interactions. All the recently published data strongly support irrelevance of the p38 kinase in regulation of MK5 and the high affinity of MAPKAPK to ERK3 [27, 31, 50]. Considering that MK5 is described as the selective substrate of ERK3, linearity of the pathway was assessed in consideration of the observed IL-8 decrease upon ERK3 depletion. Knockdown of MK5 led to a decrease in IL-8 production, which was then further confirmed on mRNA levels (Fig. 3.15 C and 3.16 D). Surprisingly, an interesting negative feedback loop was observed in MK5-depleted cells on the ERK3 protein expression (Fig. 3.15 A-B). These findings have been already suggested by Schumacher et al by testing primary embryonic fibroblasts from wild type and MK5 deficient mice, indicating stabilizing interaction between MK5 and ERK3 [31]. Our data did not show any further destabilization of labile ERK3 protein in MK5 knockdown cells (Fig. 3.16 A-B). However, CHX chase experiments performed in HT-29 and CaCo2 cells, combined with the mRNA levels analysis indicate that MK5 functions as a positive regulator of endogenous ERK3 mRNA levels in multiple cells lines (Fig. 3.16 C, 3.16 E-F). This interesting observation coupled with the downregulation of IL-8 mRNA expression in MK5-depleted cells (Fig. 3.16 D and F) further suggests that both: Direct and indirect downregulation of ERK3 expression results in reduction of CXCL8/IL-8 levels. These data suggests that MK5 functions as a positive regulator of endogenous ERK3.

As mentioned before, there is a definite cross-talk between expression levels of ERK3 and canonical MAPKs. Considering that MK5 was first discovered as a p38-regulated and activated kinase (PRAK), we tested the activity of classical MAPKs in MK5 knockdown

cells (Fig. 3.15 A and D). These results corroborate to our previous observations that in the absence of ERK3, even a very significant activation of the MEK1/2-ERK1/2 module or p38-MAPK is unable to compensate and reboot CXCL8/IL-8 levels. In addition to the strong activity of p38 and ERK1/2 upon MK5 depletion, complete degradation of IκB can also be observed in these cells (Fig. 3.15 A), indicating full activation of the canonical NF-κB pathway. These results validated the data obtained from the TFs array analysis (Fig. 3.19 C-F), where CXCL8/IL-8 levels were downregulated accordingly to the detected ERK3 expression, despite the upregulation in activity of NF-κB. All things considered, our data suggest that even an intermediate downregulation in ERK3 expression leads to a transcriptional downregulation of IL-8.

As explained in the introduction, ERK4 evolved as a paralog of ERK3, but no significant function of ERK4 neither in development nor in physiological processes has been described so far [45]. Considering the fact that ERK3 and ERK4 share distinct structural similarities and that both were identified as MK5 interacting partners, role of ERK4 in regulation of ERK3 and ERK3-dependent IL-8 phenotype needed to be addressed. Our data revealed that knockdown of ERK4 leads to an upregulation of ERK3 protein levels in both oncogenic and primary epithelial cells (Fig. 3.17 A-B and F-G respectively). Interestingly, ERK4 knockdown did not exert any strong effects on ERK3 protein stability (Fig. 3.17 A-B and F-G). Consistently, the enhanced levels of ERK3 in the ERK4 depleted cells led to a significant increase in CXCL8/IL-8 secretion (Fig. 3.17 C). Nevertheless, no significant effect of ERK4 knockdown was detected on ERK3 (Fig. 3.17 D and E), indicating a post-transcriptional/translational regulation of ERK3 by ERK4. Considering opposing effects exhibited by ERK3 and ERK4 depletion on IL-8 production, double knockdown experiments were performed, which recapitulated ERK3 knockdown phenotype (Fig. 3.18). Considering that the physiological role of ERK4 is not well established and that ERK4 controls ERK3 protein levels, further studies are clearly warranted. ERK4 is often detected in ERK3 precipitates and whether they function as a heteromeric complex is still an interesting and important issue to be addressed.

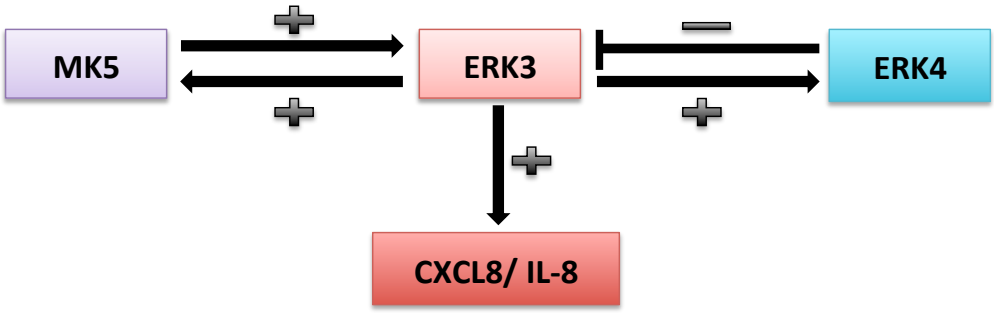

Figure 4.1 Schematic representation of the interplay between ERK3, ERK4 and MK5. ERK3 activates and interacts with MK5 regulating its phosphorylation and protein expression in return MK5 positively regulates ERK3 mRNA expression. ERK3 positively regulates ERK4 expression and levels of ERK3 expression correlate with ERK4 expression levels. In return, ERK4 negatively regulates ERK3 protein expression.

4.7 LPS as a double agent: Inducing and repressing proteasomal degradation of ERK3 in primary epithelium and colon cancer cells, respectively

Protein abundance of ERK3 seems to play a crucial role for IL-8 production. LPS-mediated downregulation of ERK3 protein expression (Fig. 3.2 A-C) provoked a drastic drop in IL-8 levels (Fig. 3.6 B and D) in HCPECs. Conversely, in HT-29 cells, LPS stimulation subsequently increased IL-8 production, while mediating sequential elevation of ERK3 protein rather than its transcription (Fig. 3.1 A-C). Protein turnover is a rapid mechanism controlling activation of signaling pathways in response to the extracellular stimuli, therefore any aberrations in the degradation rate underlie the pathogenesis of many diseases, including cancer [187-189]. ERK3 is a short-lived protein and as such is susceptible to ubiquitin-proteasome dependent regulations and its degradation by the 26 S proteasome system was reported previously [32, 35]. In our study we propose that the role of ERK3 in IL-8 regulation is at least partially sustained by a rapid synthesis and degradation of ERK3 protein. As HCPECs responded to LPS with accelerated attenuation of ERK3 protein expression, which consequently led to a significant decrease in IL-8 levels (Fig. 3.6 B and D respectively), we hypothesized that inhibition of the proteasomal degradation might restore the IL-8 phenotype. Pre-treatment of primary epithelial cells with MG-132 inhibitor blocked protein degradation and resulted in accumulation of ubiquitin conjugated ERK3 (Fig. 3.24 A), in consequence

rescuing the LPS-induced reduction in CXCL8/IL-8 levels (Fig. 3.24 B). It was also observed that the decrease in IL-8 production upon LPS stimulation and the increase following the MG-132 treatment was detected regardless of ERK1/2 activity (Fig. 3.24 A). These findings only further confirmed that ERK3 protein expression maintains high IL-8 levels in HCPECs, thus demonstrating that LPS-dependent destabilization of ERK3 in primary epithelium has a physiological relevance. Similarly to the previous observations (Fig. 3.23 A), proteasome inhibition and ERK3 protein aggregation led to overexpression of ERK4 (Fig. 3.24 A). This result provides further indication that there is a strong correlation between ERK3 and ERK4 proteins, while proving again that ERK4 protein expression is irrelevant for the IL-8 production per se, but further advocating its role as a regulator of ERK3 abundance.

Discrepancy in LPS-mediated regulation of ERK3 protein levels in HCPECs and HT-29 was further proved to be mediated by the proteasome. While LPS attenuates ubiquitination of ERK3 protein in oncogenic cells, thus leading to its stabilization, stimulation of HCPECs caused destabilization of the atypical MAPK, leading to an enhanced ubiquitination and degradation of ERK3 (Fig. 3.25 A-B). These results further confirmed that LPS exhibits opposing effects on ERK3 protein stability in primary and oncogenic epithelial cells.

More extensive studies are required to determine the E3 ligase of ERK3, but one might assume that differential expression of TLR4 in primary and cancer-derived epithelial cells plays a role in regulating the fate of ERK3 upon LPS stimulation. Furthermore, the discovery of the adverse effect of LPS on ERK3 in primary colonic epithelial cells might also be crucial in understanding how antibiotic treatments and subsequent lack of bacterial compounds in the colon are involved in the occurrence of inflammatory bowel disease [190]. As mentioned before, intestine epithelium is constantly exposed to significant levels of lumenal LPS and the low expression of TLR4 by the HCPECs might provide an explanation why they can tolerate LPS and maintain hyporesponsiveness towards lumenal bacteria. The discovery that ERK3 controls epithelial architecture and the secretome apart from shedding further insights into epithelial function also opens further avenues for targeting this kinase in pathophysiological conditions like chronic inflammation.

Conclusion and outlook

Overall, this thesis provides one of the first physiological roles of the atypical MAPKs while describing a novel non-canonical pathway regulating epithelial secretome and chemotaxis. In this study, we propose that LPS stimulation leads to a destabilization and stabilization of ERK3 protein in primary epithelium and oncogenic cells, respectively. Differences in ERK3-mediated IL-8 production in primary and cancerous epithelial cells open further possibilities in determining whether this atypical MAPK is the pivotal regulator of bowel inflammation and cancerogenesis. The fact that ERK3 regulates immune response not only by its transcriptional expression, but also by a cellular abundance grants this kinase a remarkable role in development and controlling pathological process like cancer. The cross-talk and synergism between the classical MAPK and EKR3 warrants reevaluation of roles that are assigned exclusively to the classical MAPKs. Furthermore, considering that labile nature of ERK3 has physiological relevance for maintaining proper physiological levels of IL-8, it is crucial to identify E3 ligases regulating ERK3 ubiquitination and further verify how MEK1/2-ERK1/2 pathway regulates ERK3 protein stability and identify the intersection between ERK3 and MAPK signaling pathway. Disclosure of ERK3 as a crucial regulator of innate immune responses opens new pathways of investigations, where discovered phenotypes can be used as readouts. Considering that ERK3 was already suggested to regulate epithelial architecture and data presented in this study, it is of importance to further evaluate role of this atypical MAPK in establishment and maintenance of intestinal epithelium. Animal models based evaluations are needed to further characterize tissue-specific role of ERK3 in disorders such as ulcerative colitis and colon cancer. Furthermore, ERK3 dependent regulation of c-Jun also requires further studies. Interacting region of the atypical MAPK and c-Jun as well as whether ERK3 can regulate phosphorylation of c-Jun and its homodimerization and heterodimerization with c-Fos deserves a closer look. Last but not least, verification how ERK4 regulates ERK3 protein deserves extra attention to finally identify physiological role for this atypical MAPK.

References

1. Cargnello, M. and P.P. Roux, *Activation and function of the MAPKs and their substrates, the MAPK-activated protein kinases.* Microbiol Mol Biol Rev, 2011. **75**(1): p. 50-83.
2. Raman, M., W. Chen, and M.H. Cobb, *Differential regulation and properties of MAPKs.* Oncogene, 2007. **26**(22): p. 3100-12.
3. Katz, M., I. Amit, and Y. Yarden, *Regulation of MAPKs by growth factors and receptor tyrosine kinases.* Biochim Biophys Acta, 2007. **1773**(8): p. 1161-76.
4. Rajalingam, K., et al., *Ras oncogenes and their downstream targets.* Biochim Biophys Acta, 2007. **1773**(8): p. 1177-95.
5. Yoon, S. and R. Seger, *The extracellular signal-regulated kinase: multiple substrates regulate diverse cellular functions.* Growth Factors, 2006. **24**(1): p. 21-44.
6. Gille, H., et al., *ERK phosphorylation potentiates Elk-1-mediated ternary complex formation and transactivation.* EMBO J, 1995. **14**(5): p. 951-62.
7. Hu, S., et al., *Profiling the human protein-DNA interactome reveals ERK2 as a transcriptional repressor of interferon signaling.* Cell, 2009. **139**(3): p. 610-22.
8. Fremin, C., et al., *Functional Redundancy of ERK1 and ERK2 MAP Kinases during Development.* Cell Rep, 2015. **12**(6): p. 913-21.
9. Marshall, C.J., *Specificity of receptor tyrosine kinase signaling: transient versus sustained extracellular signal-regulated kinase activation.* Cell, 1995. **80**(2): p. 179-85.
10. Osaki, L.H. and P. Gama, *MAPKs and signal transduction in the control of gastrointestinal epithelial cell proliferation and differentiation.* Int J Mol Sci, 2013. **14**(5): p. 10143-61.
11. Dikic, I., J. Schlessinger, and I. Lax, *PC12 cells overexpressing the insulin receptor undergo insulin-dependent neuronal differentiation.* Curr Biol, 1994. **4**(8): p. 702-8.
12. Traverse, S., et al., *Sustained activation of the mitogen-activated protein (MAP) kinase cascade may be required for differentiation of PC12 cells. Comparison of the effects of nerve growth factor and epidermal growth factor.* Biochem J, 1992. **288 (Pt 2)**: p. 351-5.
13. Wortzel, I. and R. Seger, *The ERK Cascade: Distinct Functions within Various Subcellular Organelles.* Genes Cancer, 2011. **2**(3): p. 195-209.
14. Geetha, N., et al., *Signal integration and coincidence detection in the mitogen-activated protein kinase/extracellular signal-regulated kinase (ERK) cascade: concomitant activation of receptor tyrosine kinases and of LRP-1 leads to sustained ERK phosphorylation via down-regulation of dual specificity phosphatases (DUSP1 and -6).* J Biol Chem, 2011. **286**(29): p. 25663-74.
15. Owens, D.M. and S.M. Keyse, *Differential regulation of MAP kinase signalling by dual-specificity protein phosphatases.* Oncogene, 2007. **26**(22): p. 3203-13.
16. Lin, Y.W. and J.L. Yang, *Cooperation of ERK and SCFSkp2 for MKP-1 destruction provides a positive feedback regulation of proliferating signaling.* J Biol Chem, 2006. **281**(2): p. 915-26.
17. Kidger, A.M. and S.M. Keyse, *The regulation of oncogenic Ras/ERK signalling by dual-specificity mitogen activated protein kinase phosphatases (MKPs).* Semin Cell Dev Biol, 2016. **50**: p. 125-32.
18. Gupta, S., et al., *Selective interaction of JNK protein kinase isoforms with transcription factors.* EMBO J, 1996. **15**(11): p. 2760-70.

19. Plotnikov, A., et al., *The MAPK cascades: signaling components, nuclear roles and mechanisms of nuclear translocation.* Biochim Biophys Acta, 2011. **1813**(9): p. 1619-33.
20. Mishra, P. and S. Gunther, *New insights into the structural dynamics of the kinase JNK3.* Sci Rep, 2018. **8**(1): p. 9435.
21. Tournier, C., et al., *Requirement of JNK for stress-induced activation of the cytochrome c-mediated death pathway.* Science, 2000. **288**(5467): p. 870-4.
22. Dhanasekaran, D.N. and E.P. Reddy, *JNK signaling in apoptosis.* Oncogene, 2008. **27**(48): p. 6245-51.
23. Jiang, Y., et al., *Characterization of the structure and function of a new mitogen-activated protein kinase (p38beta).* J Biol Chem, 1996. **271**(30): p. 17920-6.
24. Marie, C., S. Roman-Roman, and G. Rawadi, *Involvement of mitogen-activated protein kinase pathways in interleukin-8 production by human monocytes and polymorphonuclear cells stimulated with lipopolysaccharide or Mycoplasma fermentans membrane lipoproteins.* Infect Immun, 1999. **67**(2): p. 688-93.
25. Coulombe, P. and S. Meloche, *Atypical mitogen-activated protein kinases: structure, regulation and functions.* Biochim Biophys Acta, 2007. **1773**(8): p. 1376-87.
26. Rousseau, J., et al., *Targeted inactivation of Mapk4 in mice reveals specific nonredundant functions of Erk3/Erk4 subfamily mitogen-activated protein kinases.* Mol Cell Biol, 2010. **30**(24): p. 5752-63.
27. Aberg, E., et al., *Docking of PRAK/MK5 to the atypical MAPKs ERK3 and ERK4 defines a novel MAPK interaction motif.* J Biol Chem, 2009. **284**(29): p. 19392-401.
28. Bind, E., et al., *A novel mechanism for mitogen-activated protein kinase localization.* Mol Biol Cell, 2004. **15**(10): p. 4457-66.
29. Julien, C., P. Coulombe, and S. Meloche, *Nuclear export of ERK3 by a CRM1-dependent mechanism regulates its inhibitory action on cell cycle progression.* J Biol Chem, 2003. **278**(43): p. 42615-24.
30. Klinger, S., et al., *Loss of Erk3 function in mice leads to intrauterine growth restriction, pulmonary immaturity, and neonatal lethality.* Proc Natl Acad Sci U S A, 2009. **106**(39): p. 16710-5.
31. Schumacher, S., et al., *Scaffolding by ERK3 regulates MK5 in development.* EMBO J, 2004. **23**(24): p. 4770-9.
32. Coulombe, P., et al., *Rapid turnover of extracellular signal-regulated kinase 3 by the ubiquitin-proteasome pathway defines a novel paradigm of mitogen-activated protein kinase regulation during cellular differentiation.* Mol Cell Biol, 2003. **23**(13): p. 4542-58.
33. Ciechanover, A. and R. Ben-Saadon, *N-terminal ubiquitination: more protein substrates join in.* Trends Cell Biol, 2004. **14**(3): p. 103-6.
34. Tanguay, P.L., G. Rodier, and S. Meloche, *C-terminal domain phosphorylation of ERK3 controlled by Cdk1 and Cdc14 regulates its stability in mitosis.* Biochem J, 2010. **428**(1): p. 103-11.
35. Coulombe, P., et al., *N-Terminal ubiquitination of extracellular signal-regulated kinase 3 and p21 directs their degradation by the proteasome.* Mol Cell Biol, 2004. **24**(14): p. 6140-50.
36. Mikalsen, T., M. Johannessen, and U. Moens, *Sequence- and position-dependent tagging protects extracellular-regulated kinase 3 protein from 26S proteasome-mediated degradation.* Int J Biochem Cell Biol, 2005. **37**(12): p. 2513-20.
37. Mathien, S., et al., *Deubiquitinating Enzyme USP20 Regulates Extracellular Signal-Regulated Kinase 3 Stability and Biological Activity.* Mol Cell Biol, 2017. **37**(9).
38. Perander, M., et al., *Regulation of atypical MAP kinases ERK3 and ERK4 by the phosphatase DUSP2.* Sci Rep, 2017. **7**: p. 43471.

39. Wang, W., et al., *ERK3 promotes endothelial cell functions by upregulating SRC-3/SP1-mediated VEGFR2 expression.* J Cell Physiol, 2014. **229**(10): p. 1529-37.
40. Long, W., et al., *ERK3 signals through SRC-3 coactivator to promote human lung cancer cell invasion.* J Clin Invest, 2012. **122**(5): p. 1869-80.
41. Marquis, M., et al., *The non-classical MAP kinase ERK3 controls T cell activation.* PLoS One, 2014. **9**(1): p. e86681.
42. Sirois, J., et al., *The atypical MAPK ERK3 controls positive selection of thymocytes.* Immunology, 2015. **145**(1): p. 161-9.
43. Bian, K., et al., *ERK3 regulates TDP2-mediated DNA damage response and chemoresistance in lung cancer cells.* Oncotarget, 2016. **7**(6): p. 6665-75.
44. Al-Mahdi, R., et al., *A novel role for atypical MAPK kinase ERK3 in regulating breast cancer cell morphology and migration.* Cell Adh Migr, 2015. **9**(6): p. 483-94.
45. Kant, S., et al., *Characterization of the atypical MAPK ERK4 and its activation of the MAPK-activated protein kinase MK5.* J Biol Chem, 2006. **281**(46): p. 35511-9.
46. New, L., et al., *PRAK, a novel protein kinase regulated by the p38 MAP kinase.* EMBO J, 1998. **17**(12): p. 3372-84.
47. Ni, H., et al., *MAPKAPK5, a novel mitogen-activated protein kinase (MAPK)-activated protein kinase, is a substrate of the extracellular-regulated kinase (ERK) and p38 kinase.* Biochem Biophys Res Commun, 1998. **243**(2): p. 492-6.
48. Shi, Y., et al., *Elimination of protein kinase MK5/PRAK activity by targeted homologous recombination.* Mol Cell Biol, 2003. **23**(21): p. 7732-41.
49. Underwood, K.W., et al., *Catalytically active MAP KAP kinase 2 structures in complex with staurosporine and ADP reveal differences with the autoinhibited enzyme.* Structure, 2003. **11**(6): p. 627-36.
50. Seternes, O.M., et al., *Activation of MK5/PRAK by the atypical MAP kinase ERK3 defines a novel signal transduction pathway.* EMBO J, 2004. **23**(24): p. 4780-91.
51. Aberg, E., et al., *Regulation of MAPK-activated protein kinase 5 activity and subcellular localization by the atypical MAPK ERK4/MAPK4.* J Biol Chem, 2006. **281**(46): p. 35499-510.
52. Perander, M., et al., *The Ser186phospho-acceptor site within ERK4 is essential for its ability to interact with and activate PRAK/MK5.* Biochemical Journal, 2008. **411**(3): p. 613-622.
53. Deleris, P., et al., *Activation loop phosphorylation of ERK3/ERK4 by group I p21-activated kinases (PAKs) defines a novel PAK-ERK3/4-MAPK-activated protein kinase 5 signaling pathway.* J Biol Chem, 2011. **286**(8): p. 6470-8.
54. De la Mota-Peynado, A., J. Chernoff, and A. Beeser, *Identification of the atypical MAPK Erk3 as a novel substrate for p21-activated kinase (Pak) activity.* J Biol Chem, 2011. **286**(15): p. 13603-11.
55. Wan, P.T., et al., *Mechanism of activation of the RAF-ERK signaling pathway by oncogenic mutations of B-RAF.* Cell, 2004. **116**(6): p. 855-67.
56. Hoeflich, K.P., et al., *Regulation of ERK3/MAPK6 expression by BRAF.* Int J Oncol, 2006. **29**(4): p. 839-49.
57. Arthur, J.S.C. and S.C. Ley, *Mitogen-activated protein kinases in innate immunity.* Nature Reviews Immunology, 2013. **13**(9): p. 679-692.
58. Newton, K. and V.M. Dixit, *Signaling in Innate Immunity and Inflammation.* Cold Spring Harbor Perspectives in Biology, 2012. **4**(3): p. a006049-a006049.
59. Kawai, T. and S. Akira, *The role of pattern-recognition receptors in innate immunity: update on Toll-like receptors.* Nature Immunology, 2010. **11**(5): p. 373-384.
60. Lu, Y.C., W.C. Yeh, and P.S. Ohashi, *LPS/TLR4 signal transduction pathway.* Cytokine, 2008. **42**(2): p. 145-151.
61. Mogensen, T.H., *Pathogen Recognition and Inflammatory Signaling in Innate Immune Defenses.* Clinical Microbiology Reviews, 2009. **22**(2): p. 240-273.

62. Oeckinghaus, A. and S. Ghosh, *The NF-kappaB family of transcription factors and its regulation.* Cold Spring Harb Perspect Biol, 2009. **1**(4): p. a000034.
63. Hoffmann, E., et al., *Multiple control of interleukin-8 gene expression.* J Leukoc Biol, 2002. **72**(5): p. 847-55.
64. Roget, K., et al., *I B Kinase 2 Regulates TPL-2 Activation of Extracellular Signal-Regulated Kinases 1 and 2 by Direct Phosphorylation of TPL-2 Serine 400.* Molecular and Cellular Biology, 2012. **32**(22): p. 4684-4690.
65. Tseng, P.-H., et al., *Different modes of ubiquitination of the adaptor TRAF3 selectively activate the expression of type I interferons and proinflammatory cytokines.* Nature Immunology, 2009. **11**(1): p. 70-75.
66. Beck, P.L., et al., *Interleukin-8 in gastrointestinal inflammation and malignancy: induction and clinical consequences.* International Journal of Interferon, Cytokine and Mediator Research, 2016: p. 13.
67. David, J.M., et al., *The IL-8/IL-8R Axis: A Double Agent in Tumor Immune Resistance.* Vaccines (Basel), 2016. **4**(3).
68. Balkwill, F., *Cancer and the chemokine network.* Nat Rev Cancer, 2004. **4**(7): p. 540-50.
69. Sallusto, F. and M. Baggiolini, *Chemokines and leukocyte traffic.* Nat Immunol, 2008. **9**(9): p. 949-52.
70. Holtmann, H., et al., *Induction of interleukin-8 synthesis integrates effects on transcription and mRNA degradation from at least three different cytokine- or stress-activated signal transduction pathways.* Mol Cell Biol, 1999. **19**(10): p. 6742-53.
71. Harant, H., et al., *Synergistic activation of interleukin-8 gene transcription by all-trans-retinoic acid and tumor necrosis factor-alpha involves the transcription factor NF-kappaB.* J Biol Chem, 1996. **271**(43): p. 26954-61.
72. Jundi, K. and C. Greene, *Transcription of Interleukin-8: How Altered Regulation Can Affect Cystic Fibrosis Lung Disease.* Biomolecules, 2015. **5**(3): p. 1386-1398.
73. Wu, G.D., et al., *Oct-1 and CCAAT/enhancer-binding protein (C/EBP) bind to overlapping elements within the interleukin-8 promoter. The role of Oct-1 as a transcriptional repressor.* J Biol Chem, 1997. **272**(4): p. 2396-403.
74. Nourbakhsh, M., et al., *The NF-kappa b repressing factor is involved in basal repression and interleukin (IL)-1-induced activation of IL-8 transcription by binding to a conserved NF-kappa b-flanking sequence element.* J Biol Chem, 2001. **276**(6): p. 4501-8.
75. Vanden Berghe, W., et al., *The nuclear factor-kappaB engages CBP/p300 and histone acetyltransferase activity for transcriptional activation of the interleukin-6 gene promoter.* J Biol Chem, 1999. **274**(45): p. 32091-8.
76. Krause, A., et al., *Stress-activated protein kinase/Jun N-terminal kinase is required for interleukin (IL)-1-induced IL-6 and IL-8 gene expression in the human epidermal carcinoma cell line KB.* J Biol Chem, 1998. **273**(37): p. 23681-9.
77. Suzuki, M., et al., *The role of p38 mitogen-activated protein kinase in IL-6 and IL-8 production from the TNF-alpha- or IL-1beta-stimulated rheumatoid synovial fibroblasts.* FEBS Lett, 2000. **465**(1): p. 23-7.
78. Chan, L.P., et al., *IL-8 promotes inflammatory mediators and stimulates activation of p38 MAPK/ERK-NF-kappaB pathway and reduction of JNK in HNSCC.* Oncotarget, 2017. **8**(34): p. 56375-56388.
79. Zeigler, M.E., et al., *Role of ERK and JNK pathways in regulating cell motility and matrix metalloproteinase 9 production in growth factor-stimulated human epidermal keratinocytes.* J Cell Physiol, 1999. **180**(2): p. 271-84.
80. Scherle, P.A., et al., *Inhibition of MAP kinase kinase prevents cytokine and prostaglandin E2 production in lipopolysaccharide-stimulated monocytes.* J Immunol, 1998. **161**(10): p. 5681-6.

81. Babu, G.J., et al., *Phosphorylation of elk-1 by MEK/ERK pathway is necessary for c-fos gene activation during cardiac myocyte hypertrophy.* J Mol Cell Cardiol, 2000. **32**(8): p. 1447-57.
82. Li, A., et al., *IL-8 directly enhanced endothelial cell survival, proliferation, and matrix metalloproteinases production and regulated angiogenesis.* J Immunol, 2003. **170**(6): p. 3369-76.
83. Itoh, Y., et al., *IL-8 promotes cell proliferation and migration through metalloproteinase-cleavage proHB-EGF in human colon carcinoma cells.* Cytokine, 2005. **29**(6): p. 275-82.
84. Kuhns, D.B., et al., *Ca2+-dependent production and release of IL-8 in human neutrophils.* J Immunol, 1998. **161**(8): p. 4332-9.
85. Prame Kumar, K., A.J. Nicholls, and C.H.Y. Wong, *Partners in crime: neutrophils and monocytes/macrophages in inflammation and disease.* Cell Tissue Res, 2018. **371**(3): p. 551-565.
86. Van Damme, J., et al., *Granulocyte chemotactic protein-2 and related CXC chemokines: from gene regulation to receptor usage.* J Leukoc Biol, 1997. **62**(5): p. 563-9.
87. Besemer, J., *Neutrophil-activating peptides NAP-2 and IL-8 bind to the same sites on neutrophils but interact in different ways. Discrepancies in binding affinities, receptor densities, and biological effects.* J Immunol, 1995. **154**(2): p. 972-4.
88. Malawista, S.E., et al., *Chemotactic activity of human blood leukocytes in plasma treated with EDTA: chemoattraction of neutrophils about monocytes is mediated by the generation of NAP-2.* J Leukoc Biol, 2002. **72**(1): p. 175-82.
89. Benigni, G., et al., *CXCR3/CXCL10 Axis Regulates Neutrophil-NK Cell Cross-Talk Determining the Severity of Experimental Osteoarthritis.* J Immunol, 2017. **198**(5): p. 2115-2124.
90. Agostini, C., et al., *Cxcr3 and its ligand CXCL10 are expressed by inflammatory cells infiltrating lung allografts and mediate chemotaxis of T cells at sites of rejection.* Am J Pathol, 2001. **158**(5): p. 1703-11.
91. Lang, S., et al., *CXCL10/IP-10 Neutralization Can Ameliorate Lipopolysaccharide-Induced Acute Respiratory Distress Syndrome in Rats.* PLoS One, 2017. **12**(1): p. e0169100.
92. Ichikawa, A., et al., *CXCL10-CXCR3 enhances the development of neutrophil-mediated fulminant lung injury of viral and nonviral origin.* Am J Respir Crit Care Med, 2013. **187**(1): p. 65-77.
93. Volpe, S., et al., *CCR2 acts as scavenger for CCL2 during monocyte chemotaxis.* PLoS One, 2012. **7**(5): p. e37208.
94. Iwamoto, T., et al., *A role of monocyte chemoattractant protein-4 (MCP-4)/CCL13 from chondrocytes in rheumatoid arthritis.* Febs Journal, 2007. **274**(18): p. 4904-4912.
95. Iwamoto, T., et al., *Production of monocyte chemoattractant protein-4 (MCP-4)/CCL13 by interferon-gamma-activated human chondrocytes and its role in rheumatoid arthritis.* Arthritis and Rheumatism, 2006. **54**(9): p. S88-S88.
96. Iwamoto, T., et al., *Monocyte chemoattractant protein-4 (MCP-4)/CCL13 is highly expressed in cartilage from patients with rheumatoid arthritis.* Rheumatology, 2006. **45**(4): p. 421-424.
97. Katano, M., et al., *Increased expression of S100 calcium binding protein A8 in GM-CSF-stimulated neutrophils leads to the increased expressions of IL-8 and IL-16.* Clin Exp Rheumatol, 2011. **29**(5): p. 768-75.
98. Hidi, R., et al., *Role of B7-CD28/CTLA-4 costimulation and NF-kappa B in allergen-induced T cell chemotaxis by IL-16 and RANTES.* J Immunol, 2000. **164**(1): p. 412-8.

99. Laberge, S., et al., *Secretion of IL-16 (lymphocyte chemoattractant factor) from serotonin-stimulated CD8+ T cells in vitro.* J Immunol, 1996. **156**(1): p. 310-5.
100. Loosen, S.H., et al., *IL-6 and IL-8 Serum Levels Predict Tumor Response and Overall Survival after TACE for Primary and Secondary Hepatic Malignancies.* Int J Mol Sci, 2018. **19**(6).
101. Konenkov, V.I., et al., *Blood Serum Levels of Proinflammatory Cytokines (IL-1beta, IL-6, TNFalpha, IL-8, IL-12p70, and IFNgamma) in Patients with Uterine Myoma.* Bull Exp Biol Med, 2018. **165**(5): p. 698-701.
102. Feng, L., et al., *Serum levels of IL-6, IL-8, and IL-10 are indicators of prognosis in pancreatic cancer.* J Int Med Res, 2018: p. 300060518800588.
103. Long, X., et al., *IL-8, a novel messenger to cross-link inflammation and tumor EMT via autocrine and paracrine pathways (Review).* Int J Oncol, 2016. **48**(1): p. 5-12.
104. Waugh, D.J. and C. Wilson, *The interleukin-8 pathway in cancer.* Clin Cancer Res, 2008. **14**(21): p. 6735-41.
105. Rao, H.L., et al., *Increased intratumoral neutrophil in colorectal carcinomas correlates closely with malignant phenotype and predicts patients' adverse prognosis.* PLoS One, 2012. **7**(1): p. e30806.
106. Kuang, D.M., et al., *Peritumoral neutrophils link inflammatory response to disease progression by fostering angiogenesis in hepatocellular carcinoma.* J Hepatol, 2011. **54**(5): p. 948-55.
107. Wang, J., et al., *The clinical significance of tumor-infiltrating neutrophils and neutrophil-to-CD8+ lymphocyte ratio in patients with resectable esophageal squamous cell carcinoma.* J Transl Med, 2014. **12**: p. 7.
108. Trellakis, S., et al., *Peripheral blood neutrophil granulocytes from patients with head and neck squamous cell carcinoma functionally differ from their counterparts in healthy donors.* Int J Immunopathol Pharmacol, 2011. **24**(3): p. 683-93.
109. Wislez, M., et al., *Hepatocyte growth factor production by neutrophils infiltrating bronchioloalveolar subtype pulmonary adenocarcinoma: role in tumor progression and death.* Cancer Res, 2003. **63**(6): p. 1405-12.
110. Jensen, T.O., et al., *Intratumoral neutrophils and plasmacytoid dendritic cells indicate poor prognosis and are associated with pSTAT3 expression in AJCC stage I/II melanoma.* Cancer, 2012. **118**(9): p. 2476-85.
111. Ginestier, C., et al., *CXCR1 blockade selectively targets human breast cancer stem cells in vitro and in xenografts.* J Clin Invest, 2010. **120**(2): p. 485-97.
112. Brandolini, L., et al., *Targeting CXCR1 on breast cancer stem cells: signaling pathways and clinical application modelling.* Oncotarget, 2015. **6**(41): p. 43375-94.
113. Hwang, W.L., et al., *SNAIL regulates interleukin-8 expression, stem cell-like activity, and tumorigenicity of human colorectal carcinoma cells.* Gastroenterology, 2011. **141**(1): p. 279-91, 291 e1-5.
114. Khan, M.N., et al., *CXCR1/2 antagonism with CXCL8/Interleukin-8 analogue CXCL8(3-72)K11R/G31P restricts lung cancer growth by inhibiting tumor cell proliferation and suppressing angiogenesis.* Oncotarget, 2015. **6**(25): p. 21315-27.
115. Chen, L., et al., *The IL-8/CXCR1 axis is associated with cancer stem cell-like properties and correlates with clinical prognosis in human pancreatic cancer cases.* Sci Rep, 2014. **4**: p. 5911.
116. Schinke, C., et al., *IL8-CXCR2 pathway inhibition as a therapeutic strategy against MDS and AML stem cells.* Blood, 2015. **125**(20): p. 3144-52.
117. Palena, C., D.H. Hamilton, and R.I. Fernando, *Influence of IL-8 on the epithelial-mesenchymal transition and the tumor microenvironment.* Future Oncol, 2012. **8**(6): p. 713-22.

118. Pitman, R.S. and R.S. Blumberg, *First line of defense: the role of the intestinal epithelium as an active component of the mucosal immune system.* J Gastroenterol, 2000. **35**(11): p. 805-14.
119. Eckmann, L., et al., *Differential cytokine expression by human intestinal epithelial cell lines: regulated expression of interleukin 8.* Gastroenterology, 1993. **105**(6): p. 1689-97.
120. Hennig, G., et al., *Mechanisms identified in the transcriptional control of epithelial gene expression.* J Biol Chem, 1996. **271**(1): p. 595-602.
121. Takahashi, C., et al., *The atypical mitogen-activated protein kinase ERK3 is essential for establishment of epithelial architecture.* J Biol Chem, 2018. **293**(22): p. 8342-8361.
122. Zhang, J., et al., *Neural tube, skeletal and body wall defects in mice lacking transcription factor AP-2.* Nature, 1996. **381**(6579): p. 238-41.
123. Milunsky, J.M., et al., *TFAP2A mutations result in branchio-oculo-facial syndrome.* Am J Hum Genet, 2008. **82**(5): p. 1171-7.
124. Dobin, A., et al., *STAR: ultrafast universal RNA-seq aligner.* Bioinformatics, 2013. **29**(1): p. 15-21.
125. Love, M.I., W. Huber, and S. Anders, *Moderated estimation of fold change and dispersion for RNA-seq data with DESeq2.* Genome Biol, 2014. **15**(12): p. 550.
126. Zhu, A., J.G. Ibrahim, and M.I. Love, *Heavy-tailed prior distributions for sequence count data: removing the noise and preserving large differences.* Bioinformatics, 2018.
127. Abreu, M.T., et al., *TLR4 and MD-2 expression is regulated by immune-mediated signals in human intestinal epithelial cells.* J Biol Chem, 2002. **277**(23): p. 20431-7.
128. Cario, E. and D.K. Podolsky, *Differential alteration in intestinal epithelial cell expression of toll-like receptor 3 (TLR3) and TLR4 in inflammatory bowel disease.* Infect Immun, 2000. **68**(12): p. 7010-7.
129. Drost, E.M. and W. MacNee, *Potential role of IL-8, platelet-activating factor and TNF-alpha in the sequestration of neutrophils in the lung: effects on neutrophil deformability, adhesion receptor expression, and chemotaxis.* Eur J Immunol, 2002. **32**(2): p. 393-403.
130. Morland, C.M., et al., *Migration of CD18-deficient neutrophils in vitro: evidence for a CD18-independent pathway induced by IL-8.* Biochim Biophys Acta, 2000. **1500**(1): p. 70-6.
131. Burns, M.J., et al., *Production of interleukin-8 (IL-8) by cultured endothelial cells in response to Borrelia burgdorferi occurs independently of secreted [corrected] IL-1 and tumor necrosis factor alpha and is required for subsequent transendothelial migration of neutrophils.* Infect Immun, 1997. **65**(4): p. 1217-22.
132. Hammond, M.E., et al., *IL-8 induces neutrophil chemotaxis predominantly via type I IL-8 receptors.* J Immunol, 1995. **155**(3): p. 1428-33.
133. Adams, D.H. and A.R. Lloyd, *Chemokines: leucocyte recruitment and activation cytokines.* Lancet, 1997. **349**(9050): p. 490-5.
134. Singer, M. and P.J. Sansonetti, *IL-8 is a key chemokine regulating neutrophil recruitment in a new mouse model of Shigella-induced colitis.* J Immunol, 2004. **173**(6): p. 4197-206.
135. Deleris, P., et al., *Activation loop phosphorylation of the atypical MAP kinases ERK3 and ERK4 is required for binding, activation and cytoplasmic relocalization of MK5.* J Cell Physiol, 2008. **217**(3): p. 778-88.
136. Hartman, M.L., et al., *Vemurafenib and trametinib reduce expression of CTGF and IL-8 in (V600E)BRAF melanoma cells.* Lab Invest, 2017. **97**(2): p. 217-227.
137. Magnaldo, T., et al., *On the role of AP2 in epithelial-specific gene expression.* Gene Expr, 1993. **3**(3): p. 307-15.

138. Kelly, C.P., et al., *Human colon cancer cells express ICAM-1 in vivo and support LFA-1-dependent lymphocyte adhesion in vitro.* Am J Physiol, 1992. **263**(6 Pt 1): p. G864-70.
139. Kelly, C.P., et al., *IL-8 secretion and neutrophil activation by HT-29 colonic epithelial cells.* Am J Physiol, 1994. **267**(6 Pt 1): p. G991-7.
140. Round, J.L. and S.K. Mazmanian, *The gut microbiota shapes intestinal immune responses during health and disease.* Nat Rev Immunol, 2009. **9**(5): p. 313-23.
141. Geuking, M.B., et al., *The interplay between the gut microbiota and the immune system.* Gut Microbes, 2014. **5**(3): p. 411-8.
142. Pott, J. and M. Hornef, *Innate immune signalling at the intestinal epithelium in homeostasis and disease.* EMBO Rep, 2012. **13**(8): p. 684-98.
143. Elkhadragy, L., et al., *Activation loop phosphorylation of ERK3 is important for its kinase activity and ability to promote lung cancer cell invasiveness.* J Biol Chem, 2018.
144. Elkhadragy, L., et al., *A regulatory BMI1/let-7i/ERK3 pathway controls the motility of head and neck cancer cells.* Mol Oncol, 2017. **11**(2): p. 194-207.
145. Kostenko, S., G. Dumitriu, and U. Moens, *Tumour promoting and suppressing roles of the atypical MAP kinase signalling pathway ERK3/4-MK5.* J Mol Signal, 2012. **7**(1): p. 9.
146. Broom, O.J., et al., *Mitogen activated protein kinases: a role in inflammatory bowel disease?* Clin Exp Immunol, 2009. **158**(3): p. 272-80.
147. Tang, X.Y., et al., *Expression and functional research of TLR4 in human colon carcinoma.* Am J Med Sci, 2010. **339**(4): p. 319-26.
148. Fan, Y. and B. Liu, *Expression of Toll-like receptors in the mucosa of patients with ulcerative colitis.* Exp Ther Med, 2015. **9**(4): p. 1455-1459.
149. Furrie, E., et al., *Toll-like receptors-2, -3 and -4 expression patterns on human colon and their regulation by mucosal-associated bacteria.* Immunology, 2005. **115**(4): p. 565-74.
150. Yesudhas, D., et al., *Multiple roles of toll-like receptor 4 in colorectal cancer.* Front Immunol, 2014. **5**: p. 334.
151. Gross, V., et al., *Regulation of interleukin-8 production in a human colon epithelial cell line (HT-29).* Gastroenterology, 1995. **108**(3): p. 653-61.
152. Ji, H., et al., *K-ras activation generates an inflammatory response in lung tumors.* Oncogene, 2006. **25**(14): p. 2105-12.
153. Sparmann, A. and D. Bar-Sagi, *Ras-induced interleukin-8 expression plays a critical role in tumor growth and angiogenesis.* Cancer Cell, 2004. **6**(5): p. 447-58.
154. Xu, L. and I.J. Fidler, *Interleukin 8: an autocrine growth factor for human ovarian cancer.* Oncol Res, 2000. **12**(2): p. 97-106.
155. Johnston, S.L., et al., *Low grade rhinovirus infection induces a prolonged release of IL-8 in pulmonary epithelium.* J Immunol, 1998. **160**(12): p. 6172-81.
156. van Deventer, S.J., *Review article: Chemokine production by intestinal epithelial cells: a therapeutic target in inflammatory bowel disease?* Aliment Pharmacol Ther, 1997. **11 Suppl 3**: p. 116-20; discussion 120-1.
157. Yuan, T., et al., *Inhibition of Ubiquitin-Specific Proteases as a Novel Anticancer Therapeutic Strategy.* Front Pharmacol, 2018. **9**: p. 1080.
158. Dogan, T., et al., *Role of the E3 ubiquitin ligase RNF157 as a novel downstream effector linking PI3K and MAPK signaling pathways to the cell cycle.* J Biol Chem, 2017. **292**(35): p. 14311-14324.
159. Lee, S.H., et al., *Osmotic stress inhibits proteasome by p38 MAPK-dependent phosphorylation.* J Biol Chem, 2010. **285**(53): p. 41280-9.
160. Cohen, P. and M. Tcherpakov, *Will the ubiquitin system furnish as many drug targets as protein kinases?* Cell, 2010. **143**(5): p. 686-93.

161. Holt, L.J., *Regulatory modules: Coupling protein stability to phopshoregulation during cell division.* FEBS Lett, 2012. **586**(17): p. 2773-7.
162. Skowyra, D., et al., *F-box proteins are receptors that recruit phosphorylated substrates to the SCF ubiquitin-ligase complex.* Cell, 1997. **91**(2): p. 209-19.
163. Rauch, J., et al., *The secret life of kinases: functions beyond catalysis.* Cell Commun Signal, 2011. **9**(1): p. 23.
164. Ehrenreiter, K., et al., *Raf-1 regulates Rho signaling and cell migration.* J Cell Biol, 2005. **168**(6): p. 955-64.
165. Karin, M., *The regulation of AP-1 activity by mitogen-activated protein kinases.* Philos Trans R Soc Lond B Biol Sci, 1996. **351**(1336): p. 127-34.
166. Leppa, S. and D. Bohmann, *Diverse functions of JNK signaling and c-Jun in stress response and apoptosis.* Oncogene, 1999. **18**(45): p. 6158-62.
167. Whitmarsh, A.J. and R.J. Davis, *Transcription factor AP-1 regulation by mitogen-activated protein kinase signal transduction pathways.* J Mol Med (Berl), 1996. **74**(10): p. 589-607.
168. Schreck, I., et al., *c-Jun localizes to the nucleus independent of its phosphorylation by and interaction with JNK and vice versa promotes nuclear accumulation of JNK.* Biochem Biophys Res Commun, 2011. **407**(4): p. 735-40.
169. Deng, T. and M. Karin, *c-Fos transcriptional activity stimulated by H-Ras-activated protein kinase distinct from JNK and ERK.* Nature, 1994. **371**(6493): p. 171-5.
170. Gazon, H., et al., *Hijacking of the AP-1 Signaling Pathway during Development of ATL.* Front Microbiol, 2017. **8**: p. 2686.
171. Dippold, W., et al., *Expression of intercellular adhesion molecule 1 (ICAM-1, CD54) in colonic epithelial cells.* Gut, 1993. **34**(11): p. 1593-7.
172. Maeda, K., et al., *Expression of intercellular adhesion molecule-1 and prognosis in colorectal cancer.* Oncol Rep, 2002. **9**(3): p. 511-4.
173. Alexiou, D., et al., *Serum levels of E-selectin, ICAM-1 and VCAM-1 in colorectal cancer patients: correlations with clinicopathological features, patient survival and tumour surgery.* Eur J Cancer, 2001. **37**(18): p. 2392-7.
174. Schroder, C., et al., *Prognostic value of intercellular adhesion molecule (ICAM)-1 expression in breast cancer.* J Cancer Res Clin Oncol, 2011. **137**(8): p. 1193-201.
175. Parkos, C.A., et al., *Expression and polarization of intercellular adhesion molecule-1 on human intestinal epithelia: consequences for CD11b/CD18-mediated interactions with neutrophils.* Mol Med, 1996. **2**(4): p. 489-505.
176. Kim, D.H., et al., *Epithelial Mesenchymal Transition in Embryonic Development, Tissue Repair and Cancer: A Comprehensive Overview.* J Clin Med, 2017. **7**(1).
177. Cao, L., et al., *Zinc-finger protein 471 suppresses gastric cancer through transcriptionally repressing downstream oncogenic PLS3 and TFAP2A.* Oncogene, 2018. **37**(26): p. 3601-3616.
178. Berlato, C., et al., *Alternative TFAP2A isoforms have distinct activities in breast cancer.* Breast Cancer Res, 2011. **13**(2): p. R23.
179. Zhang, X., Y.K. Leung, and S.M. Ho, *AP-2 regulates the transcription of estrogen receptor (ER)-beta by acting through a methylation hotspot of the 0N promoter in prostate cancer cells.* Oncogene, 2007. **26**(52): p. 7346-54.
180. Zhou, R., P. Chen, and G.S. Zhang, *[AP-2 expression and significance in the lung cancer tissues].* Zhong Nan Da Xue Xue Bao Yi Xue Ban, 2004. **29**(2): p. 195-7.
181. Pellikainen, J., et al., *Expression of HER2 and its association with AP-2 in breast cancer.* Eur J Cancer, 2004. **40**(10): p. 1485-95.
182. Pellikainen, M.J., et al., *p21WAF1 expression in invasive breast cancer and its association with p53, AP-2, cell proliferation, and prognosis.* J Clin Pathol, 2003. **56**(3): p. 214-20.

183. Pellikainen, J., et al., *Reduced nuclear expression of transcription factor AP-2 associates with aggressive breast cancer.* Clin Cancer Res, 2002. **8**(11): p. 3487-95.
184. Beger, M., et al., *Expression pattern of AP-2 transcription factors in cervical cancer cells and analysis of their influence on human papillomavirus oncogene transcription.* J Mol Med (Berl), 2001. **79**(5-6): p. 314-20.
185. Turner, B.C., et al., *Expression of AP-2 transcription factors in human breast cancer correlates with the regulation of multiple growth factor signalling pathways.* Cancer Res, 1998. **58**(23): p. 5466-72.
186. Schulte, J.H., et al., *Transcription factor AP2alpha (TFAP2a) regulates differentiation and proliferation of neuroblastoma cells.* Cancer Lett, 2008. **271**(1): p. 56-63.
187. Nakayama, K.I. and K. Nakayama, *Ubiquitin ligases: cell-cycle control and cancer.* Nat Rev Cancer, 2006. **6**(5): p. 369-81.
188. Ciechanover, A. and A.L. Schwartz, *The ubiquitin system: pathogenesis of human diseases and drug targeting.* Biochim Biophys Acta, 2004. **1695**(1-3): p. 3-17.
189. Ciechanover, A., *The ubiquitin proteolytic system and pathogenesis of human diseases: a novel platform for mechanism-based drug targeting.* Biochem Soc Trans, 2003. **31**(2): p. 474-81.
190. Theochari, N.A., et al., *Antibiotics exposure and risk of inflammatory bowel disease: a systematic review.* Scand J Gastroenterol, 2018. **53**(1): p. 1-7.